



The Abdus Salam
International Centre for Theoretical Physics



2168-5

**Joint ICTP-IAEA Workshop on Dense Magnetized Plasma and Plasma
Diagnostics**

15 - 26 November 2010

Z-Pinch, concept, experiment

G. Hall
Imperial College of Science & Technology
London
UK

The Physics of Wire-Array Z-pinches

Gareth Hall, Imperial College, London, UK

Overview

- Why are people interested in wire arrays? Fusion!
- Brief introduction to pulsed power drivers
- Observing and modeling the process of a “basic” wire array implosion
- Implosion dynamics and X-ray production from wire arrays
- Developments in wire array technology
- Another application for wire arrays – Laboratory astrophysics
- The future of wire array ICF

Why are we interested in wire arrays?

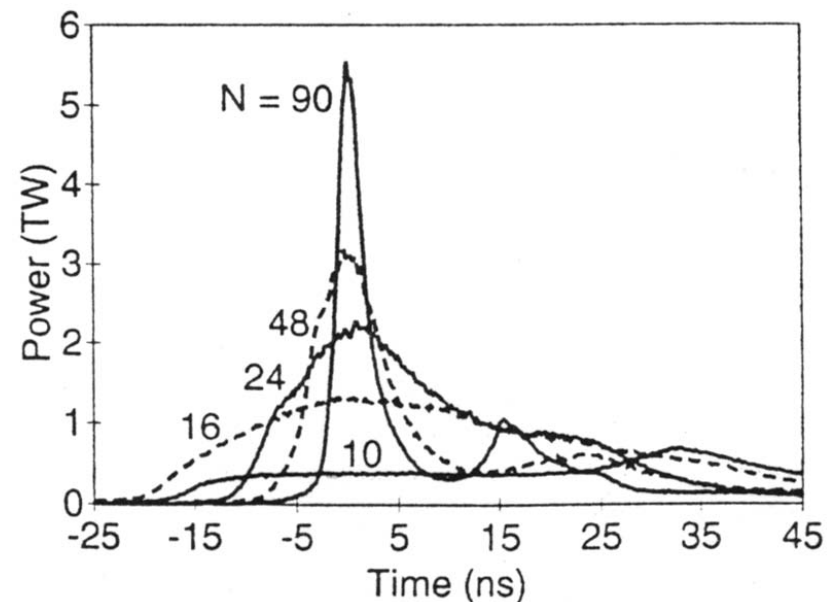
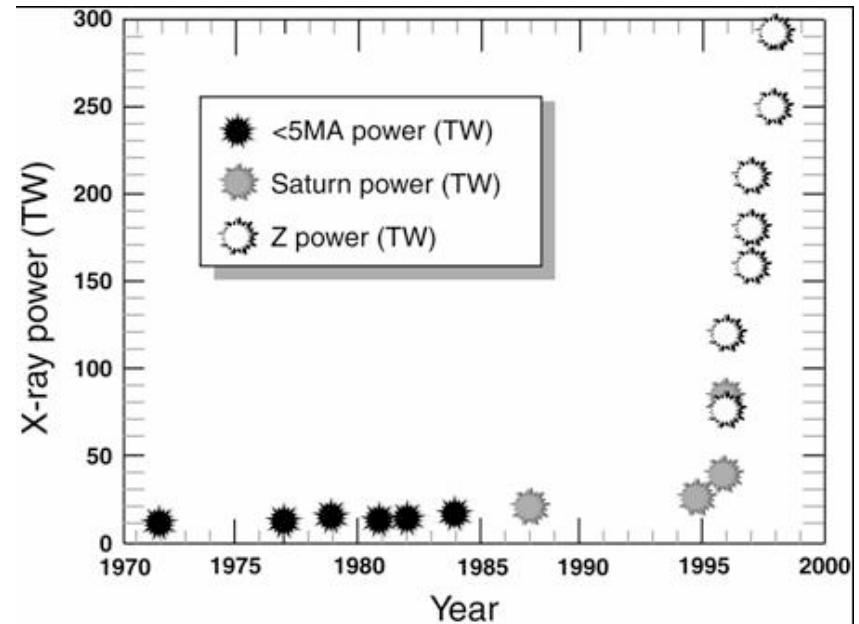
Why are we interested in wire arrays?

- Dramatic increase in soft x-ray power output since 1970s, mainly due to
 - Driver Technology (larger currents)
 - Use of high wire arrays (>100)
 - Wire array design (e.g. nested arrays see later)
- Peak soft x-ray yield energies of 1.8 MJ at 280 TW
- High efficiency: Stored energy of 11.4 MJ give ~15% (Z-machine)
- Regularly used as an x-ray drive for radiation/opacity studies, HEDP, photoionisation, hydrodynamics

T.W.L. Sanford et al, Phys Rev Lett, **77**, 5062 (1995)

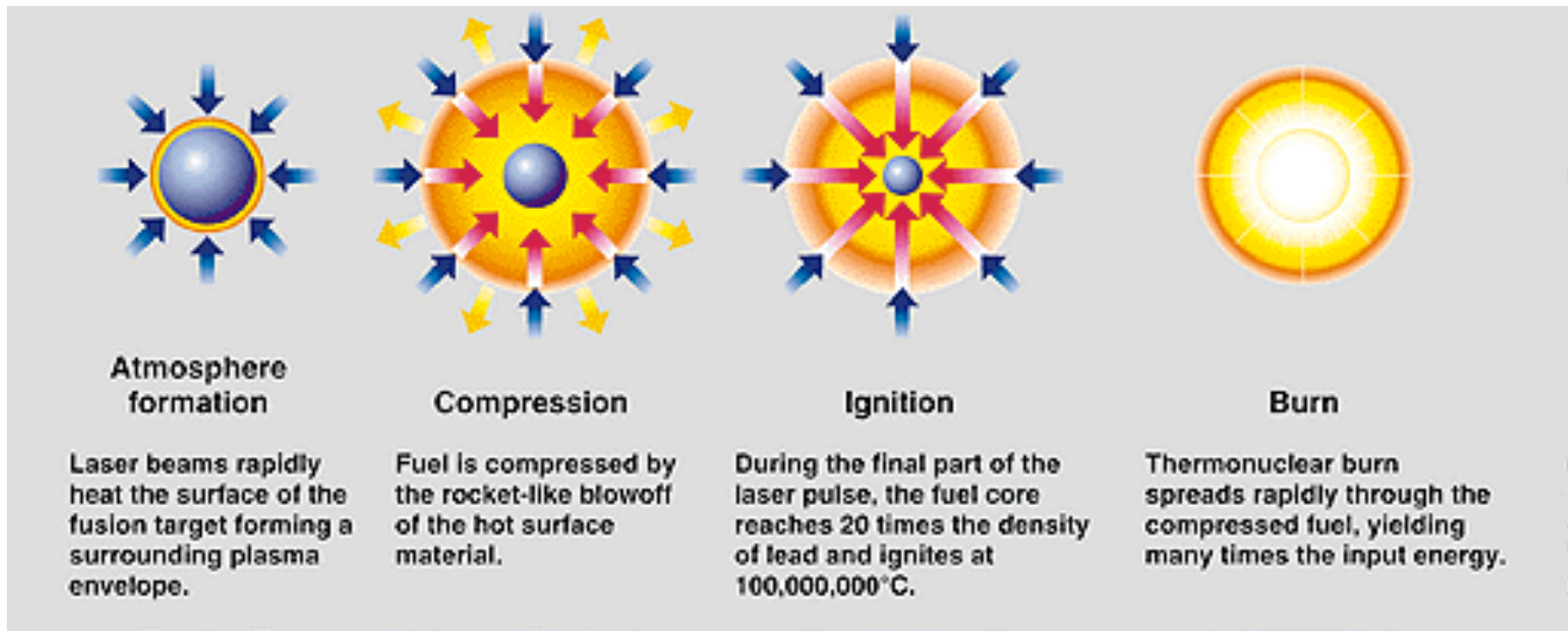
C. Deeney et al, **81**, 4883 1998

W. Stygar et al Phys Rev , **69** 046403 (2004)



High power soft X-rays...Fusion driver?

Inertial Confinement Fusion (ICF) requires large yields (mega joule level) of soft X-rays at high power (100's of TW) to compress and ignite fuel capsule.

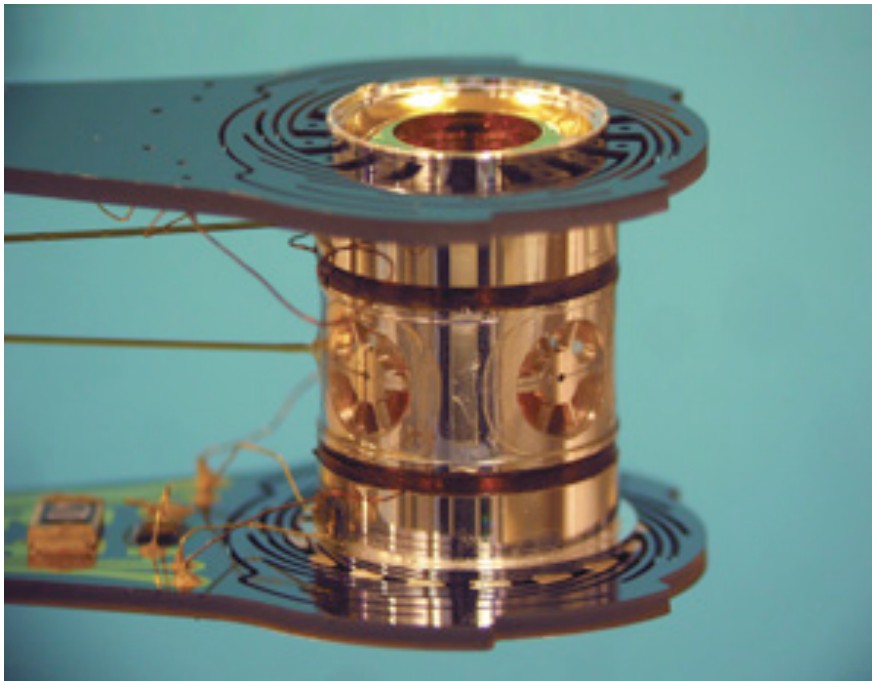


Laser driven ICF is a familiar concept

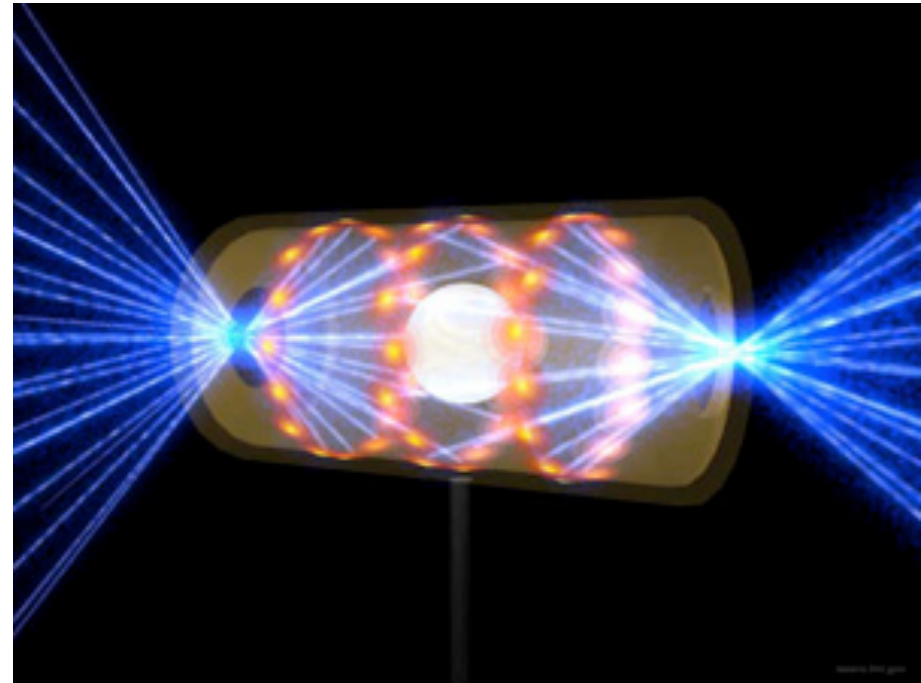
National Ignition Facility in a nutshell

- 192 lasers focussed onto hohlraum walls
- UV Laser light (351nm) heats walls, and is reradiated as soft X-ray onto fuel capsule
- 1.8MJ of laser into the hohlraum to ignite

NIF indirect-drive hohlraum



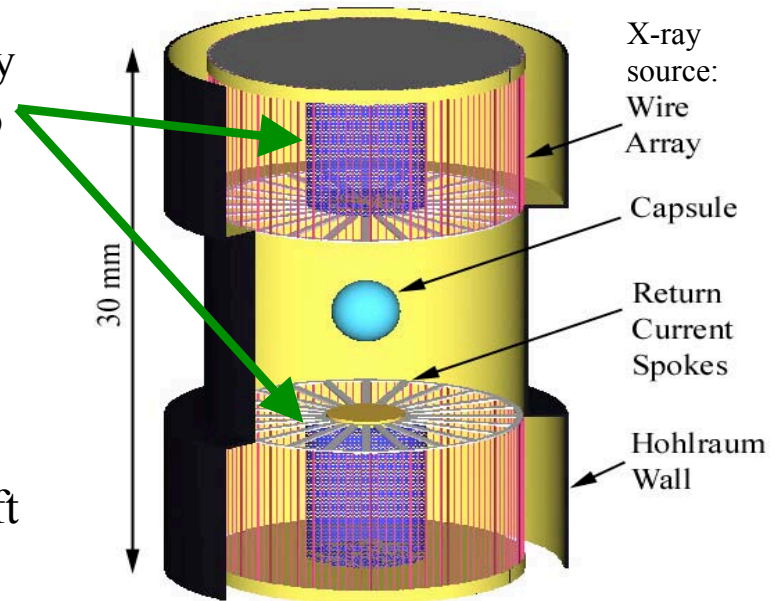
Laser-driven ICF concept



- **Z produced 1.8MJ of soft x-rays from a wire array in 1998. Of course, there's a lot more (!!) to the problem than this, but it is a promising result.**
- **So, can we use wire arrays to do ICF?**

Double Ended Hohlräum (DEH) concept

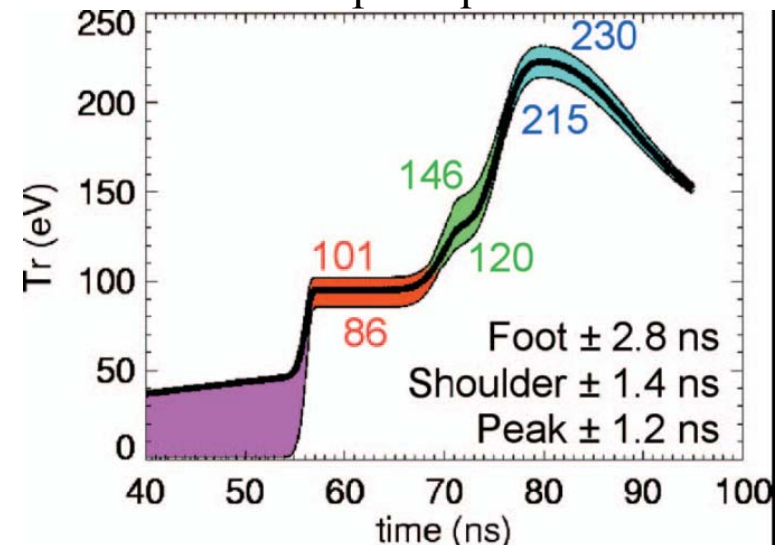
- Implosion of a wire array converts electrical energy into soft x-rays – use this as the radiation source to energise a hohlraum (instead of a laser)
- Wire arrays in two primary hohlraums, fuel capsule in secondary hohlraum. No direct illumination onto capsule: secondary is driven by primaries for radiation uniformity.
- Ignition requires each pinch to produce 1PW of soft X-ray (60MA driver at current scaling)



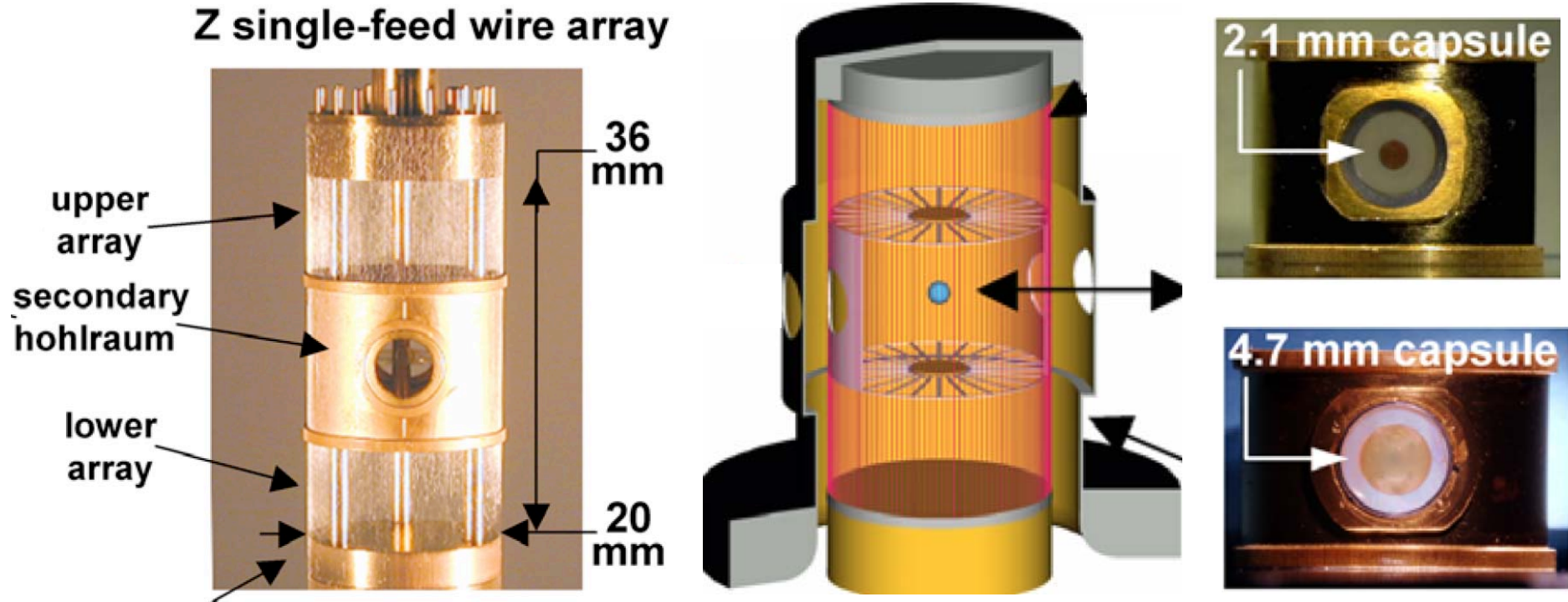
Ignition design for high yield

CAPSULE	NIF 300eV	Double Z-pinch 220eV
Radius (mm)	1.1	2.65
Fuel thickness (μm)	80	280
Drive Pressure (MB)	160	60
Peak pr (g/cm ²)	1.9	3.1
Absorbed Energy (MJ)	0.14	1.21
Yield (MJ)	13	520

Pulse shape requirements



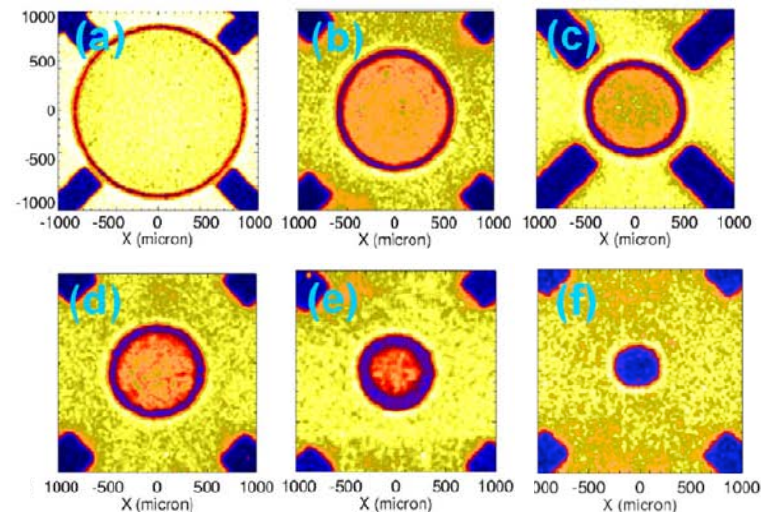
DEH experiments at Sandia National Laboratories



Experimental work with the DEH concept on the 20MA Z-machine achieved:

- Drive symmetry within 2- 4%
- Secondary hohlraum temp 65-75eV
- Capsule Convergence ratio of ~ 13
- Energy into capsule ~ 7 kJ

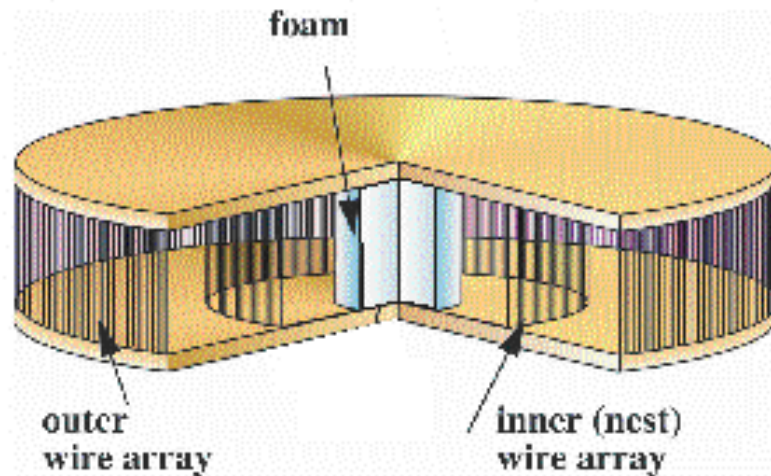
This was performed with 50TW single arrays (i.e. no pulse shaping). Nested arrays can do much better...



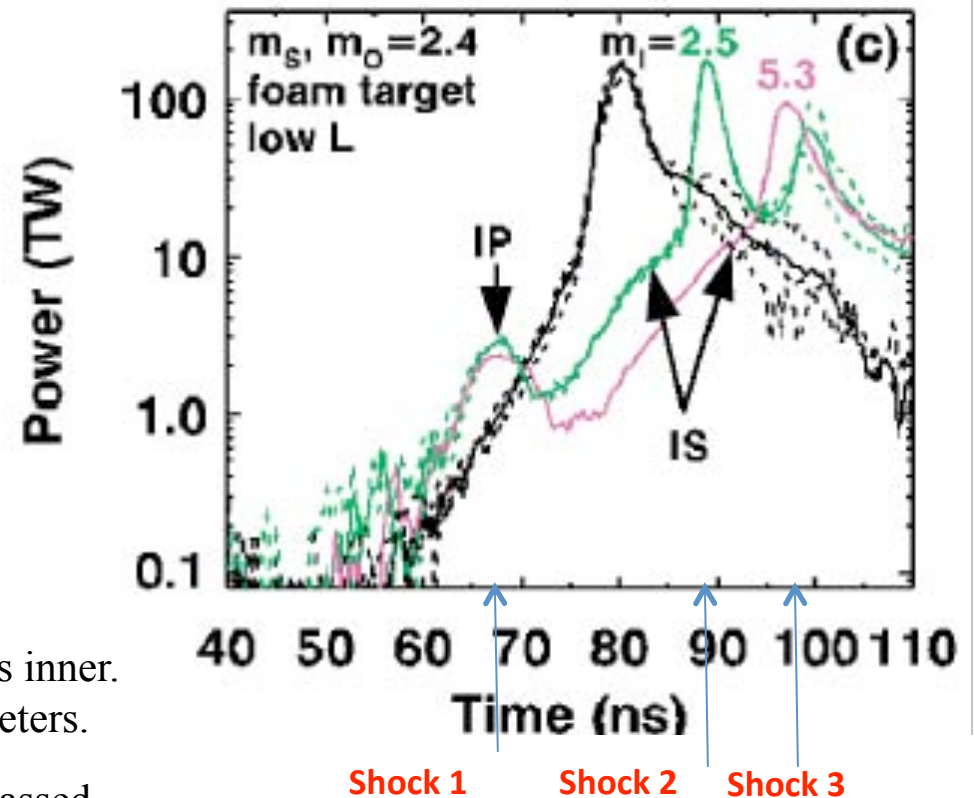
Pulse Shaping for ICF

Need multiple shocks (as many as possible, but minimum 3) onto the capsule to drive the implosion isentropically, otherwise the fuel becomes too hot and won't compress.

Use two arrays "nested" one inside the other, and place a foam on axis:



- Shock 1: Interaction pulse (IP) as outer array passes inner. Control timing by ratio of outer to inner array diameters.
- Shock 2: Interaction shock as outer array (having passed through the inner) reaches the axis and hits the foam. Timing is determined by the foam diameter.
- Shock 3: Final (peak) shock as inner array hits the axis. Timing is controlled by the inner array diameter and mass.

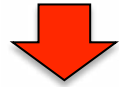


M.E.Cuneo, *Phys Rev Lett*, **95**, 185001 (2005)

M.E.Cuneo, *Phys. Plasmas Control. Fusion*, **48**, R1 (2006)

Main problem with the DEH - size

Double ended hohlraum suffers because it is big: wire arrays are typically ~20mm in diameter, ~10mm tall.



Radiation intensity of blackbody (watts/area) $\propto \sigma T^4$



Need a large hohlraum to couple radiation from pinches

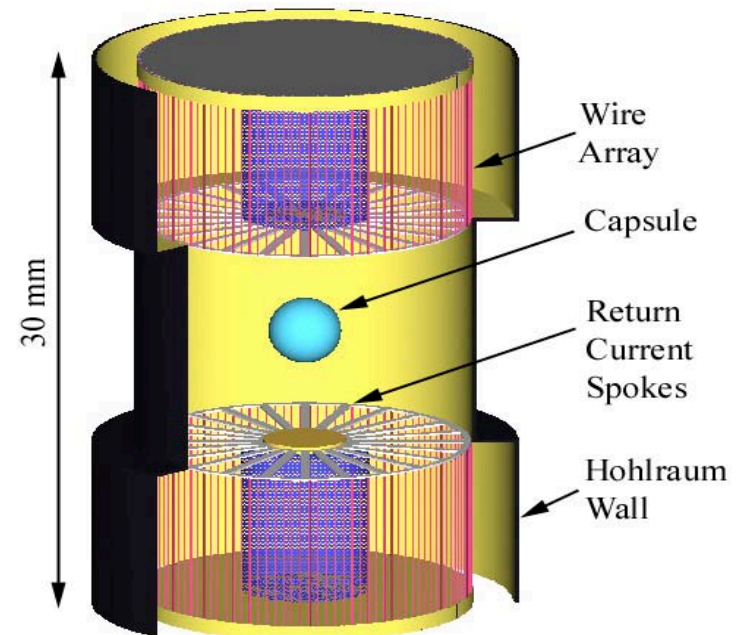


Large hohlraum = large hohlraum wall (blackbody) area



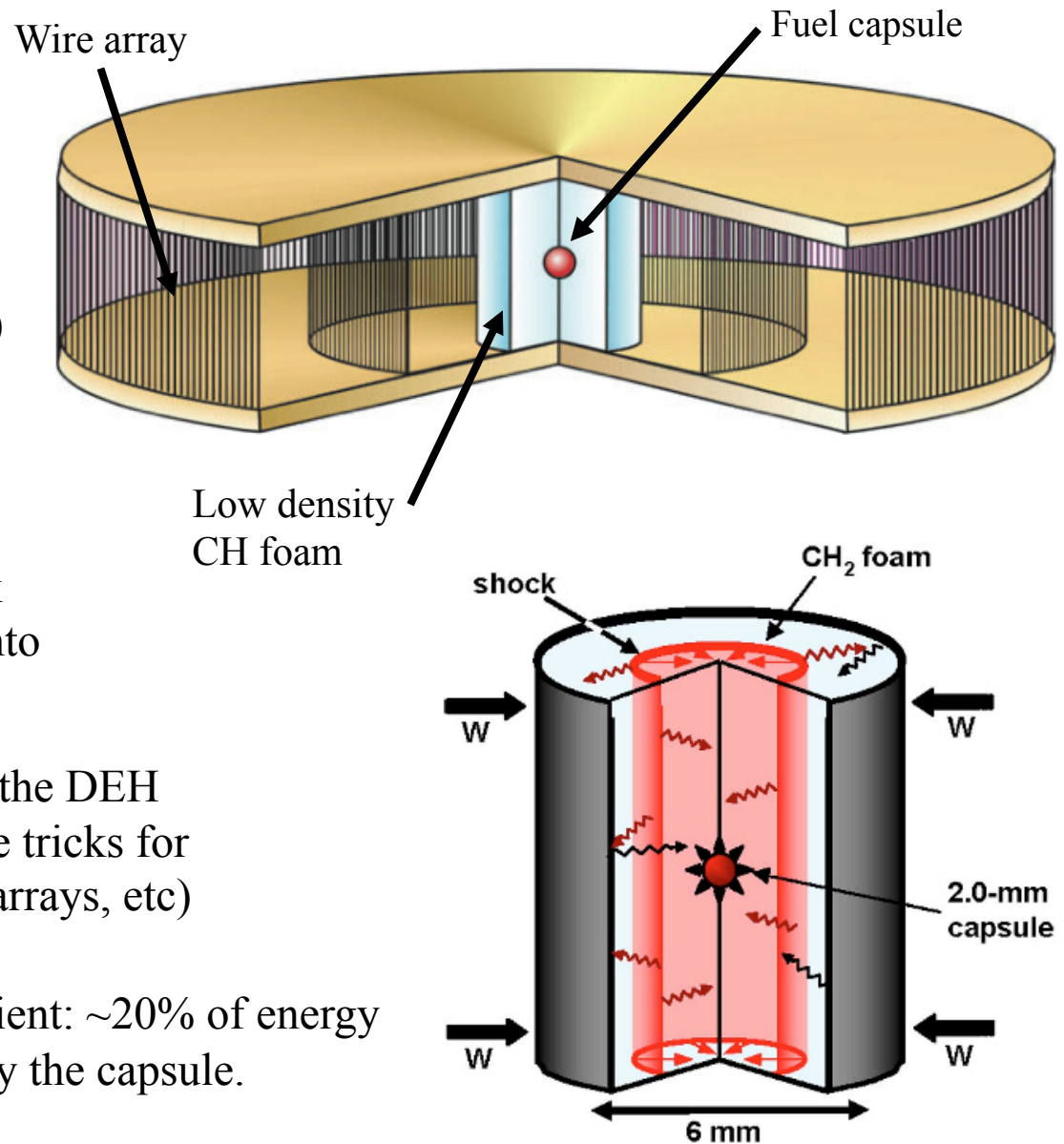
Low radiation temperature for a given pinch x-ray power, i.e. need very high radiation power (1PW) to get to high temperatures (220eV) required to drive a capsule to ignition.

- The DEH is ~1% efficient, throwing away the efficiency advantage of wire arrays.
- Good concept, but need smaller hohlraum, hence smaller radiation source – see later
- Another solution – place the fuel capsule inside the foam



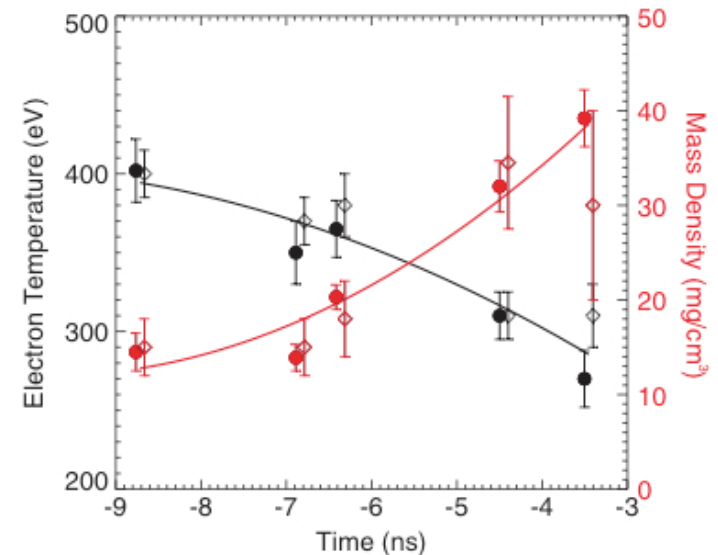
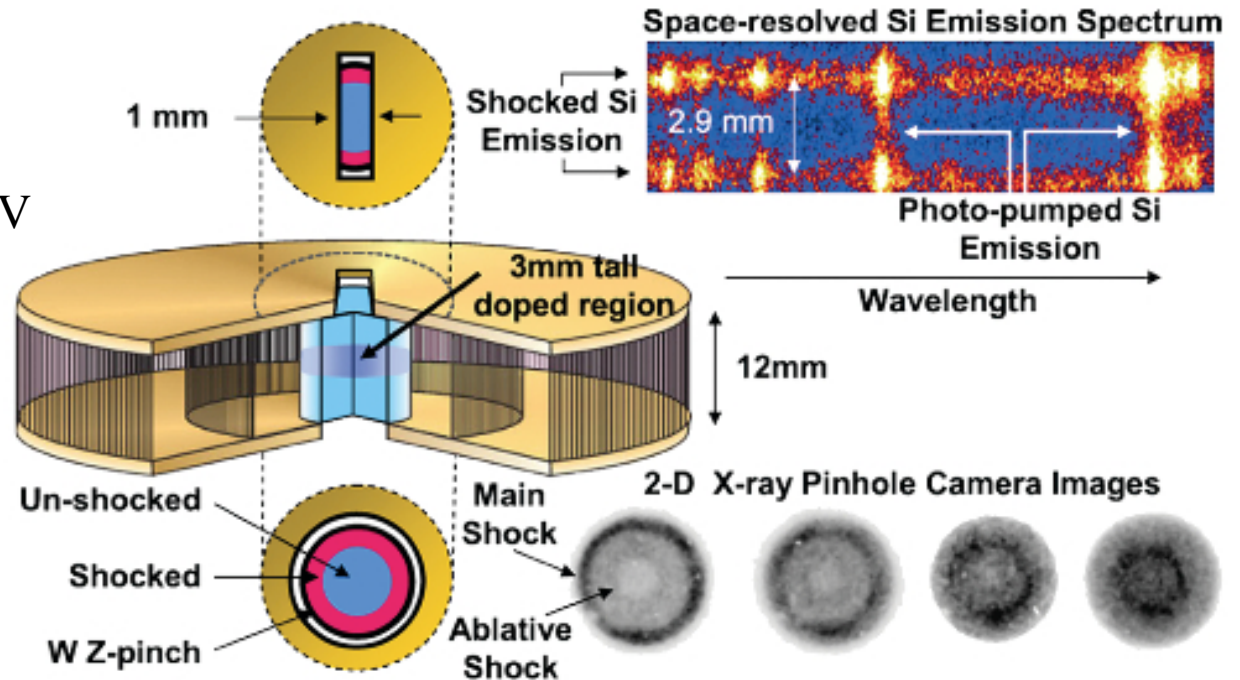
Dynamic hohlraum (DH) concept

- Place fuel inside hydrocarbon foam on axis of array
- Implosion of array onto foam forms hot, high-Z (e.g. tungsten) plasma on surface of the foam. This acts as the hohlraum wall.
- The implosion compresses the foam, drives radiative shock inwards (dynamic hohlraum) onto the capsule.
- Hohlraum is much smaller than the DEH concept, and can use the same tricks for pulse shaping as before (nested arrays, etc)
- Dynamic hohlraum is very efficient: ~20% of energy into the hohlraum is absorbed by the capsule.



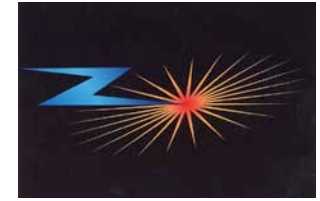
DH experiments at Sandia National Laboratories

- Experiments on the 20MA Z-machine produced radiation temperatures $>200\text{eV}$
- Radiative shock delivers 180kJ to the hohlraum.
- ICF capsule absorbs $>40\text{kJ}$ (c.f. 7kJ for the DEH)
- Experiments have observed thermonuclear DD neutron yields of 8×10^{10} (10 times higher than any other indirect drive experiments)
- Radiation symmetry not good enough for ignition; tries to perform spherical implosion with cylindrical drive.
- Can we make a dynamic hohlraum with a more spherical radiation drive? See later...



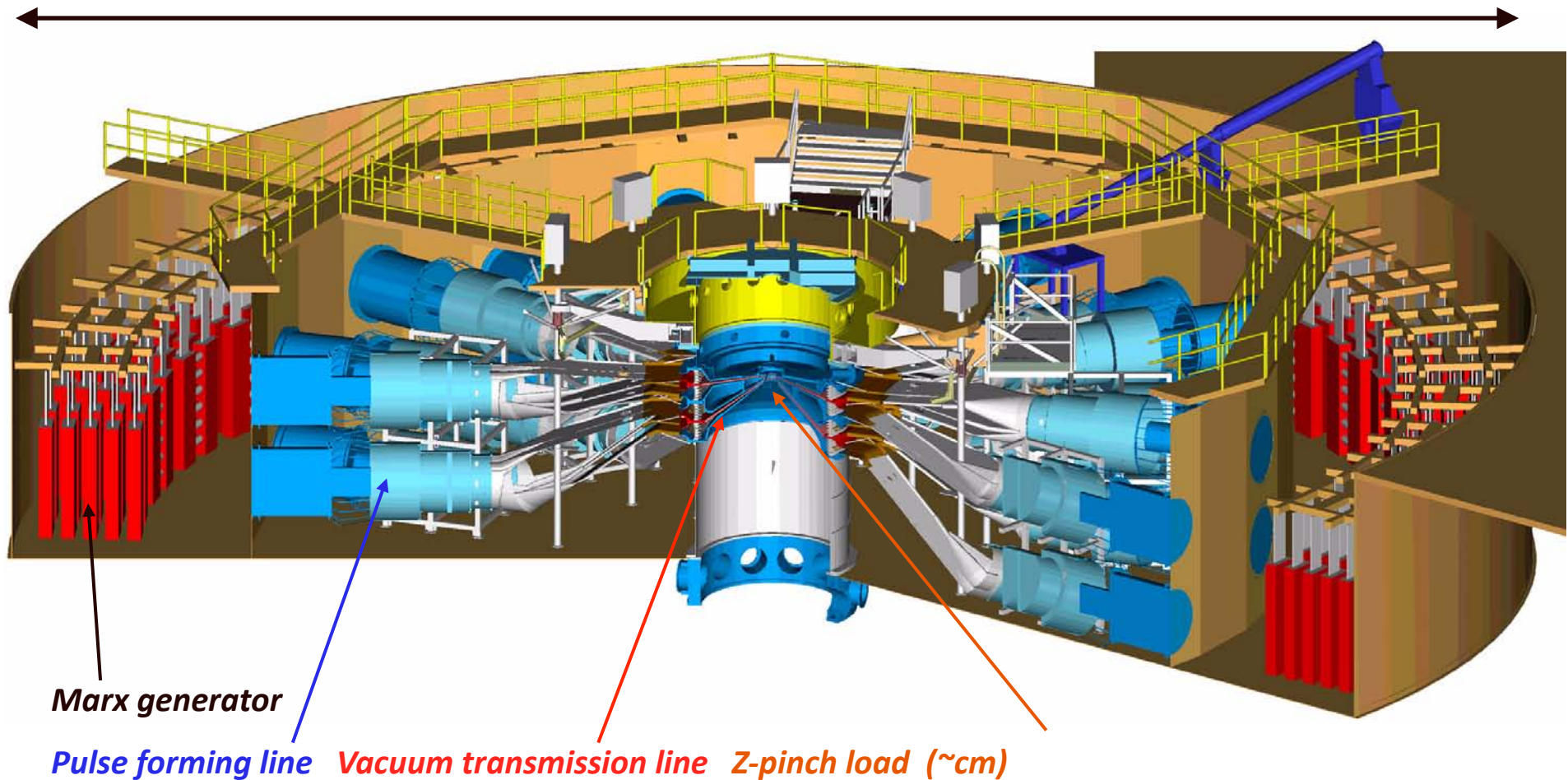
Brief introduction to pulsed power drivers

Z-machine at Sandia National Labs



- Largest wire array driver in the world: recently refurbished, now firing at 26MA
- Discharges 2160 x 2.2 μ F capacitors (36 MARX banks) to produce 5.6MV

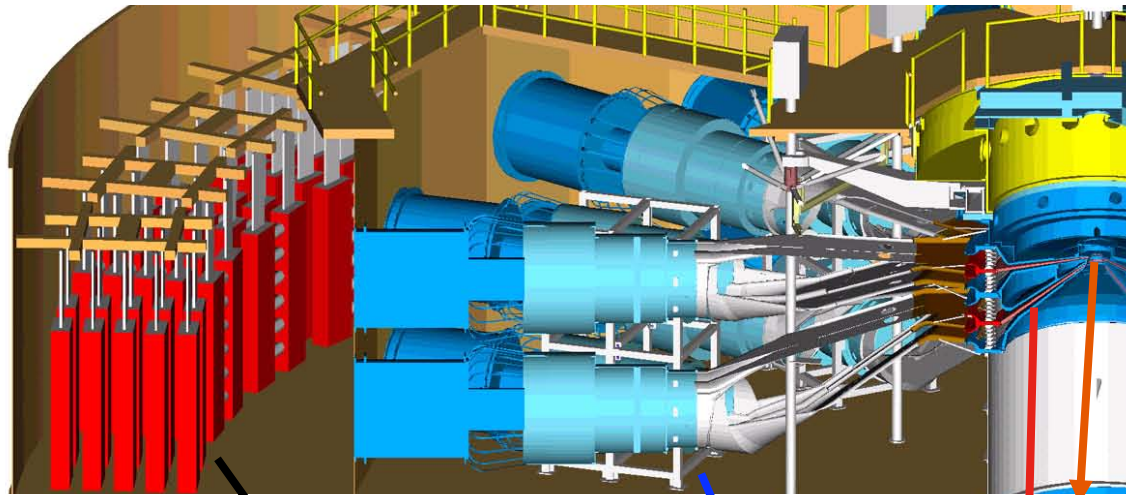
33m diameter



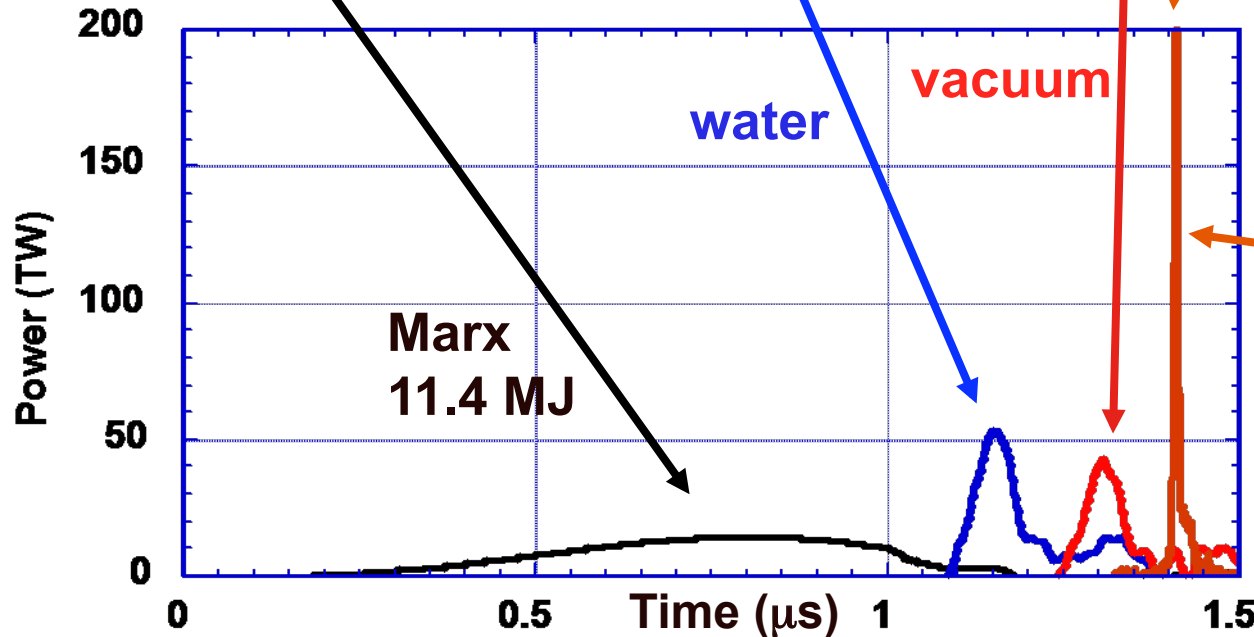
Z-machine at Sandia National Labs



- Energy is compressed in time and space between the marx banks and the load



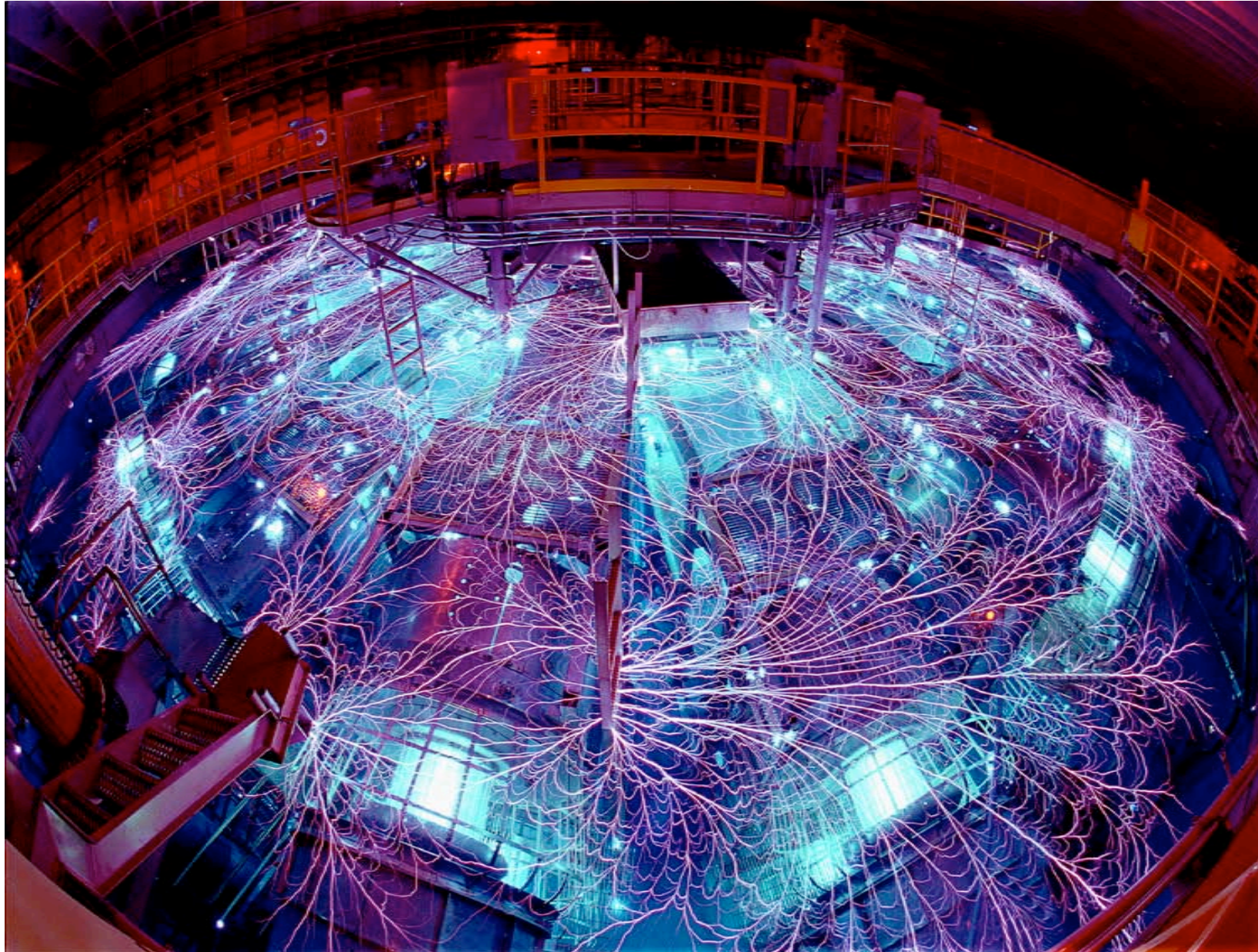
- 11.4MJ of stored electrical energy discharged in 1 μ s
- Water-filled pulse forming lines compress this to 100ns
- Machine diameter is 33m, wire array load is 20-40mm
- Last stage of energy compression come from plasma/wire array physics



X-ray output
~300 TW or 0.3 PW

Electrical to X-ray energy
conversion efficiency ~15%

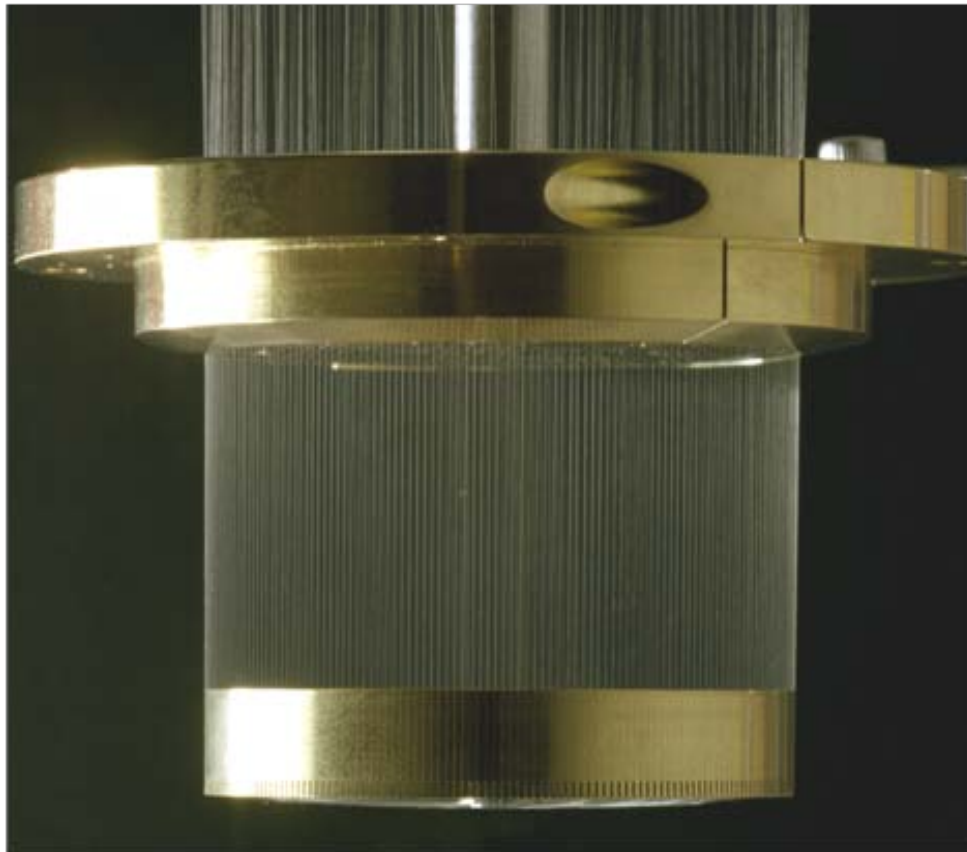
Z-machine firing



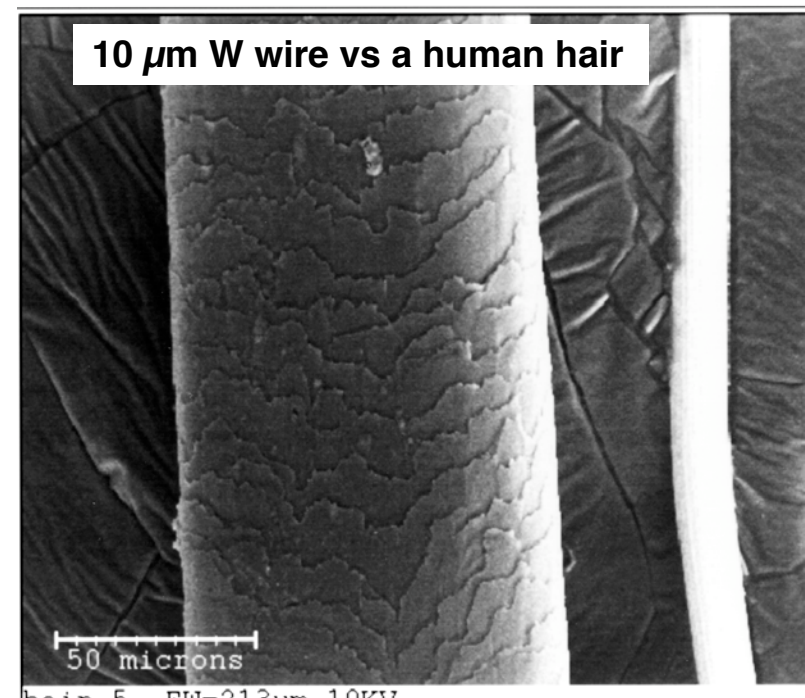
Wire arrays use fine metallic wires

- On the Z-machine, arrays with up to 600 wires were used in experiments
- Wire are typically ~ 5 times thinner than a human hair

40mm diameter array: 240 x $7.5\mu\text{m}$ tungsten wires



40mm

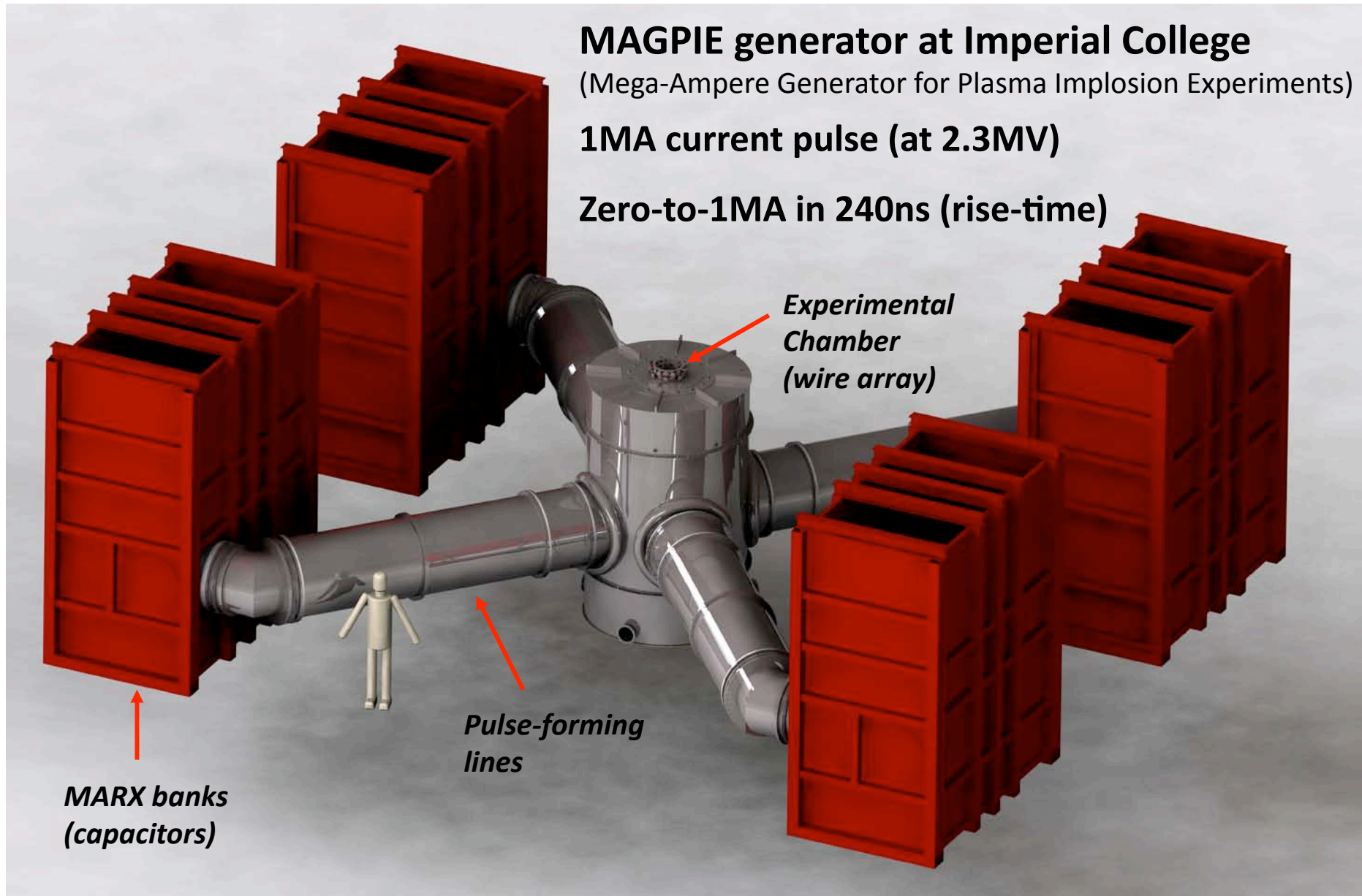


hair 5 50 microns EW-212um 10KV

S.E.M. courtesy of John McKenney

wire

University-based machines are typically 1MA

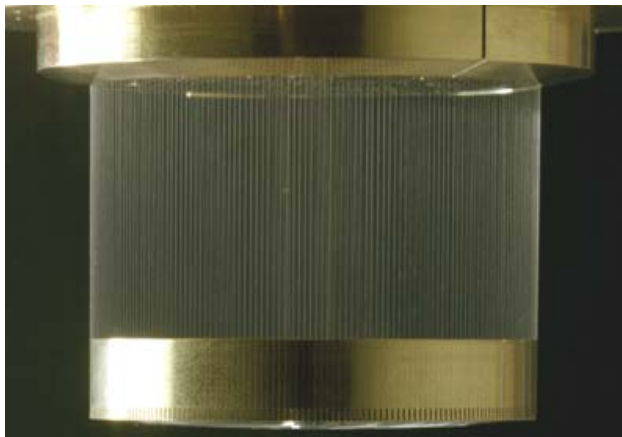


What role do these smaller machines play?

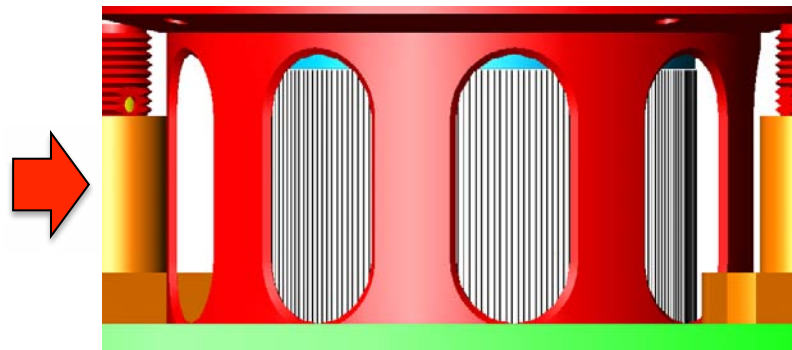
- Z-machine is low impedance (0.12Ω) to achieve fast rise time (100ns). If load develops high impedance (i.e. inductance) current losses occur or, at worst, breakdown across the transmission lines.
- At lower current/voltage, smaller machines are less susceptible to damaged in this way, so can safely investigate new array configurations before transferring to a larger machine.
- MAGPIE has *very* high impedance (1.25Ω) so can drive full current through highly inductive loads – can try some really crazy stuff!
- To maintain low impedance, the Z-machine current return path must be close to the array edge ($\sim 2\text{mm}$) and diagnostic access is limited to 9 narrow slots – makes it hard to observe experiments.
- With large impedance, MAGPIE can afford narrow return posts a long way ($\sim 8\text{cm}$) from the array without losing current. This provides an uninterrupted view of the array and unsurpassed diagnostic access.

	MAGPIE	Z
R (mm)	4-8mm	10-20mm
N	~ 32	~ 300
$t_{\text{implosion}}$	$\sim 250\text{ns}$	$\sim 100\text{ns}$
Current per wire	30 kA	60 kA

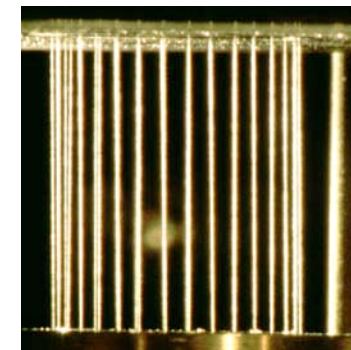
Z-machine array outside machine



Z-machine array inside machine



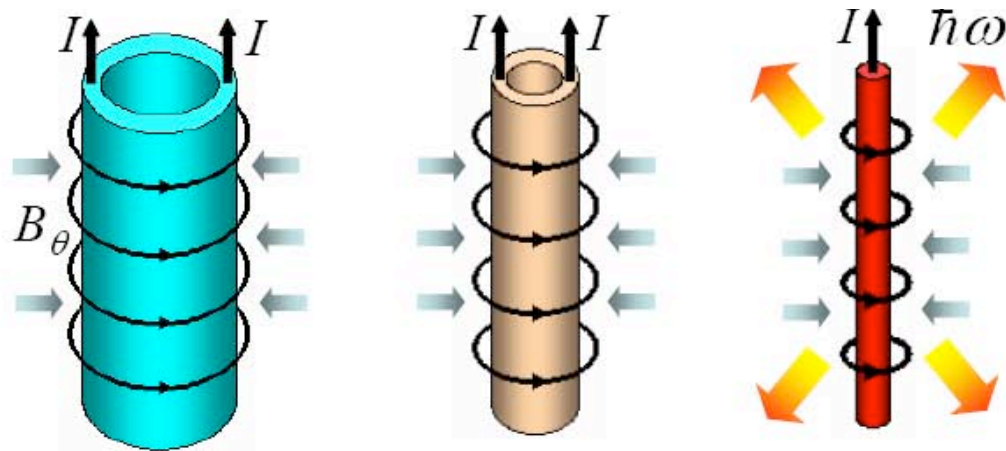
MAGPIE array inside machine



Observing and modeling
“basic” wire array implosions

Imploding shell concept

Electrical energy \Rightarrow Magnetic \Rightarrow Kinetic \Rightarrow Thermal/Radiation



Stagnation to a very small diameter:
High T and strong soft x-ray radiation

e.g. 2mg plasma shell imploding at
1000km/s has 1MJ of kinetic energy

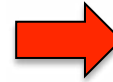
(Kinetic energy of 30 Ton pile-hammer is 0.5MJ)

Mechanical analogue



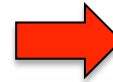
The 0D model of a shell Implosion

Magnetic pressure = Force / area of cylinder



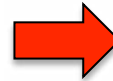
$$\frac{-B^2}{2\mu_0} = \frac{\text{Mass of shell} \cdot \frac{d^2 r}{dt^2}}{2\pi r l}$$

Substituting $B = \frac{\mu_0 I}{2\pi r}$ and $\hat{m} = \text{mass/length}$



$$\hat{m} \ddot{r} = \frac{-\mu_0 I^2}{4\pi r}$$

Introduce dimensionless variables



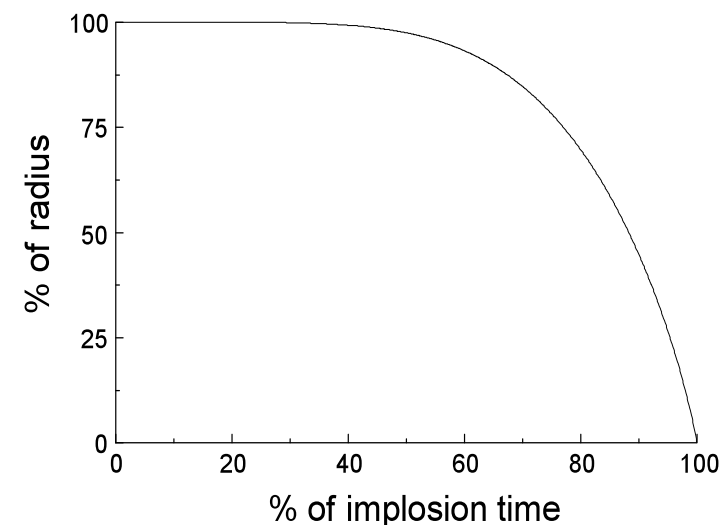
$$\tilde{r} = \frac{r}{r_0}, \tilde{t} = \frac{t}{\tau} \text{ and } \tilde{I} = \frac{I}{I_{\max}}$$

$$\tilde{r} \ddot{\tilde{r}} = - \underbrace{\left(\frac{\mu I_{\max}^2 \tau^2}{4\pi \hat{m} r_0^2} \right)}_{\Pi} \tilde{I}^2$$

D. D. Ryutov, Rev. Mod. Phys 72, 1, (2000)

Scaling parameter: Π

- Gives implosion trajectory for a shell to compare with experimentally measured implosion trajectories
- If the scaling parameter is the same for two shells, driving them with the same current pulse will produce identical implosion trajectories.
- Typically $I = I_{\max} \sin^2\left(\frac{\pi t}{2\tau}\right)$



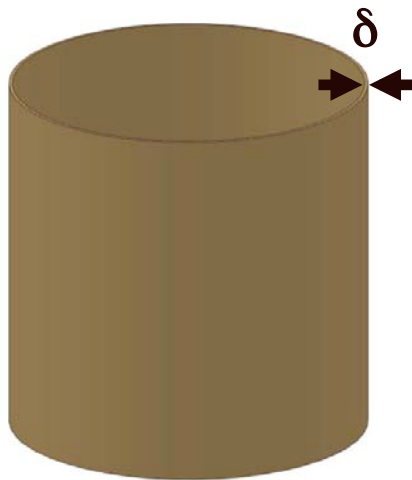
Use the 0D model to design a load

- How do we design a load to give the best X-ray output? Try to maximise kinetic energy
- Model implosions to find implosion time (when shell hits the axis) that maximises kinetic energy: occurs when shell hits axis at $t \sim 1.2\tau$ (i.e. 20% after peak current), which gives $\Pi \sim 8$
- For $\Pi \sim 8$, what would be the mass of a load for the Z-machine?

$$\Pi = \frac{\mu_0 I_{\max}^2 \tau^2}{4\pi \hat{m} r_0^2} = 8 \quad \text{and use} \quad \tau = 100\text{ns}, \quad I_{\max} = 20\text{MA},$$

$r_0 = 15\text{mm}, \quad \text{shell length} = 10\text{mm} \quad \rightarrow \quad m = 2\text{mg}$

How do we make such a large object with so little mass?

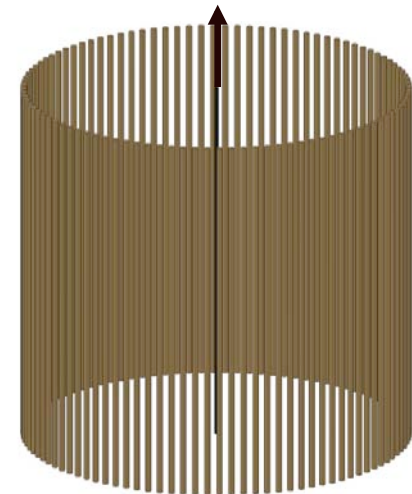


Free standing metal foil?

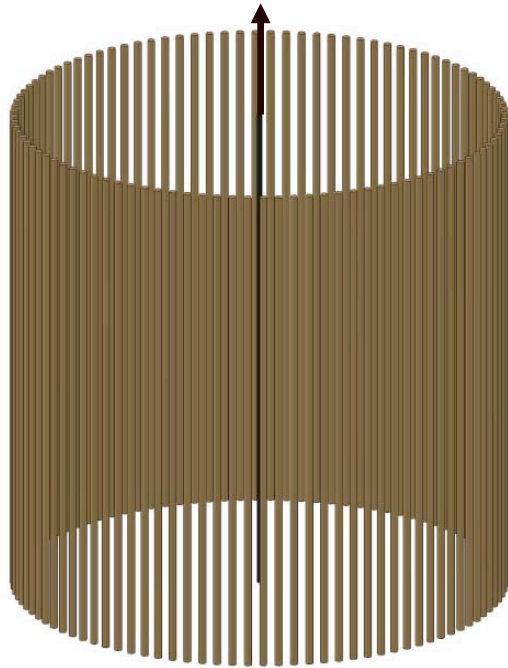
- Need $\delta \sim 50\text{-}100\text{nm}$, difficult to make!
- Very prone to Rayleigh Taylor instability
- Good current contacts?



Replace foil by cylindrical array of thin wires with the required total mass



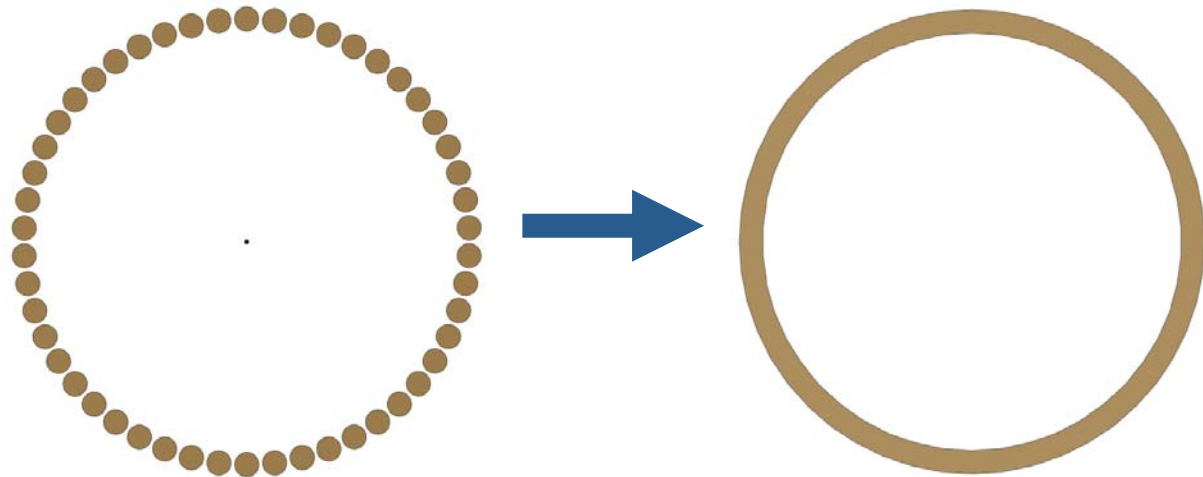
What do we expect to happen?



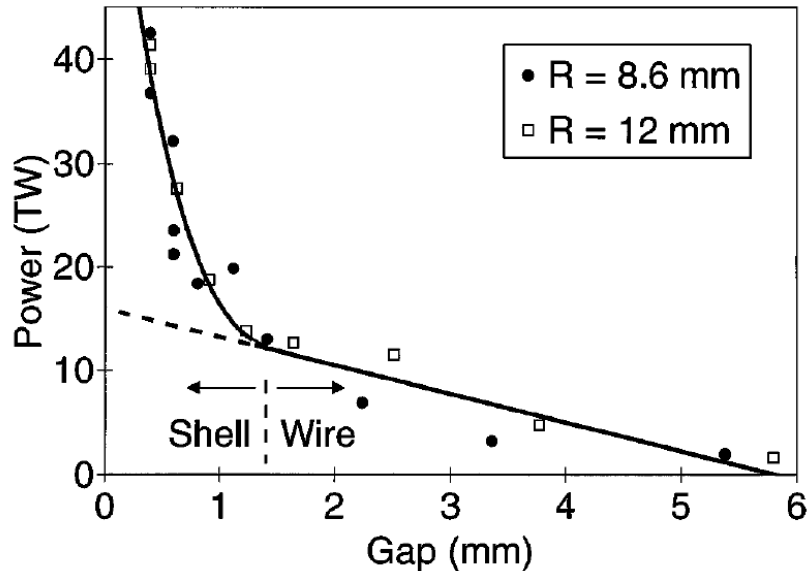
Wires start off as discrete objects, but rapidly explode as they are heated by the current...

e.g. 20MA on Z-machine, 200 wires in an array => 100kA per wire!

Expect wires to merge into a plasma shell of thickness approximately the inter-wire gap



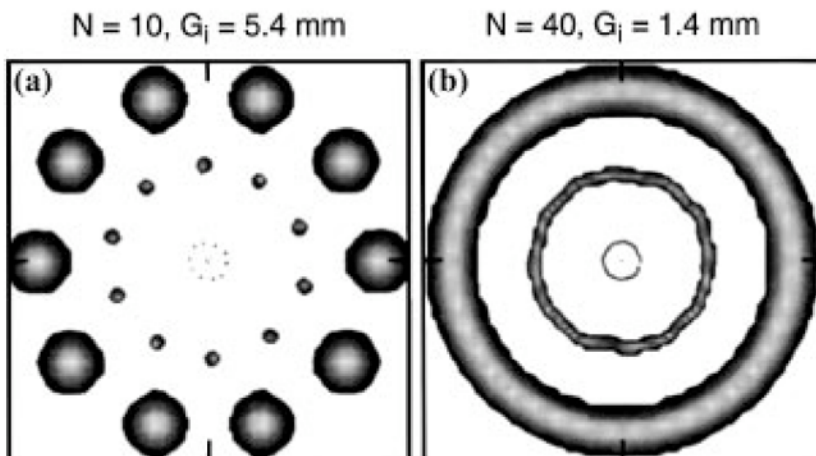
X-ray measurements appeared to agree...



Experimental scans of x-ray power vs. wire-number observed a dramatic increase of x-ray power below a certain inter-wire gap.

Sanford et. Al. PRL 1996

40TW x-ray pulse from the 8MA Saturn generator.

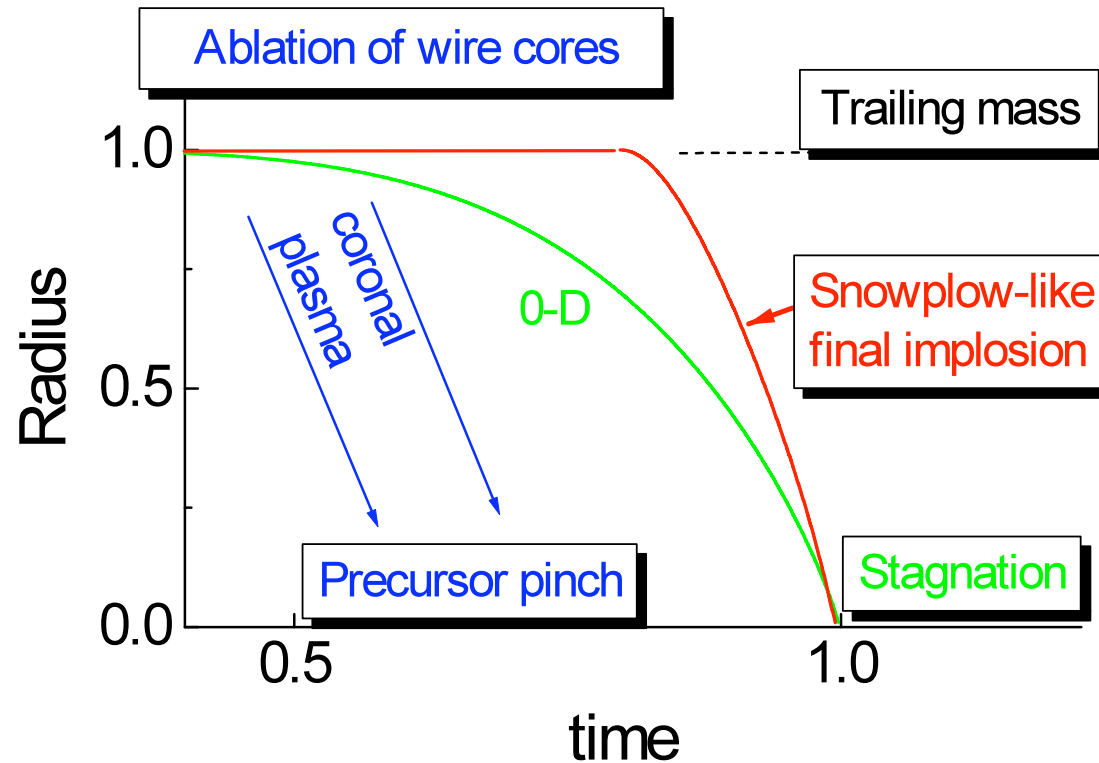


This was interpreted, from 2-D simulations, as evidence of plasma shell forming.

Basic picture of a wire array implosion

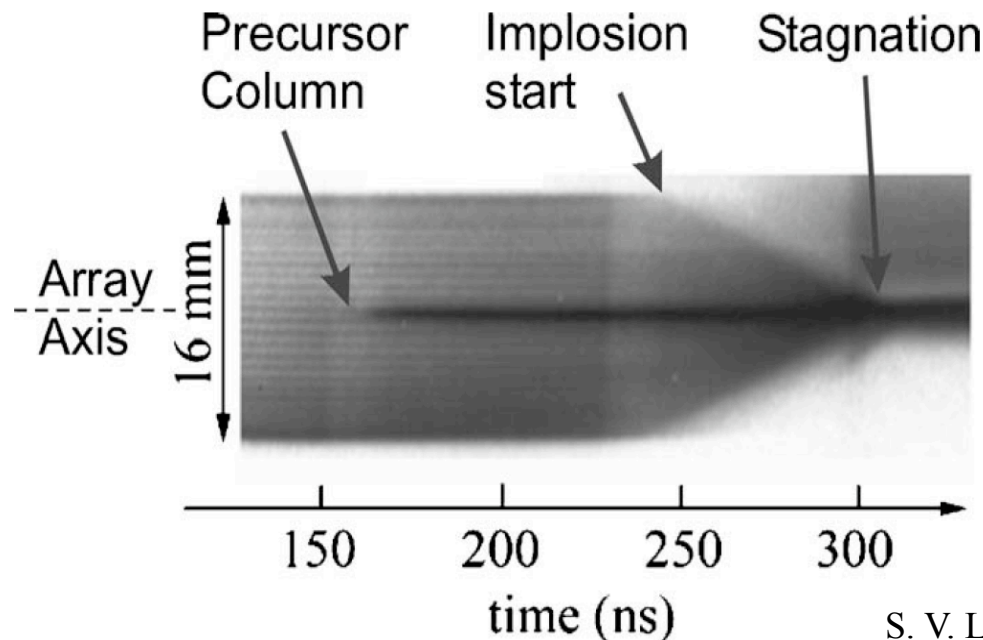
Two-stage implosion dynamics

- Extended period of ablation, radial redistribution of mass
- Snowplough-like implosion phase, stabilised by peaked on-axis density profile

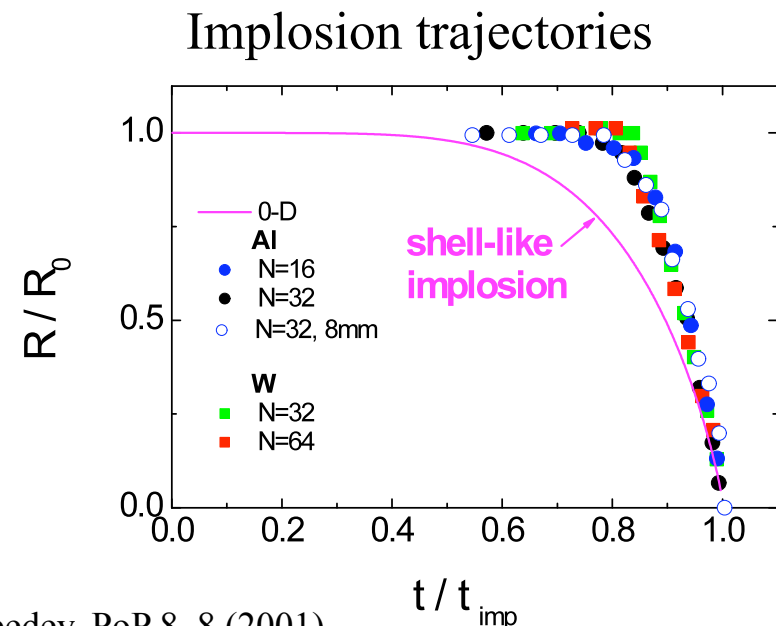


What is actually observed?

On MAGPIE, radial streak photography (i.e. image a thin radial slice of the array through time) was used to measure the implosion trajectory of the wire array.



S. V. Lebedev, PoP 8, 8 (2001)



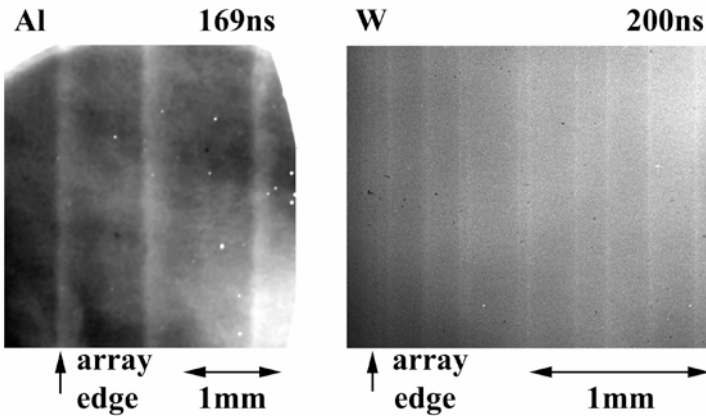
- The 0D model is wrong for wire arrays ! The observed implosion trajectories are not shell-like, even for large wire numbers (small inter-wire gap).
- It appears that the “wires” remain at the initial array radius for 80% of implosion time. What is going on at this position for all this time?

Observation of wire core/corona structure

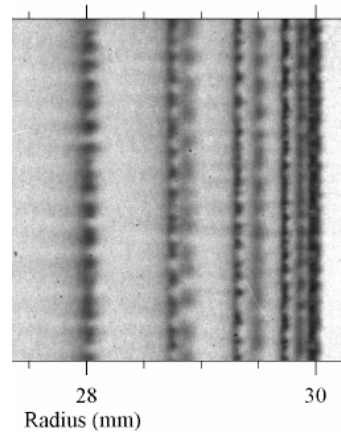
Dense, stationary wire cores surrounded by low density coronal plasma

Radiography (dense wire cores)

MAGPIE

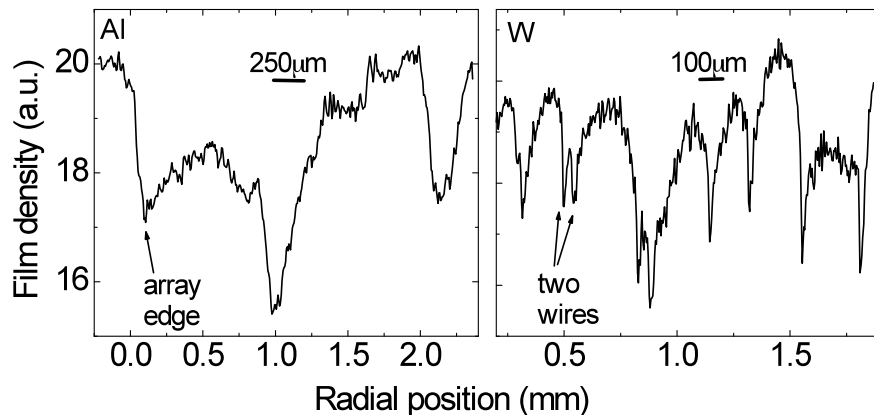
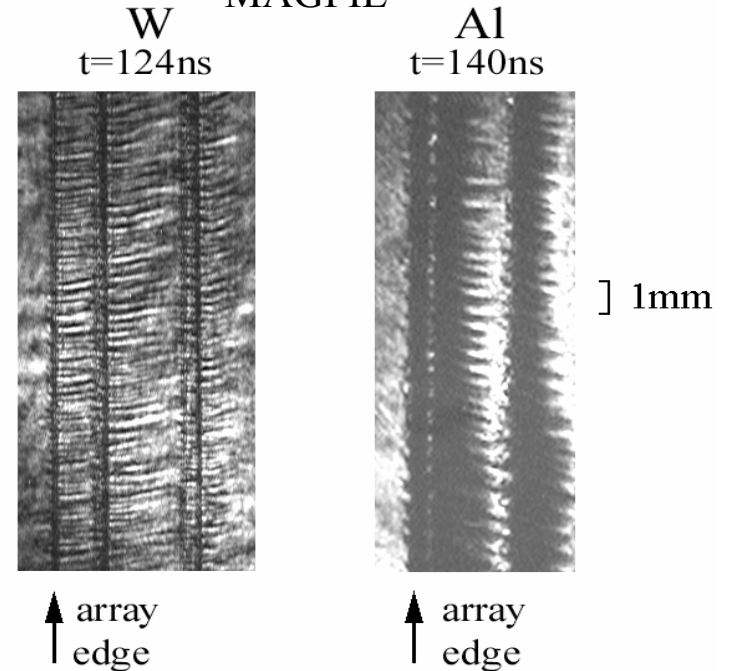


Radiography on Z-machine



Laser probing (low density coronae)

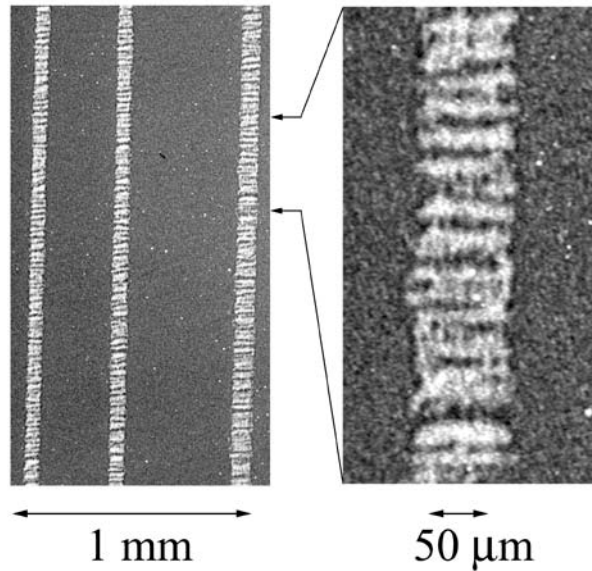
MAGPIE



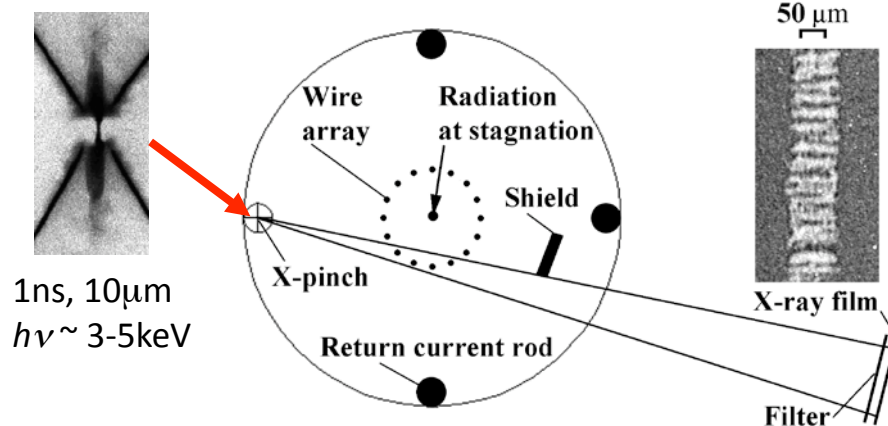
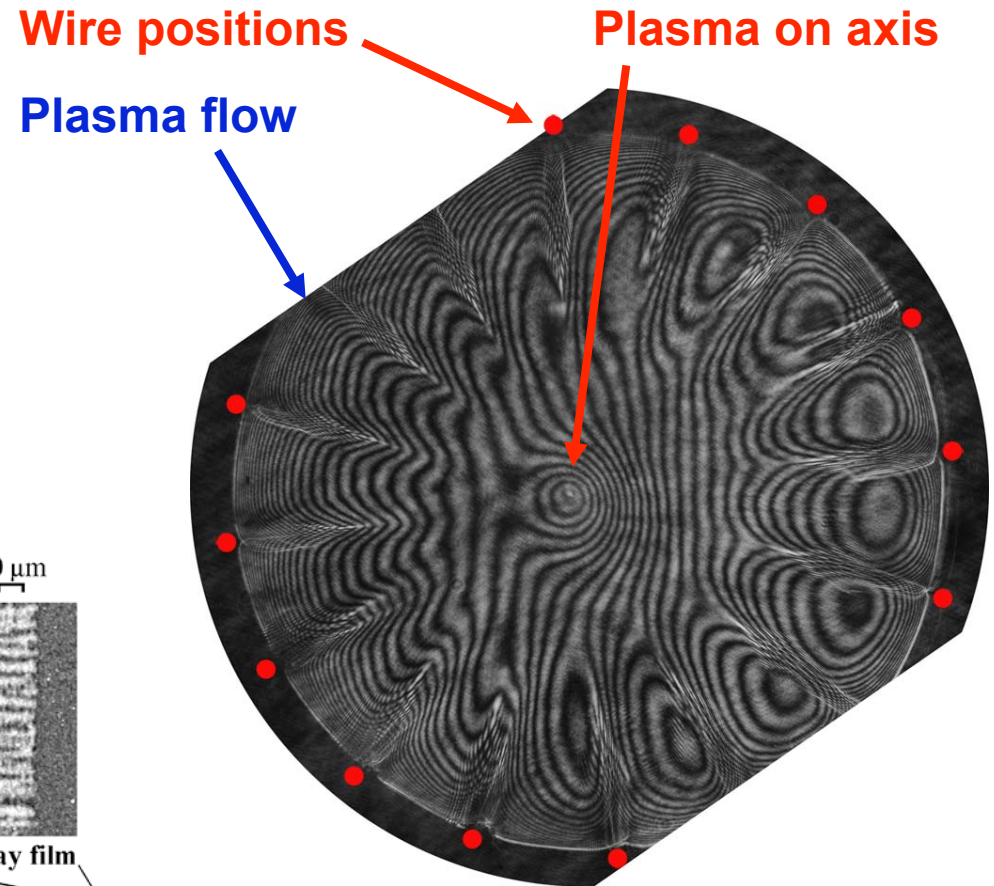
- Non-uniformity of the coronal plasma imprints on the wire core (more on this later!)
- The core-corona structure is not cylindrical – sharp outward and shallow inward edge to the density.

Observation of wire core/corona structure

High-res radiography reveals cores have complex internal structure (still not understood)

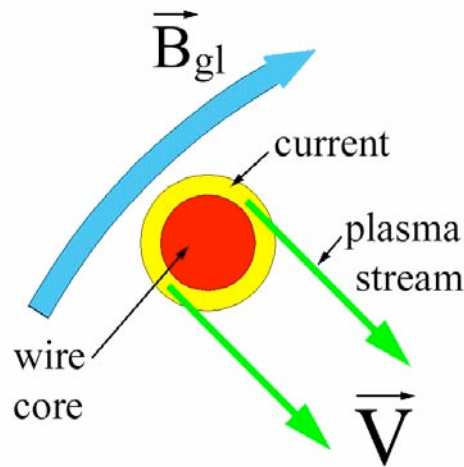


End-on laser interferometry shows that coronal plasma flows into the array whilst wire cores remain stationary.



“Rocket” model of ablation and mass redistribution

Ablation of stationary wire cores: $\mathbf{J} \times \mathbf{B}$ acts on coronal plasma, which flows inwards at V_{abl}



Balance between magnetic pressure and momentum imparted to coronal plasma at R_0

$$V_{abl} \frac{dm}{dt} = -\frac{\mu_0 I^2}{4\pi R_0}$$

This concept of “ablation velocity” (V_{abl}) illustrates the strong dependence of the ablation rate on current and array radius (V_{abl} varies fairly weakly in most situations)

Ablation rate:

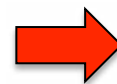
$$\frac{dm}{dt} = -\frac{\mu_0 I^2}{4\pi R_0 V_{abl}}$$

Integration yields the ablated mass as a function of time \rightarrow

$$\delta m(t) = \frac{\mu_0}{4\pi V_{abl} R_0} \int_0^t I^2 dt$$

Assume plasma coasts inwards at V_{abl} .

From the ablation rate equation, $dm/dt = \rho \cdot 2\pi r \cdot V_{abl}$. Take into account time of flight from R_0 to ‘r’ by using $I(t - (R_0 - r)/V_{abl})$

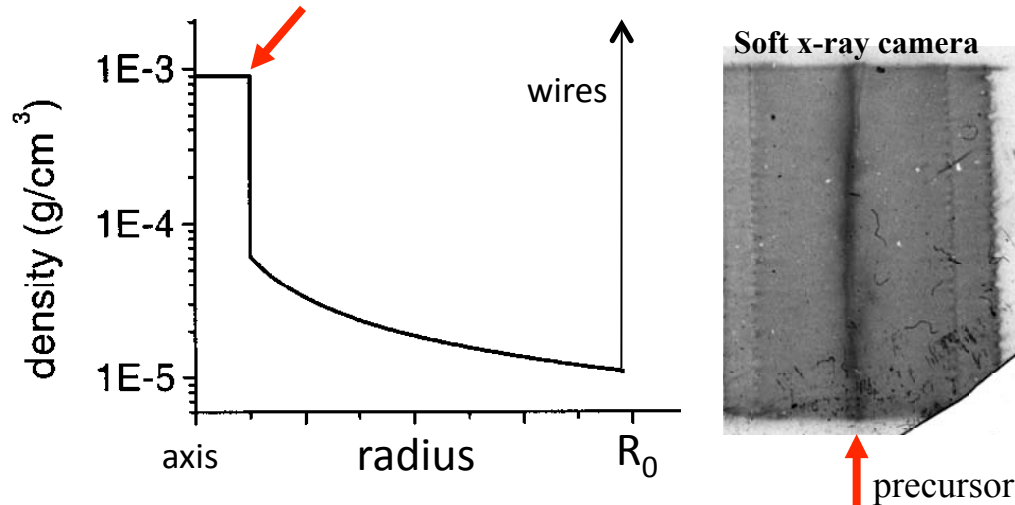


$$\rho(r, t) = \frac{\mu_0}{8\pi^2 R_0 r V_{abl}^2} \cdot \left[I\left(t - \frac{R_0 - r}{V_{abl}}\right) \right]^2$$

Density inside array: precursor plasma column

- From rocket model, can calculate $\rho(r, t)$

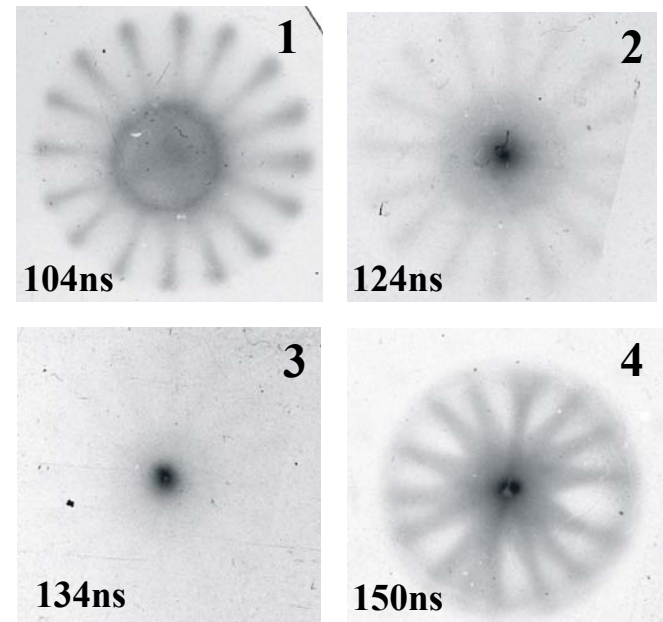
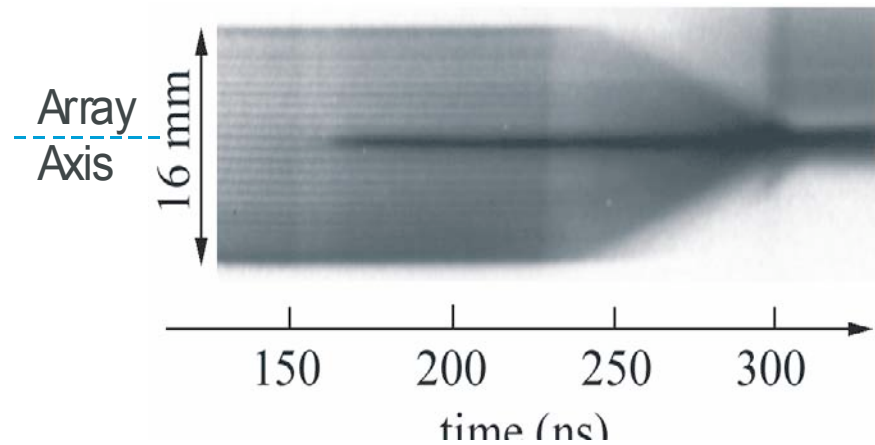
To avoid ∞ on axis, measure precursor diameter, use mass inside diameter/precursor volume to get ρ



Formation of precursor

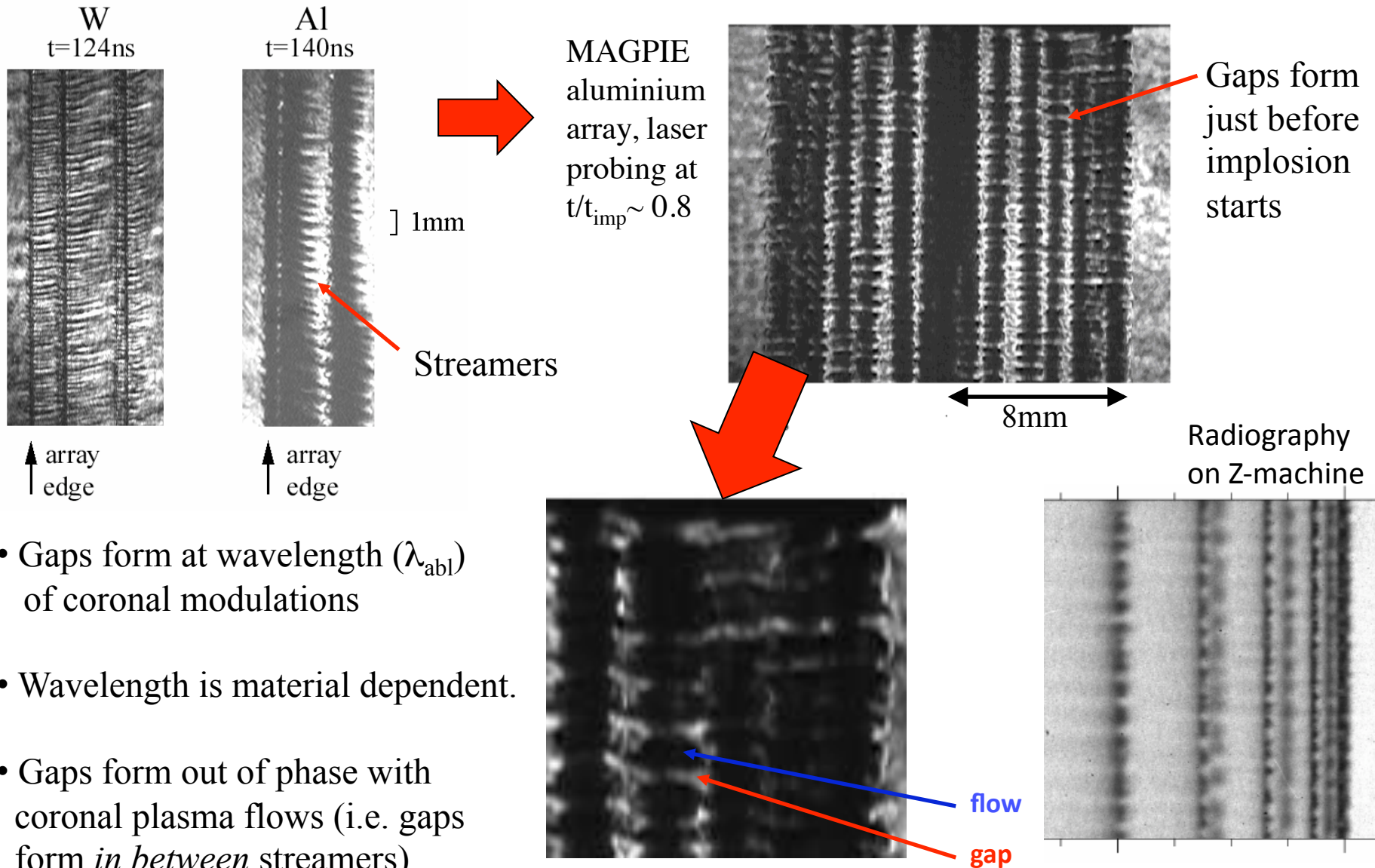
1. Broad initial density profile as streams collide at axis
2. Density increases at axis, until radiation loss rate ($\propto n_{\text{ion}}^2$) is sufficiently high for plasma to cool
3. Rapid collapse to small diameter as plasma compressed by stream kinetic pressure.
4. Column in pressure balance (kinetic vs. thermal), with slow expansion and hollow radiation profile.

- During the ablation phase, a well-defined plasma column forms on the axis



When does ablation stop and implosion begin?

Axial modulation in ablation rate (streamers) results in formation of gaps in cores:

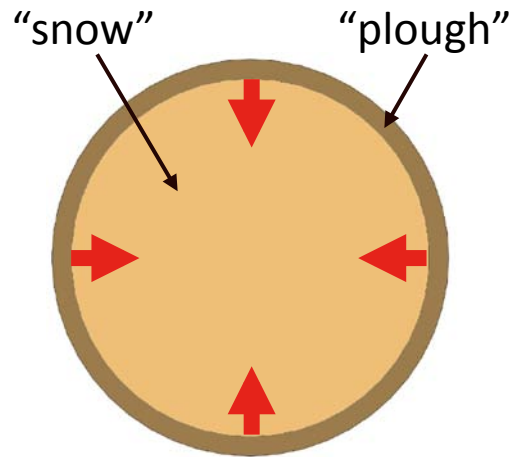


- Gaps form at wavelength (λ_{abl}) of coronal modulations
- Wavelength is material dependent.
- Gaps form out of phase with coronal plasma flows (i.e. gaps form *in between* streamers)

S. V. Lebedev, Las. Part. Beams 19, 355 (2001)

D. B. Sinars, PoP 12, 056303 (2005)

Formation of gaps triggers “snowplough” implosion



The implosion gathers up the previously ablated mass (snowplough)

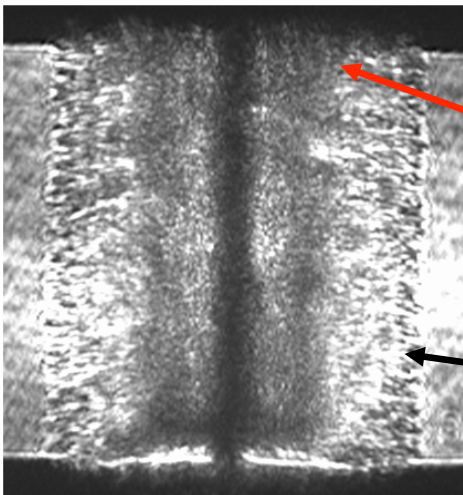
Inelastic accretion



heating and emission

Side-on laser probing, $t/t_{\text{imp}}=0.93$

224ns



32 wire W experiments.

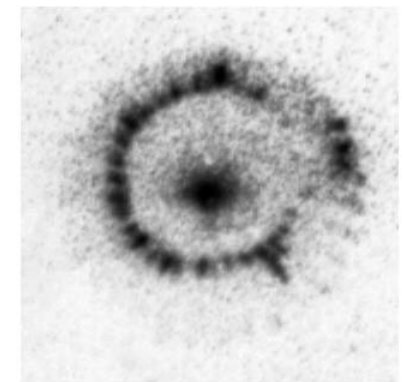
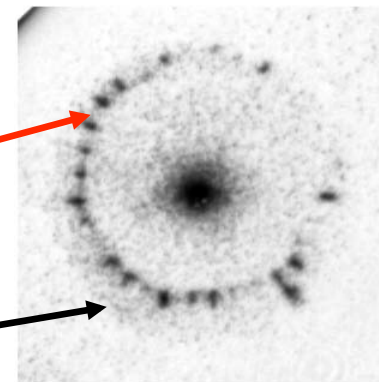
Imploding “piston” of current “snowploughs” mass inside the array ablated from the wires

Mass left behind by snowplough

End-on soft-x-ray imaging

$t/t_{\text{imp}}=0.90$

$t/t_{\text{imp}}=0.93$



X-ray images (>190eV)

s0909

The rocket model and implosion dynamics

Can use rocket model to calculate how much mass has ablated when the implosion starts:

Ablated mass fraction

$$\frac{\delta m(t)}{m_0} = \frac{\mu_0}{4\pi V_{abl} R_0 m_0} \int_0^t I^2 dt = 40 - 50\% \text{ of array mass}$$



The rocket model is then used to calculate the pre-fill density profile:

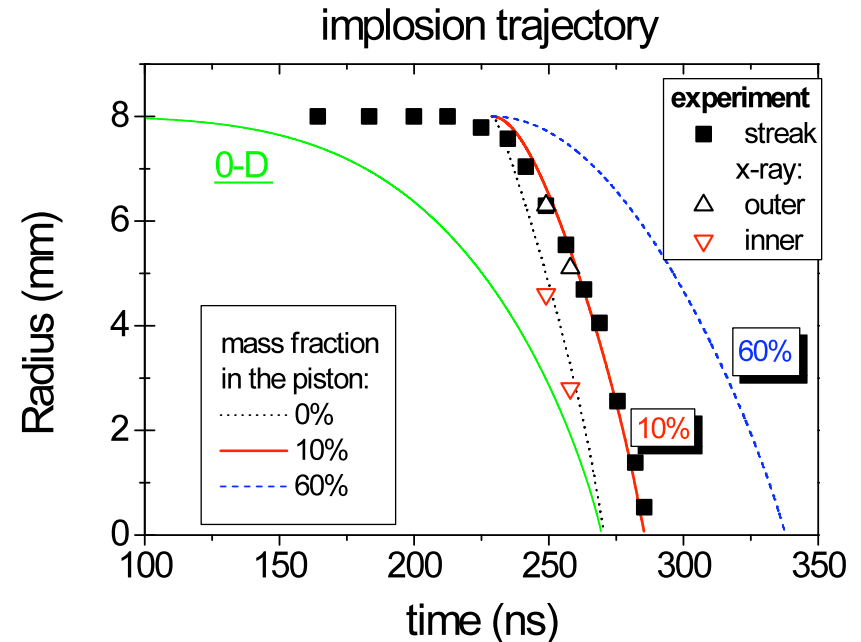
$$\rho(r, t) = \frac{\mu_0}{8\pi^2 R_0 r V_{abl}^2} \cdot \left[I \left(t - \frac{R_0 - r}{V_{abl}} \right) \right]^2$$



By varying the initial mass of the imploding “piston” (i.e. the amount of mass driven inwards from R_0 just as the implosion starts) an implosion trajectory is calculated to fit the observations.

S. V. Lebedev, PoP 9, 5 (2002)

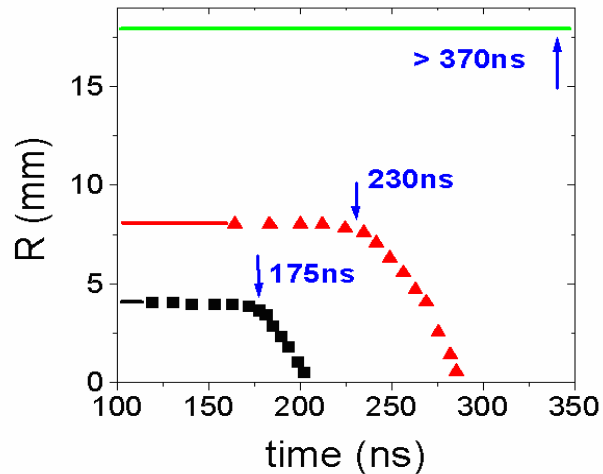
32 x 15 μ m Al array on MAGPIE



- Piston starts as 10-20% array mass
- 40-50% mass pre-fills the array
- Up to 50% of the array mass is left behind as “trailing mass”.

Inferring ablation velocity using the rocket model

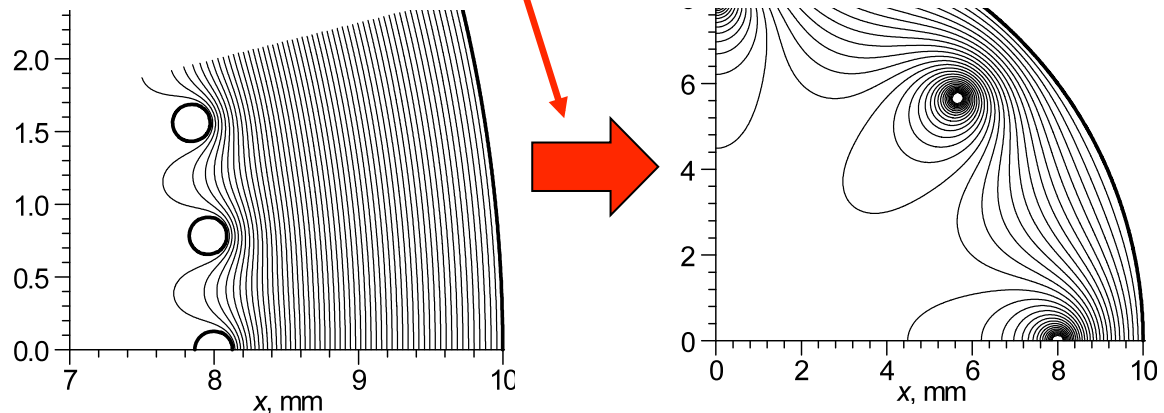
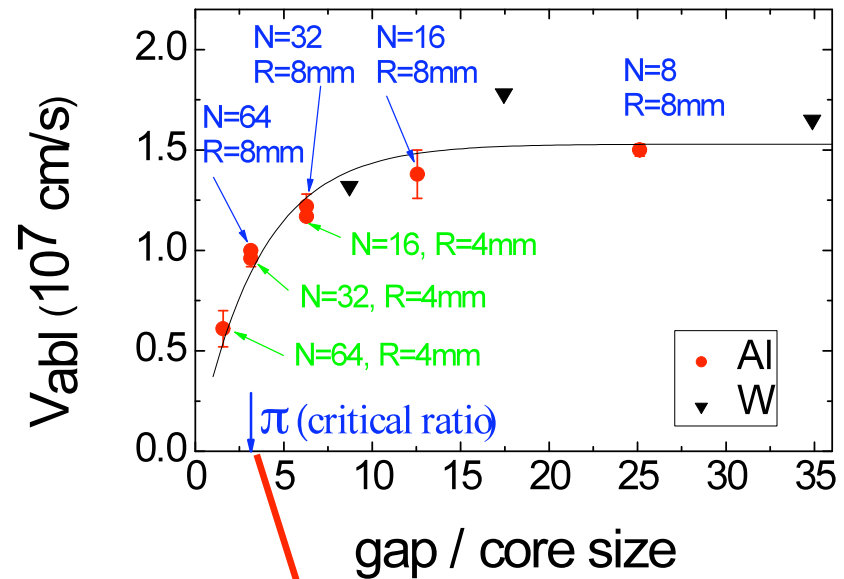
Measure implosion times for different wire number/array radii and use rocket model to infer the ablation velocity.



$$\frac{\delta m(t)}{m_0} = \frac{\mu_0}{4\pi V_{abl} R_0 m_0} \int_0^t I^2 dt$$

The magnetic field topology changes from local-dominated to global-dominated below critical gap/core ratio

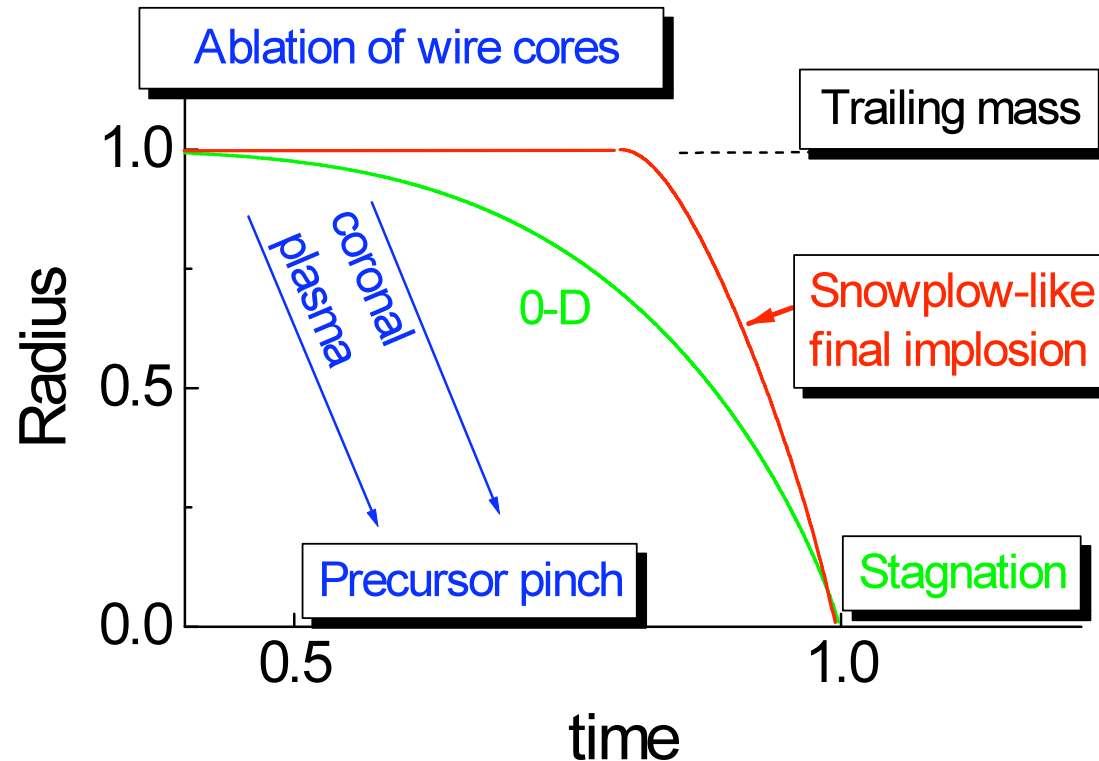
Rapid decrease of V_{abl} below “critical” gap/core size. Gap = distance between the wires, core = diameter of core/corona structure



Basic picture of a wire array implosion

Two-stage implosion dynamics

- Extended period of ablation, radial redistribution of mass
- Snowplough-like implosion phase, stabilised by peaked on-axis density profile



What does the implosion structure look like?

Implosion dynamics and X-ray production from wire arrays

Wire array implosions are unstable to Rayleigh Taylor

- Rayleigh Taylor instability occurs when a light fluid is used to accelerate/support a heavy fluid: this is an unstable equilibrium
- A small perturbation to a flat interface is amplified, leading to the classic “bubble and spike” structure

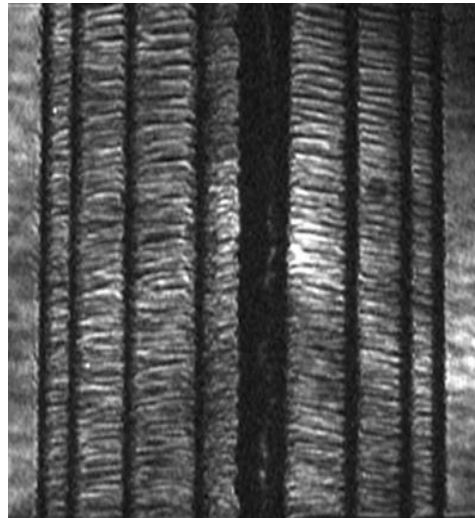


- In a wire array implosion, the plasma (heavy fluid) is accelerated by the light fluid (massless magnetic field) and goes RT unstable
- **What creates the perturbations?**

Wire breakage seeds RT instability

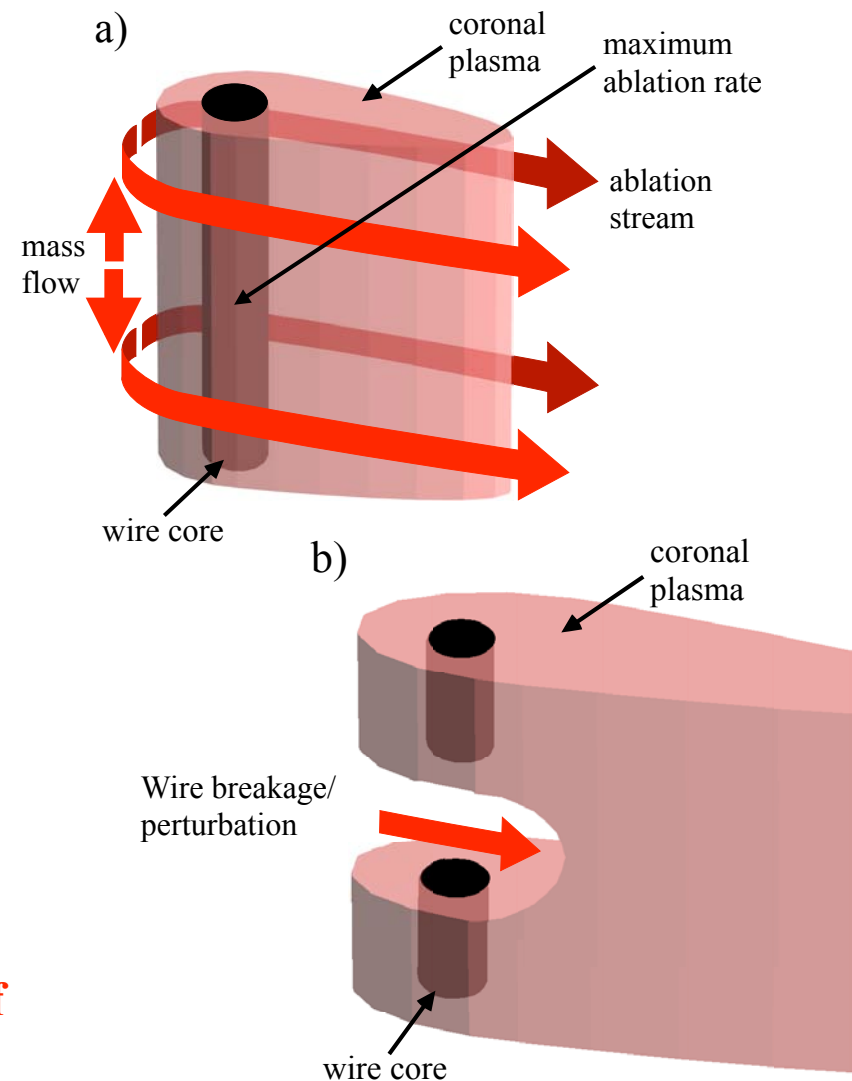
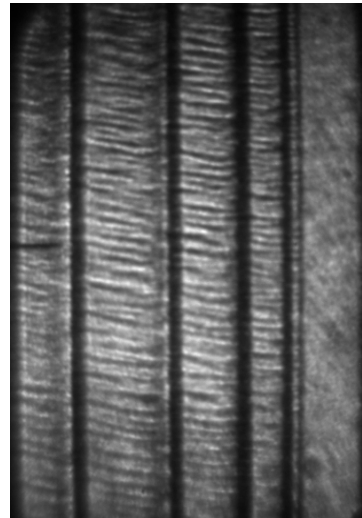
- The wire cores are ablated at the same wavelength as the ablation streams, λ_{abl} .
- Implosion triggered as wire cores develop gaps, allowing implosion to break through.

Laser probing on
MAGPIE (1MA)



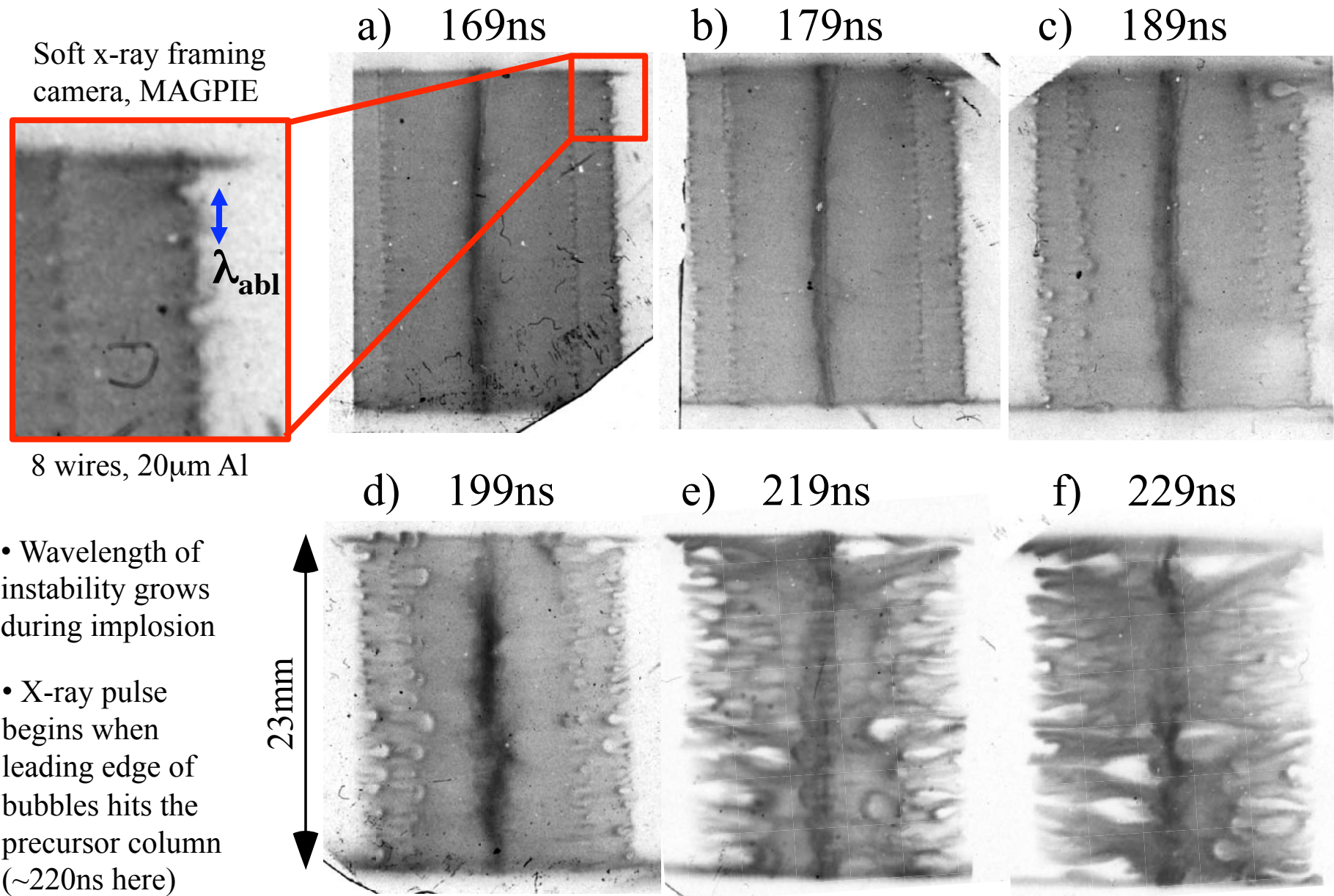
16mm

Z-machine,
20MA



- Wavelength is dependent only on material
- Ablation streams are ubiquitous to wire arrays, and process is the same for 1-20MA.
- **This process is responsible for the seeding of RT instabilities at start of implosion.**

Rayleigh Taylor growth during implosion

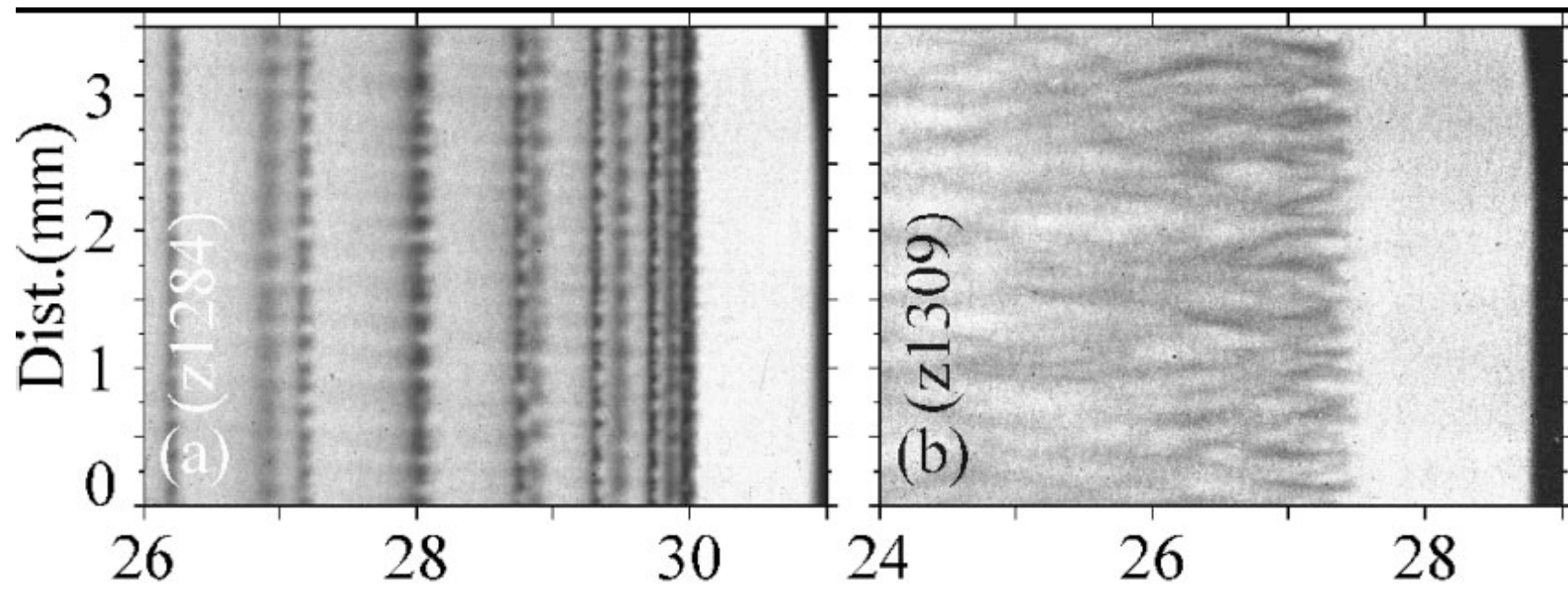


Wire breakage seeds RT instability: same at 20MA

Same process occurs at all current levels...

- The wire cores are ablated at the same wavelength as the ablation streams, λ_{abl} .
- RT instability is seeded from the gaps that develop in the wire cores.

Radiograph of 30mm Tungsten array on Z-machine



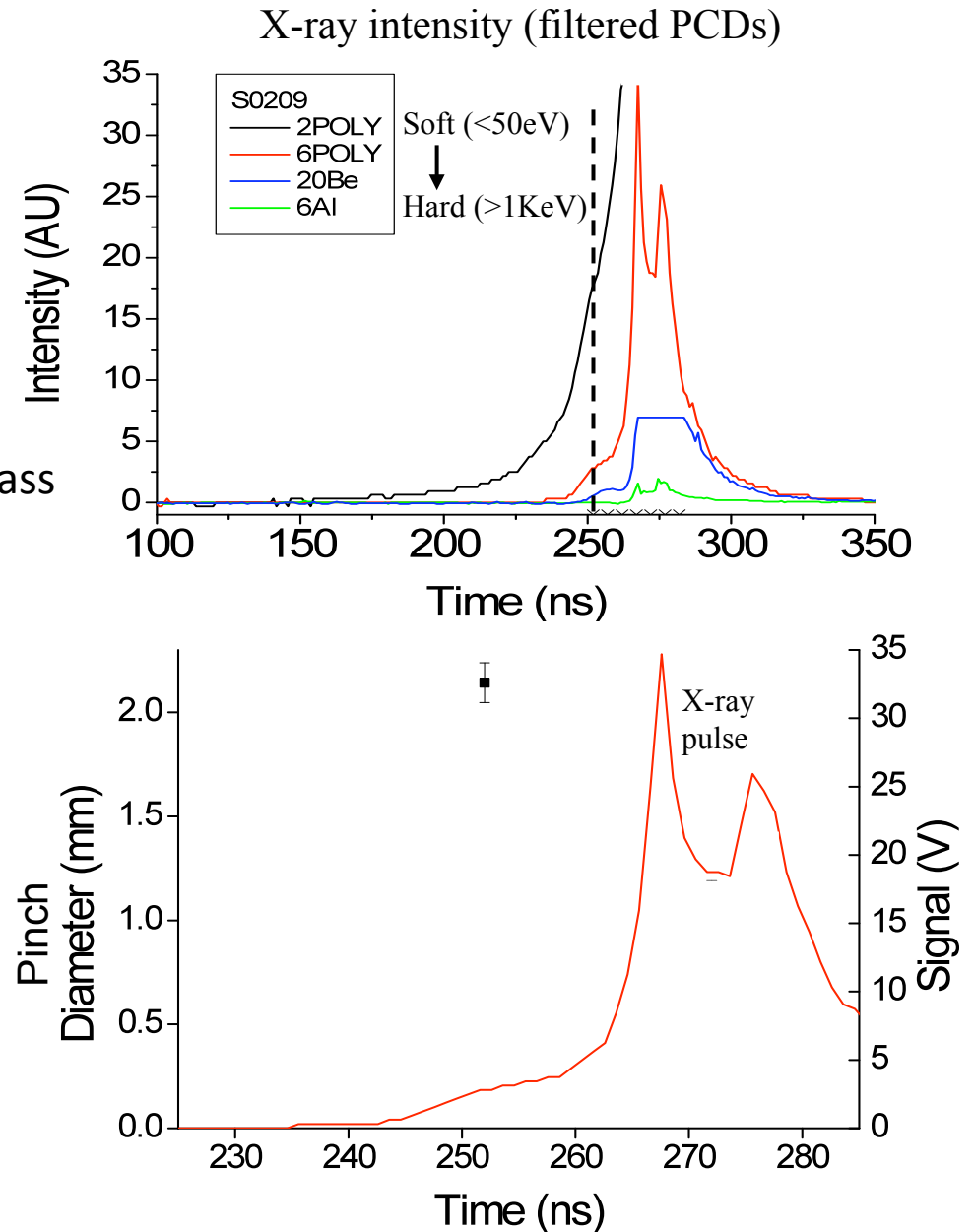
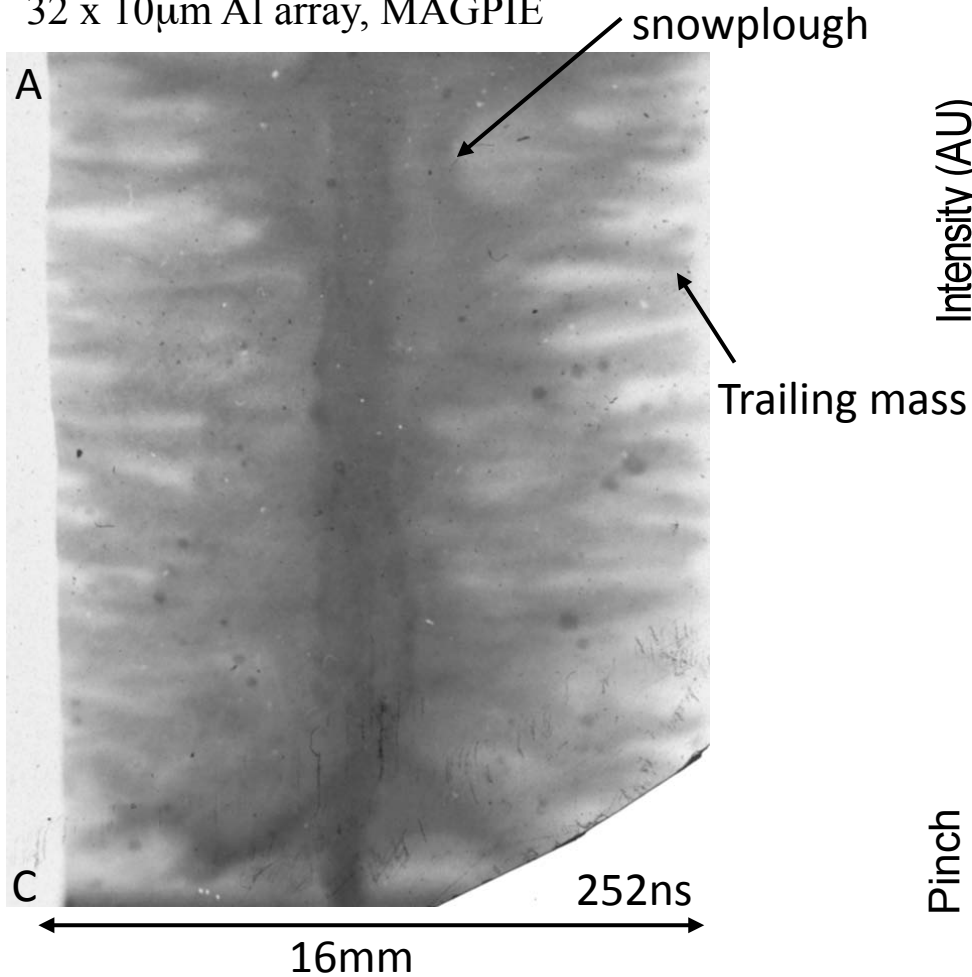
D. B. Sinars, PoP 12, 056303 (2005)

Ablation determines everything!

Implosion dynamics, pinch structure, X-ray power and pulse shape, are all strongly dependent on the seeding of the RT instability.

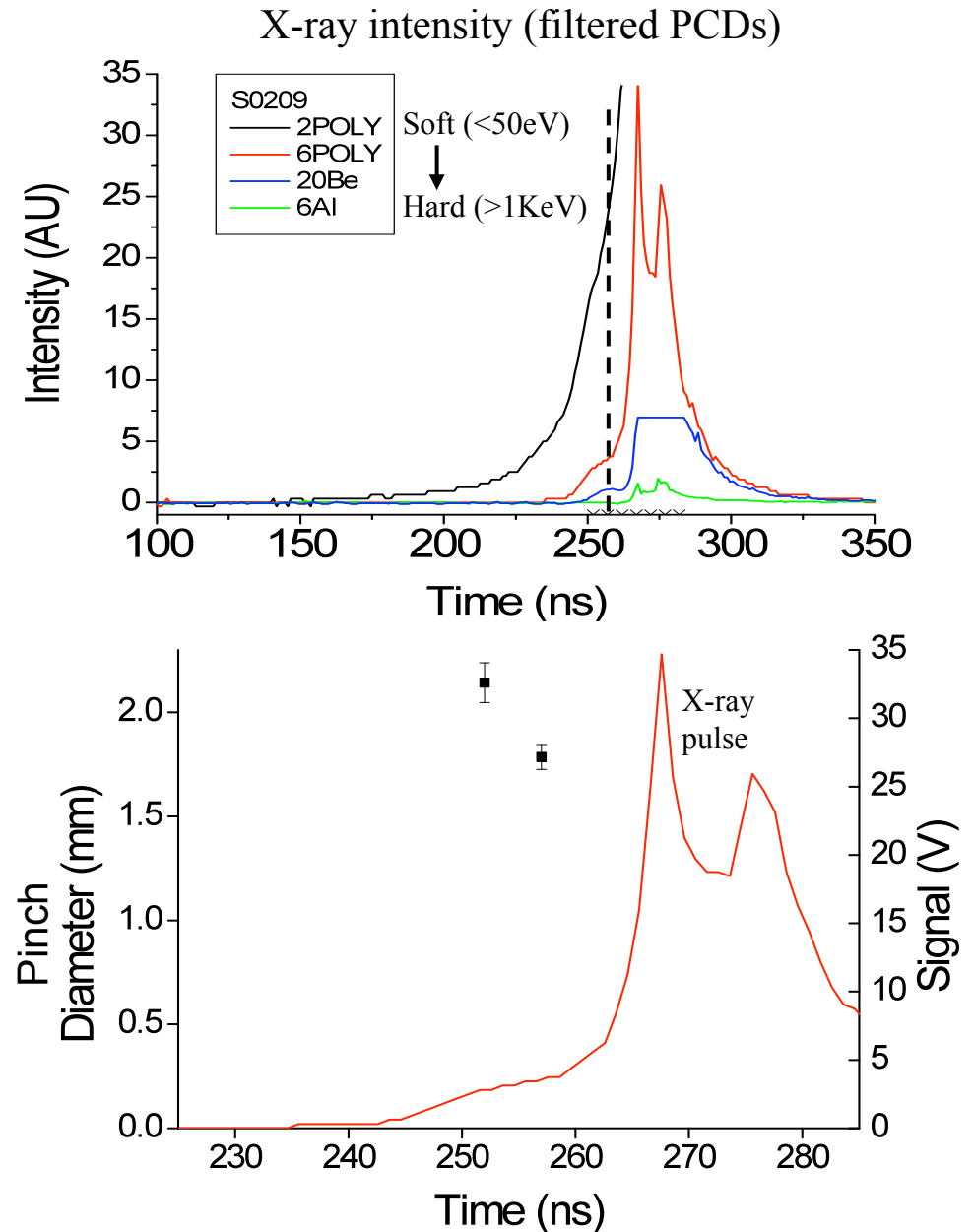
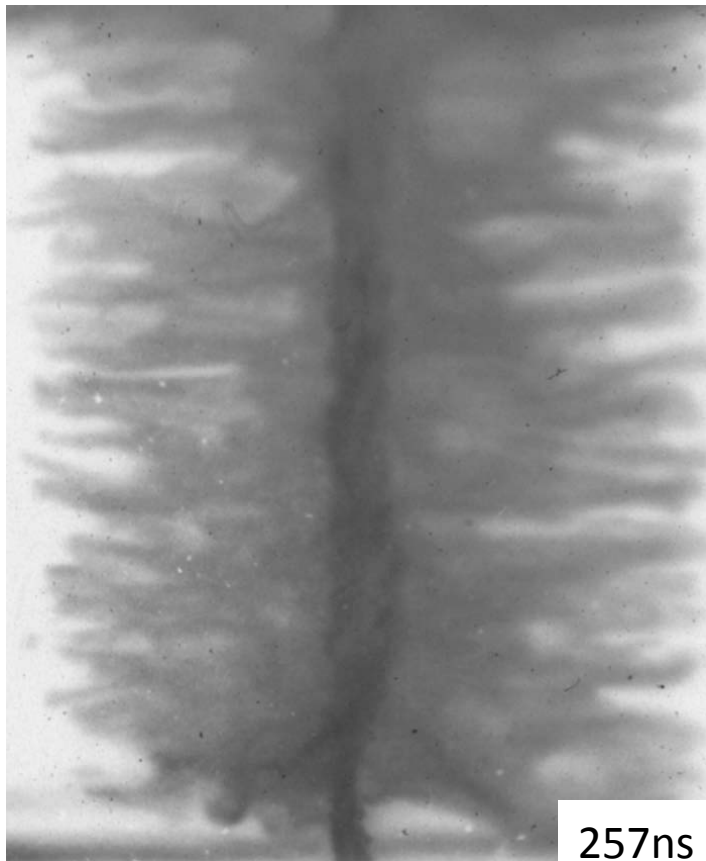
Implosion dynamics and X-ray production

Soft x-ray framing camera ($>36\text{eV}$)
32 x 10 μm Al array, MAGPIE



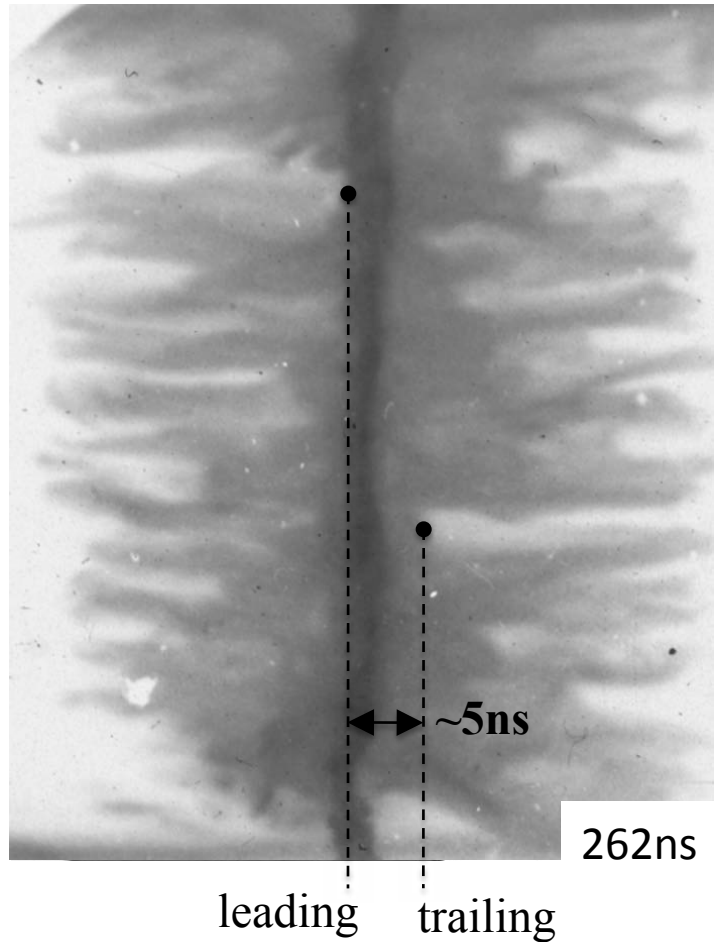
Implosion dynamics and X-ray production

Soft x-ray framing camera ($>36\text{eV}$)
32 x 10 μm Al array, MAGPIE

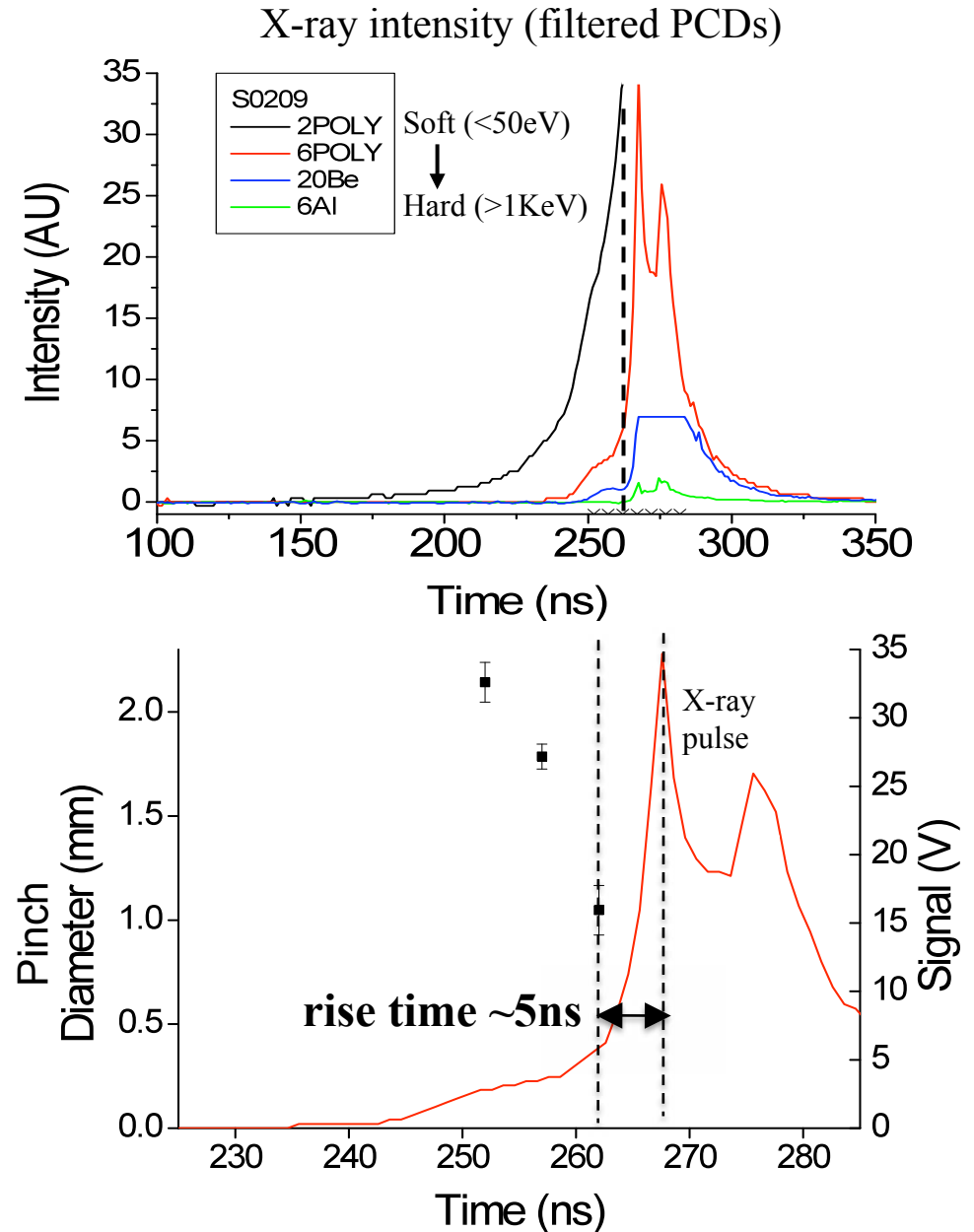


Implosion dynamics and X-ray production

Soft x-ray framing camera ($>36\text{eV}$)
32 x 10 μm Al array, MAGPIE

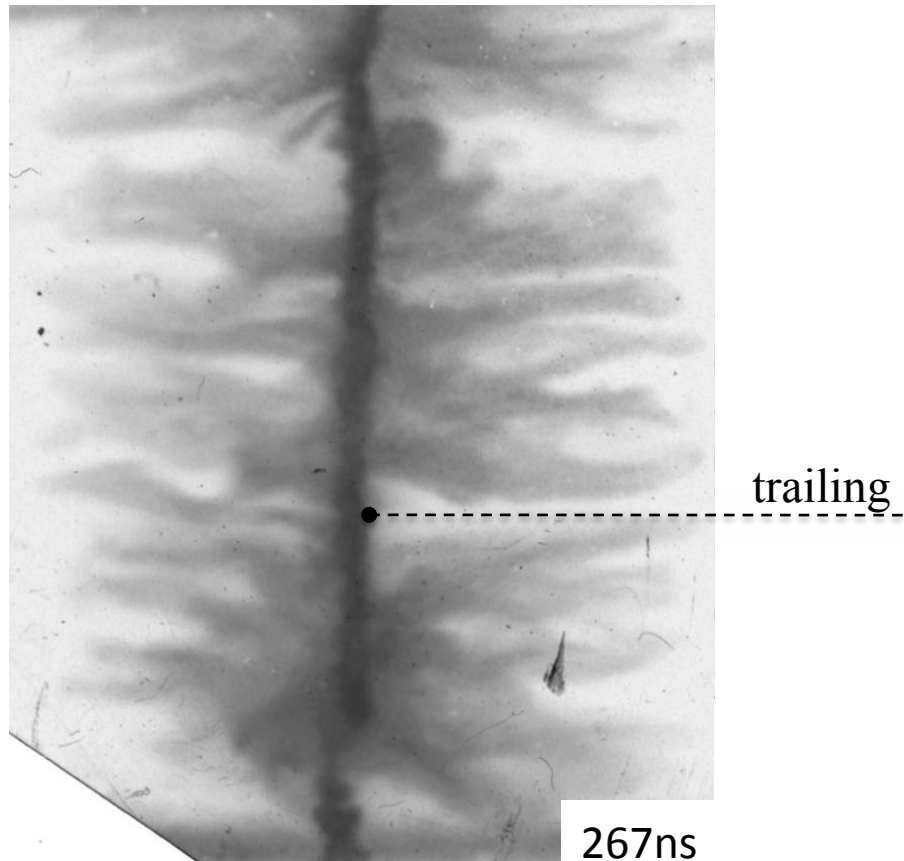


Temporal spread of the piston (grows during implosion) determines rise time of pulse

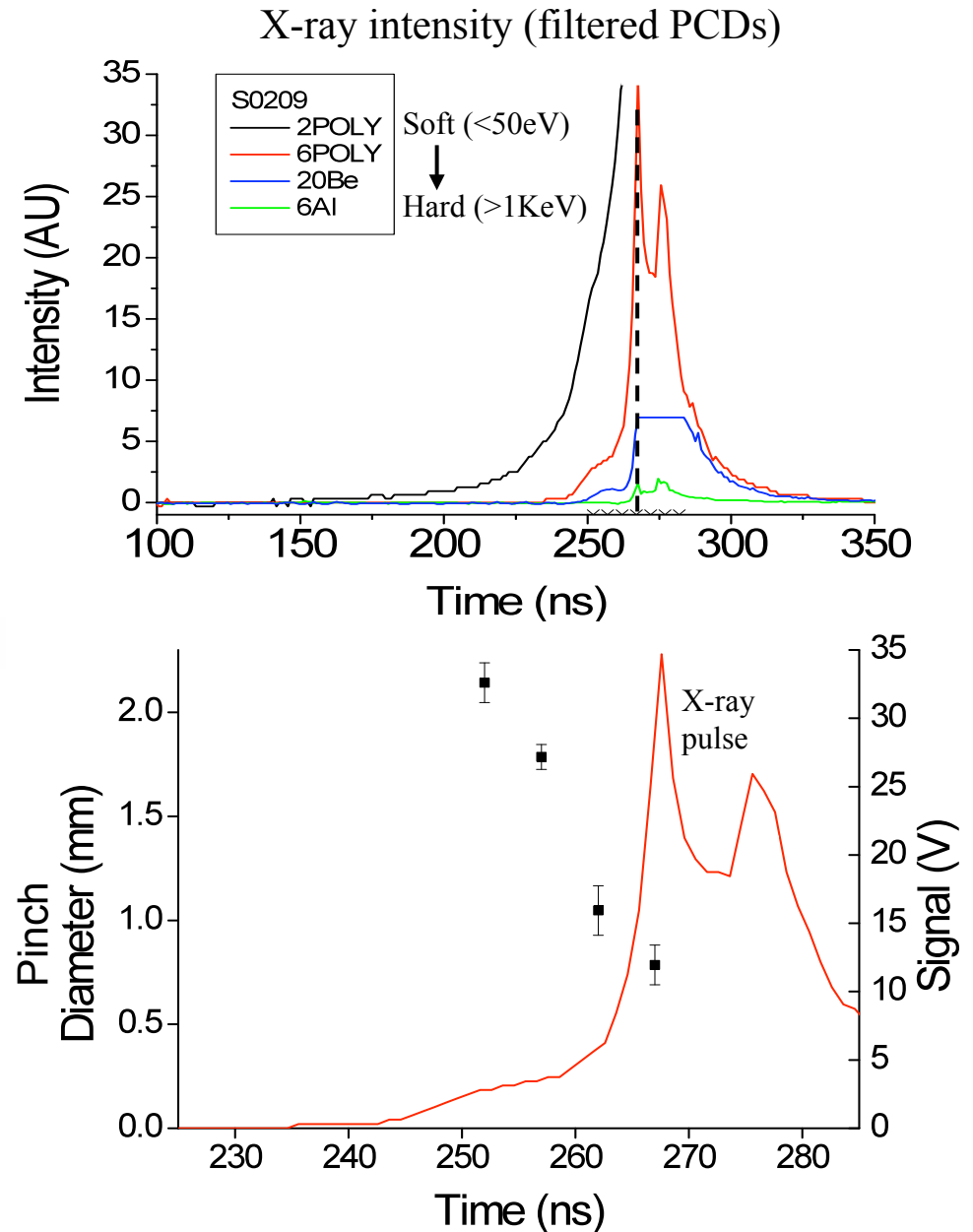


Implosion dynamics and X-ray production

Soft x-ray framing camera ($>36\text{eV}$)
 32 x 10 μm Al array, MAGPIE

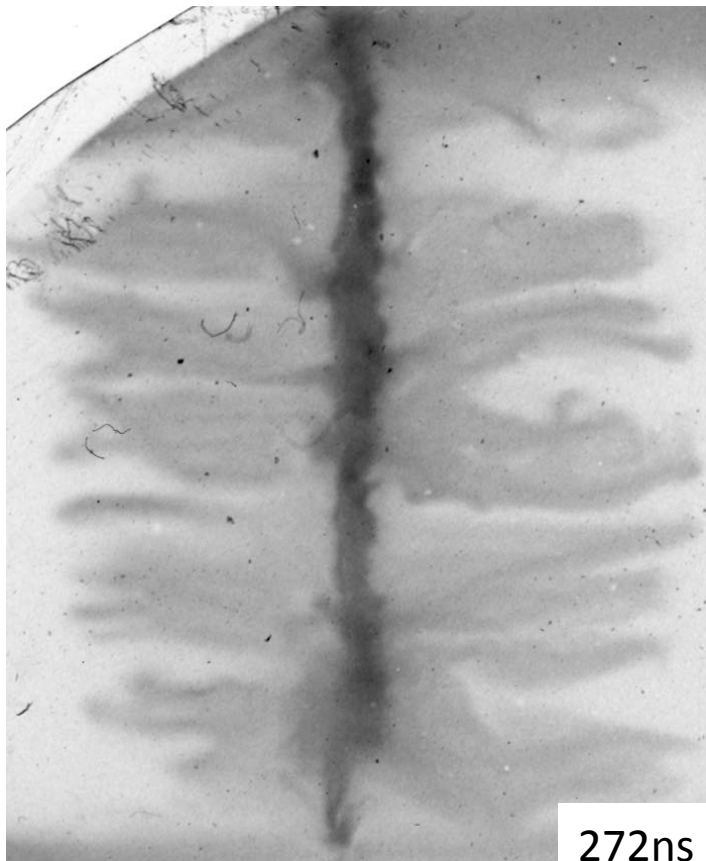


- Peak X-rays correspond to minimum pinch radius
- Trailing mass continues to implode, indicating presence of current

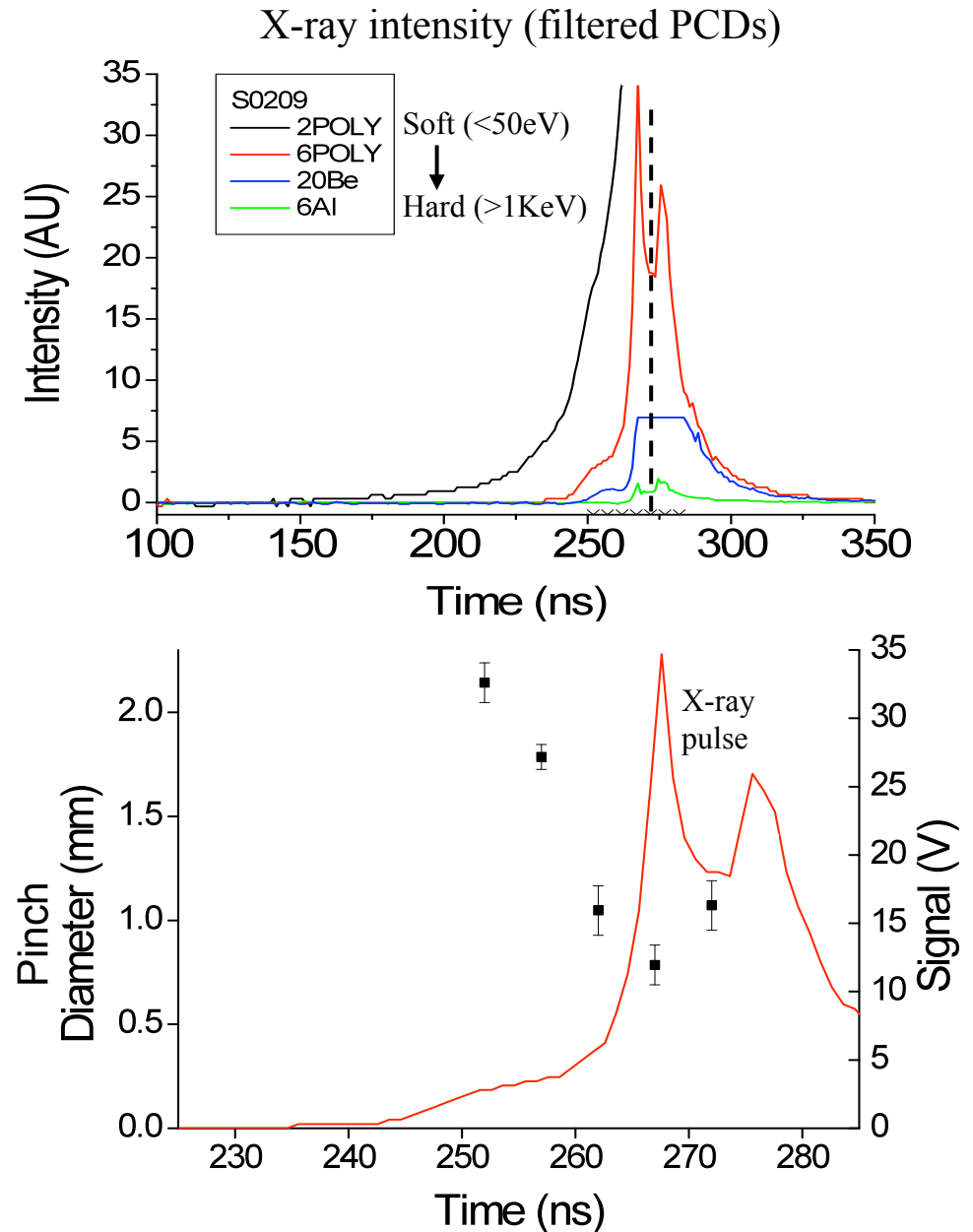


Implosion dynamics and X-ray production

Soft x-ray framing camera ($>36\text{eV}$)
32 x 10 μm Al array, MAGPIE



- After peak X-ray pulse / compression, pinch column begins to go unstable (MHD instabilities)

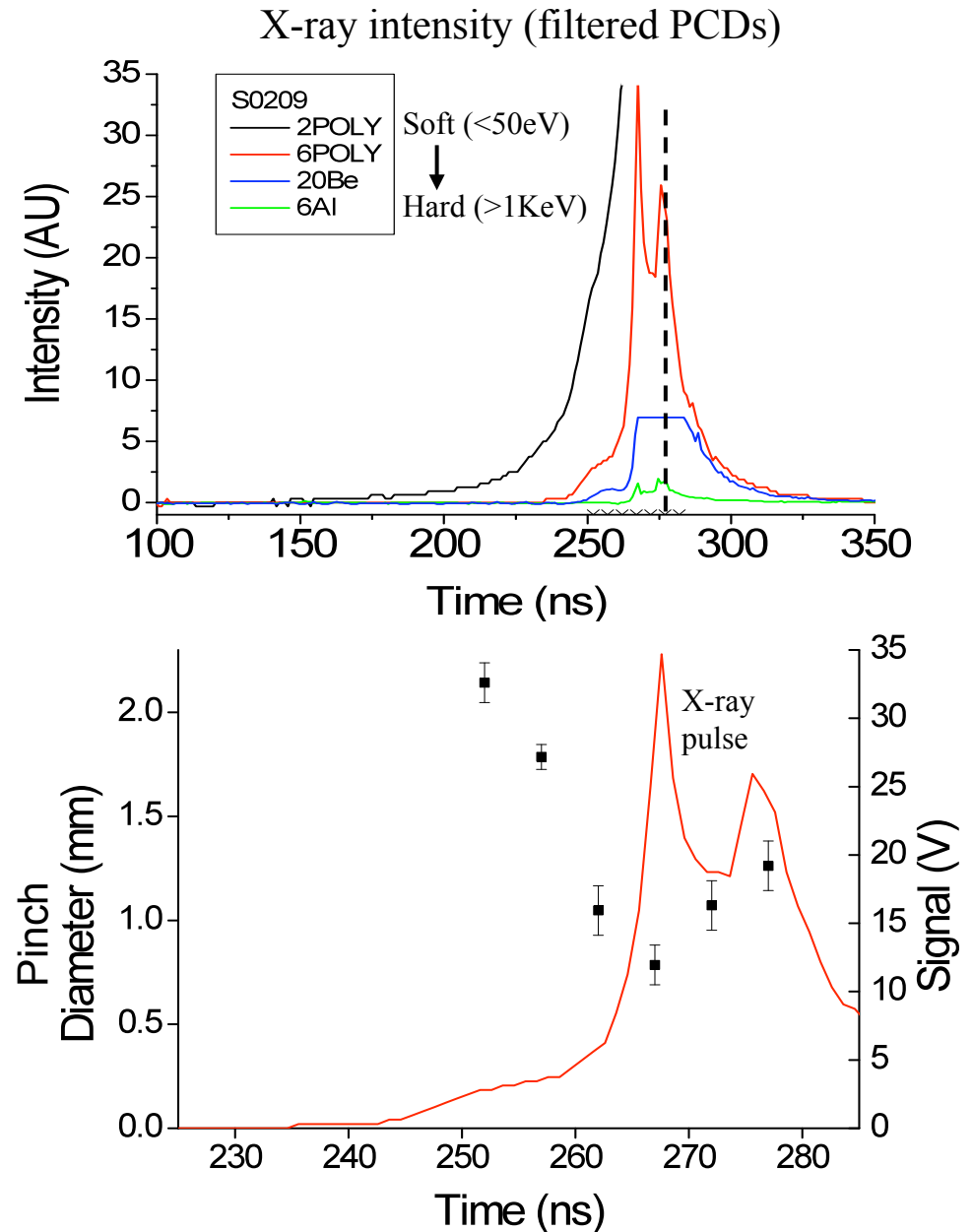


Implosion dynamics and X-ray production

Soft x-ray framing camera ($>36\text{eV}$)
32 x 10 μm Al array, MAGPIE

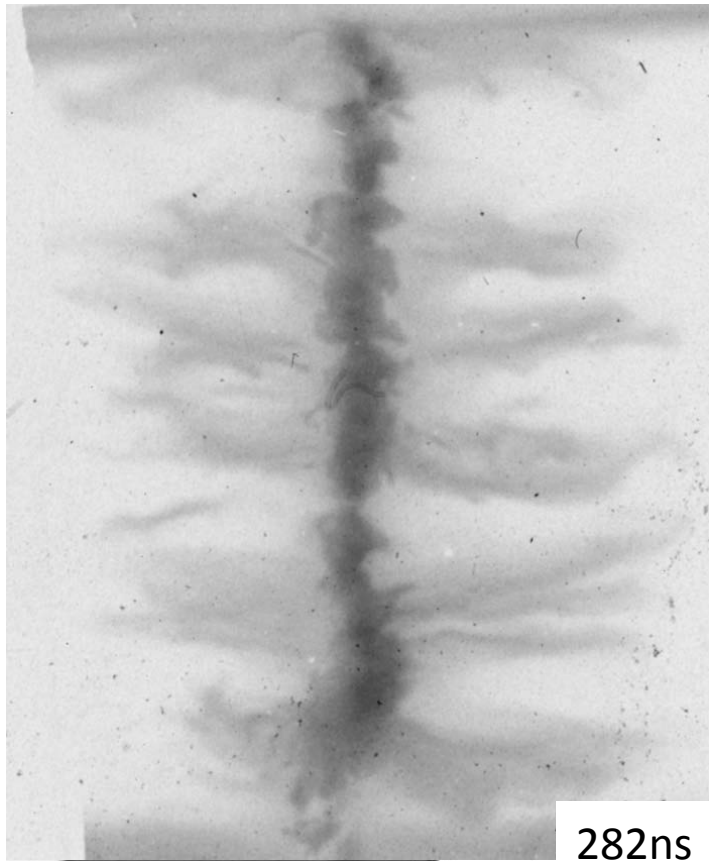


- Bright spots correspond to regions of “cleared out” trailing mass (secondary implosions / x-ray peaks)

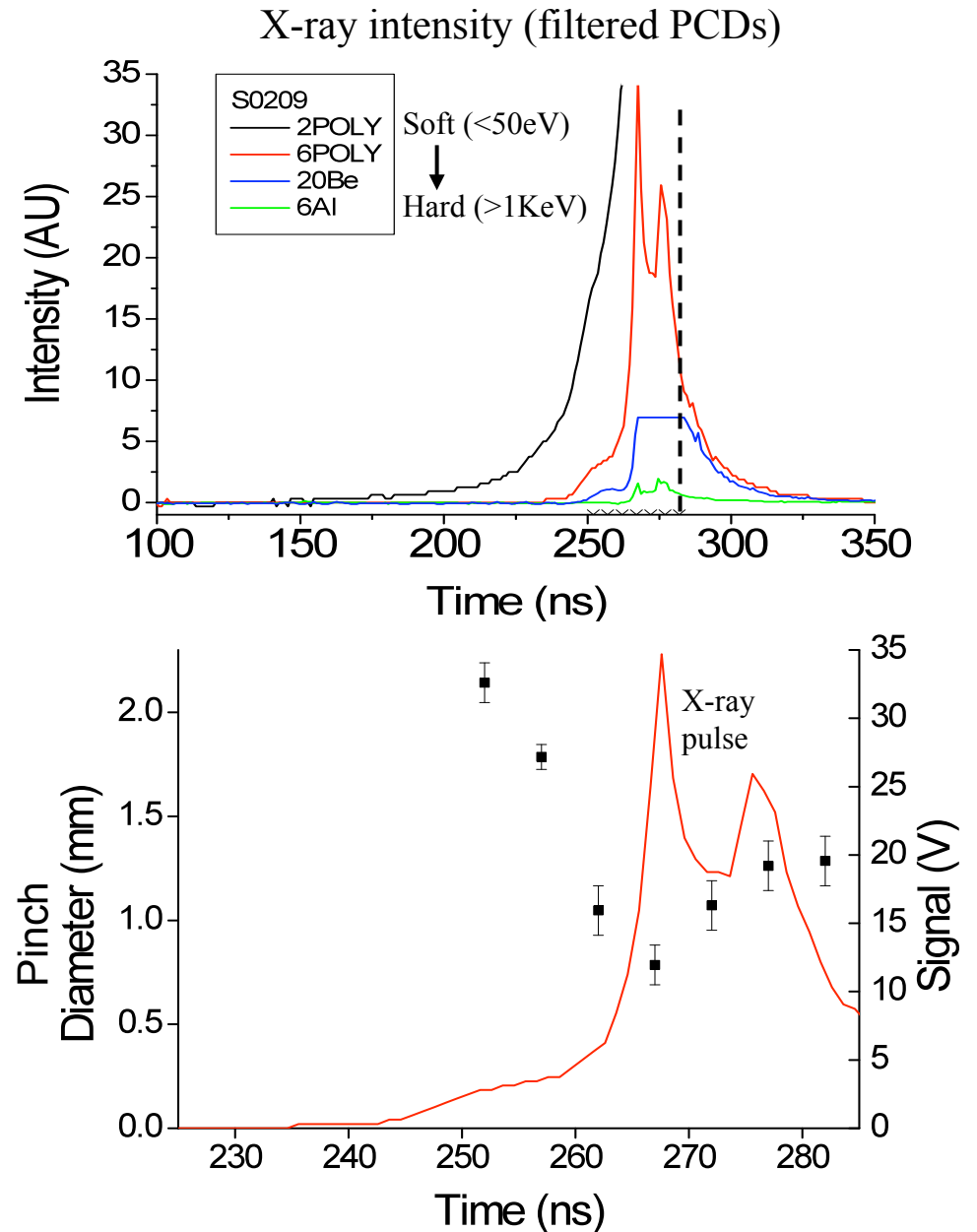


Implosion dynamics and X-ray production

Soft x-ray framing camera ($>36\text{eV}$)
32 x 10 μm Al array, MAGPIE



- Pinch breaks up



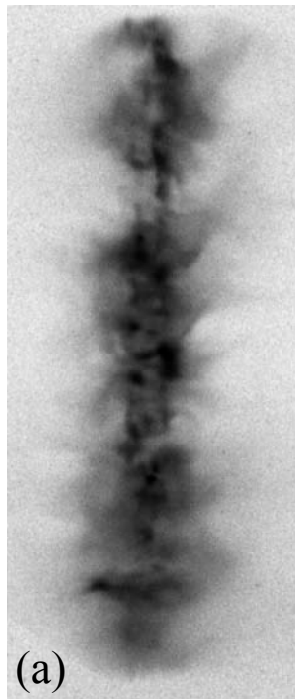
Stagnated pinch structure

- Pinches show significant amount of structure in the x-ray region of the spectrum
- Many small scale features and instabilities are visible: can use x-ray pinhole cameras to image pinch structure

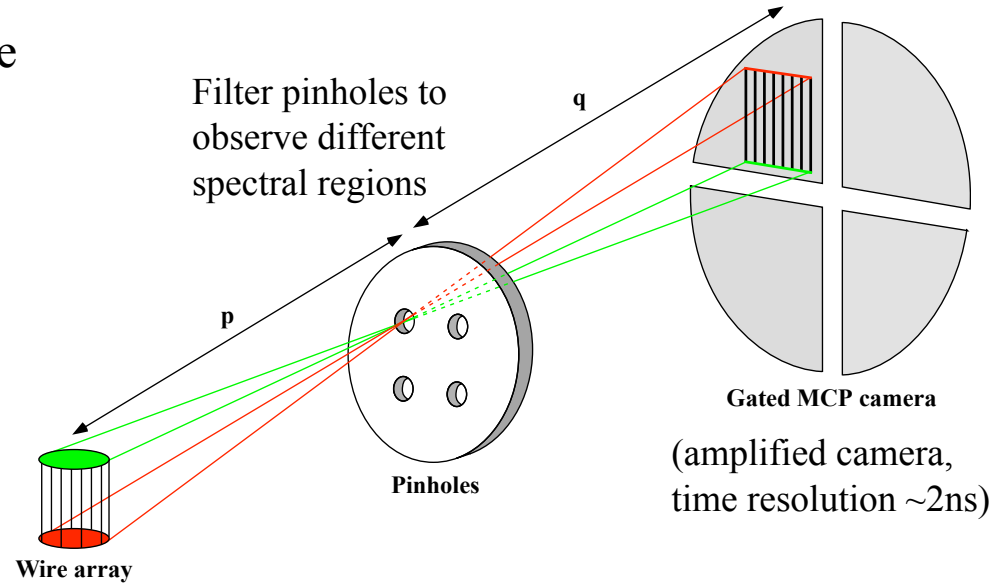
Wire array pinches on MAGPIE

Time integrated Al pinch (6 μ m Al filter)

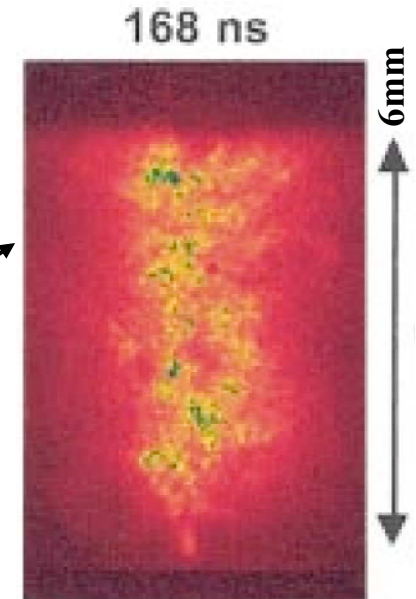
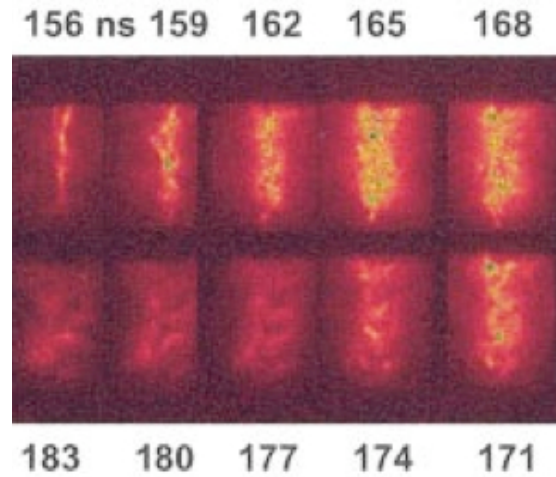
Time resolved Al pinch (7 μ m Be filter)



23mm



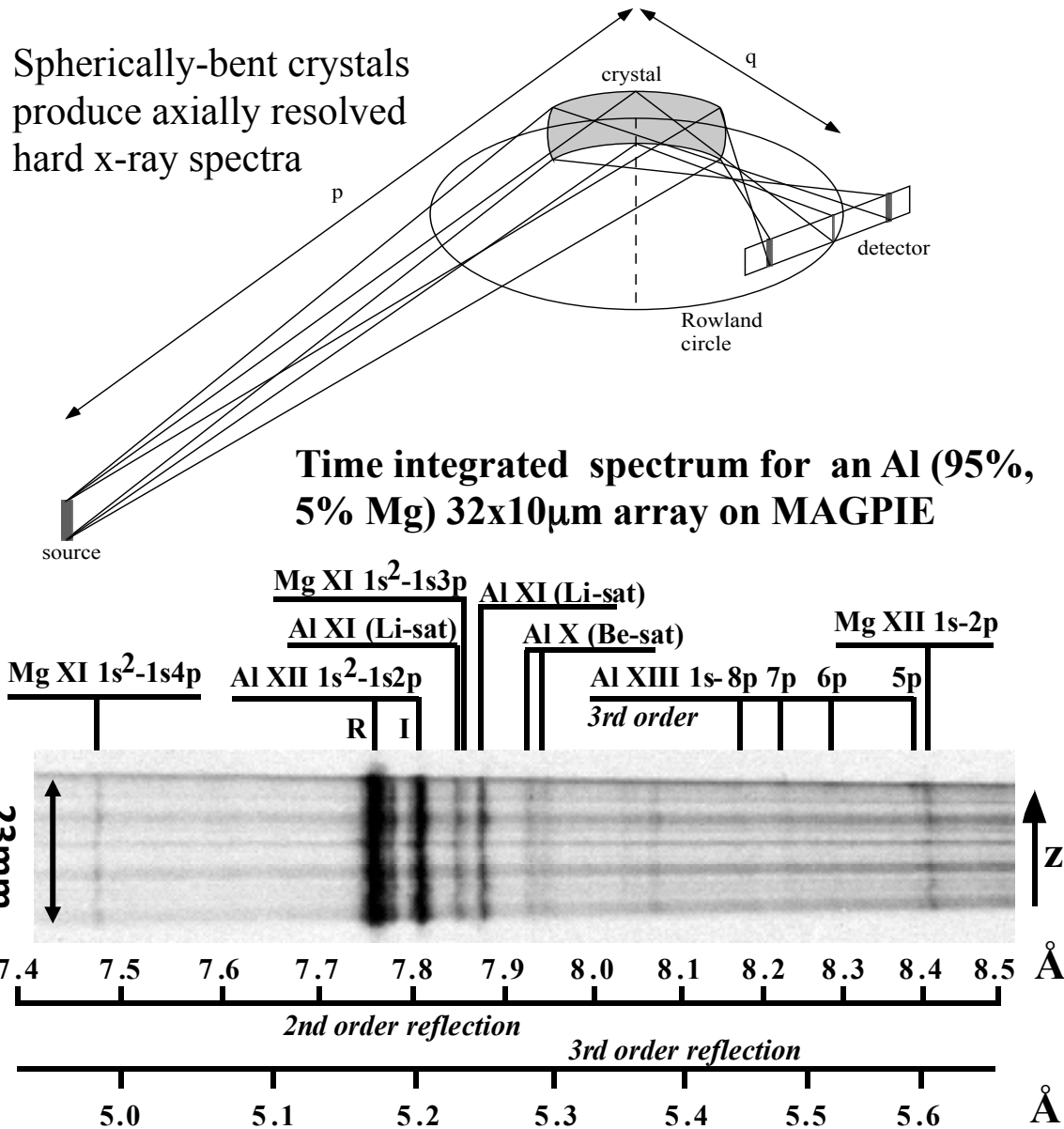
K-shell images of Al pinch on Saturn (7MA)



J. P. Apruzese, PoP 8, 3799 (2001)

G. N. Hall, PoP 13, 082701 (2006)

Pinches produce K-shell X-ray radiation

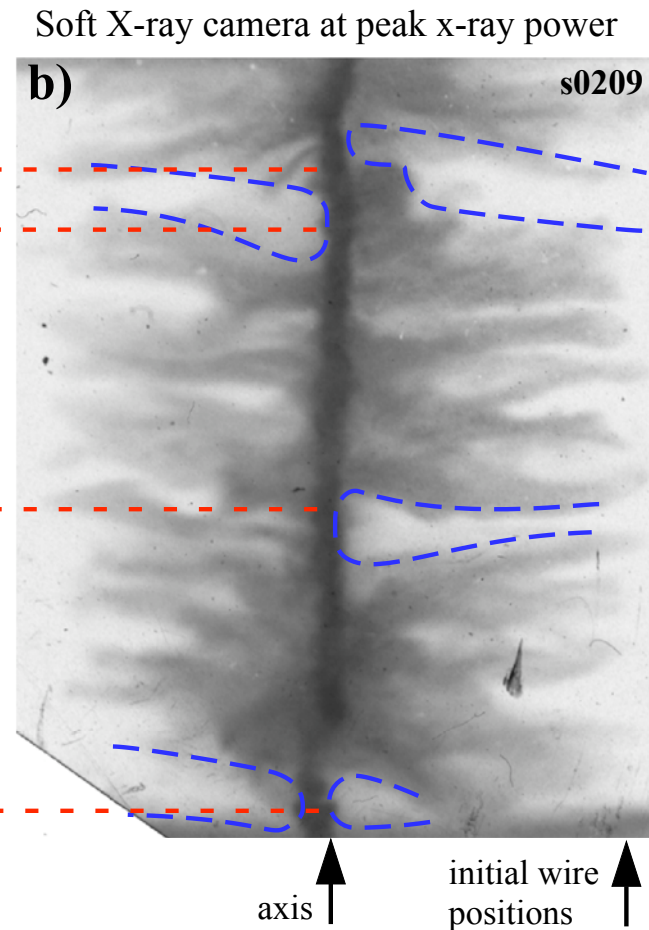
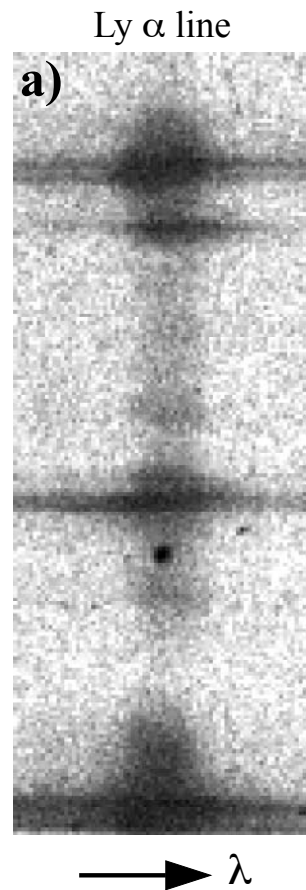
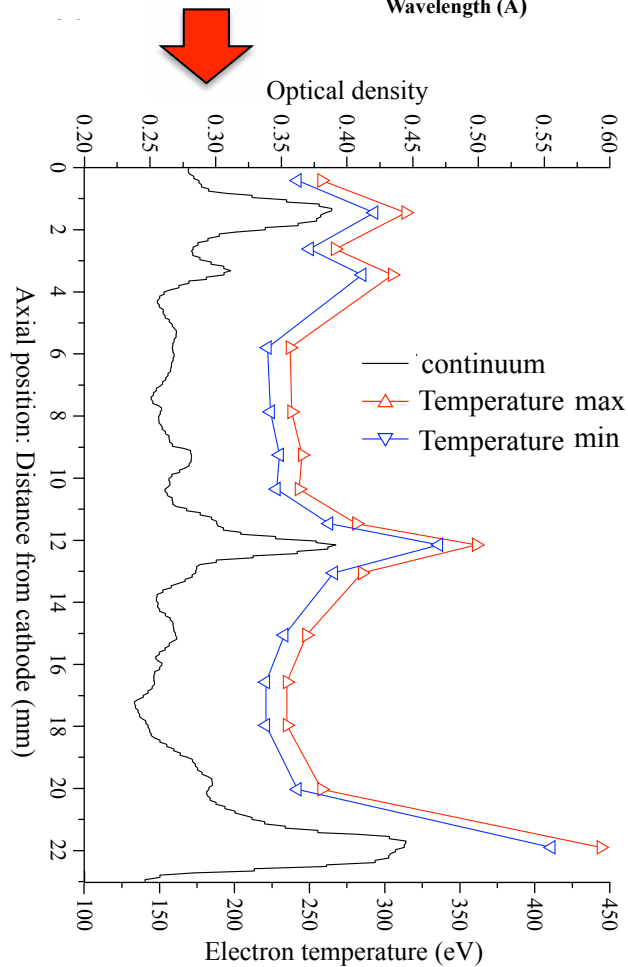
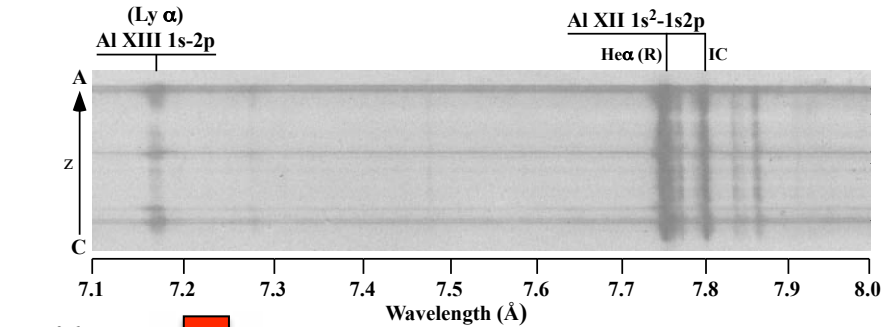


G. N. Hall, PoP 13, 082701 (2006)

- K-shell = radiation from hydrogen and helium-like ions (1-2 electrons left)
- Large machines (Z, Saturn) can perform efficient K-shell production (need large kinetic energy per ion to produce large population of H-like and He-like ions)
- Use low-medium Z elements to get good K-shell yield (aluminium, stainless steel, copper on Z-machine)
- Smaller machines cannot produce K-shell radiation efficiently, but can use it as a diagnostic to get temperature, density, etc.
- K-shell radiation is not produced uniformly along the pinch: bright spots (continuum radiation, more radiation from H-like lines) occur.
- K-shell spectra can relate implosion dynamics to pinch characteristics.

K-shell as a diagnostic for implosion/stagnation

- Compare experimentally measured line ratios (here, Ly α to He- α) to models to estimate temperature, density.
- Can tell you a lot about how dynamics affect pinch conditions. Here, RT bubbles = hot spots = less trailing current (more on axis) at these positions?

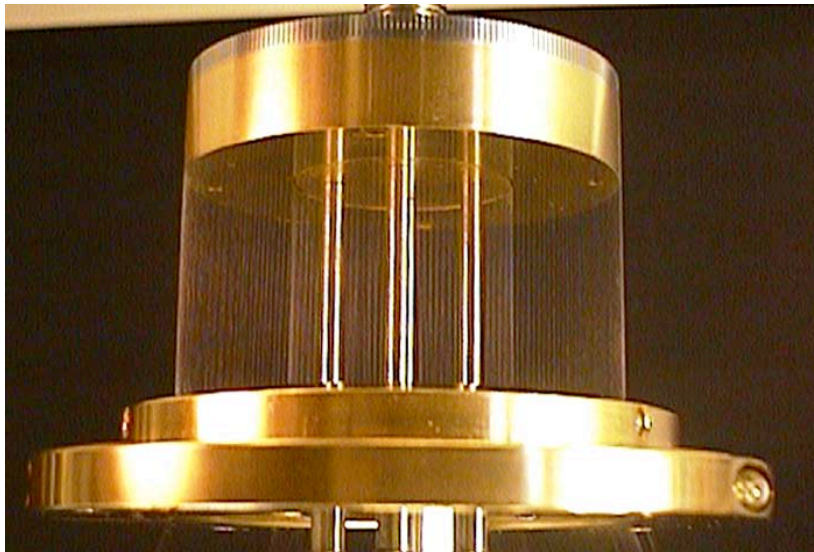


Developments in wire array technology

Control RT growth = control the pulse shape

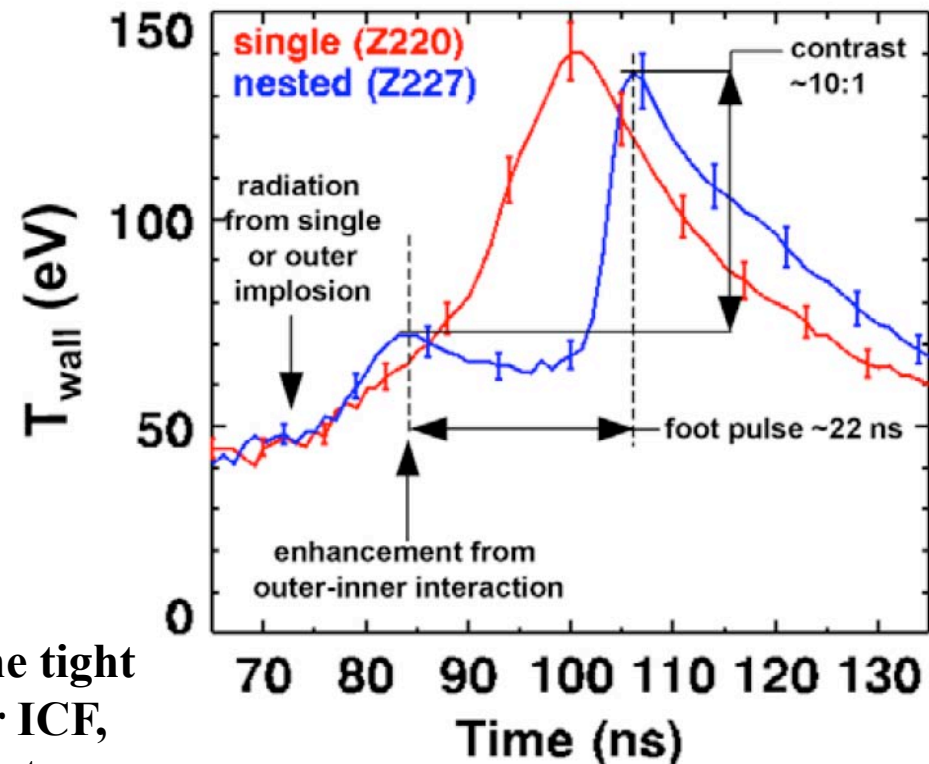
- The temporal width of the implosion (i.e. time between leading and trailing edge hitting the axis) sets the rise time / shape of the X-ray pulse.
- Temporal width set by growth of RT instability: controlling RT growth gives pulse shaping
- Use nested array: interaction of outer array with inner should “reset” the RT growth and decrease the rise time of the main X-ray pulse.

Z-machine “nested” wire array = 2 concentric arrays



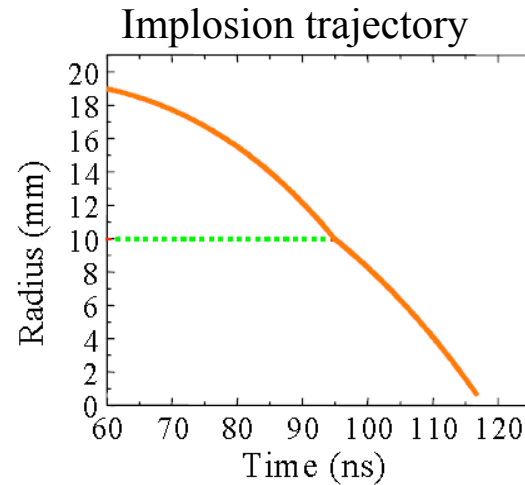
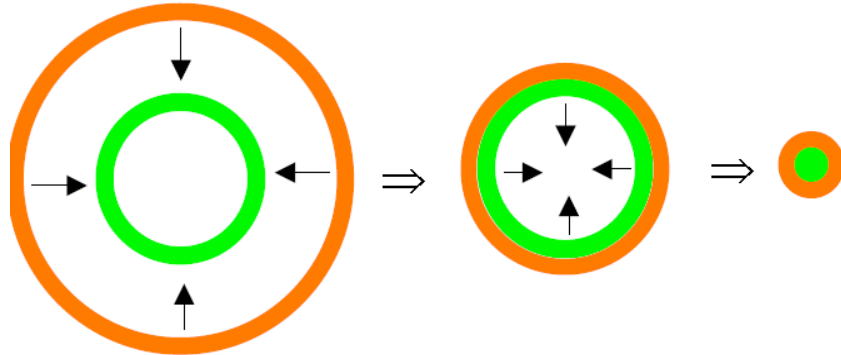
The idea obviously works, but to achieve the tight constraints of timing and pulse contrast for ICF, we need to know how the two arrays interact...

Hohlraum driven by nested array on Z-machine



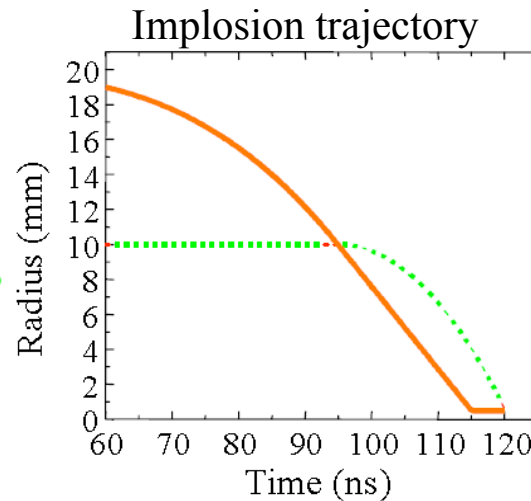
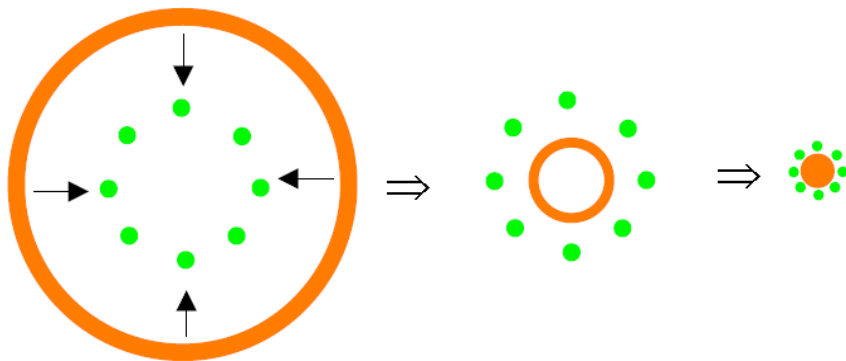
Two possible modes of nested array interaction

- Low transparency: ‘Hydro Collision’



- Assumes inner shell is non-transparent
- Outer shell transfers momentum to inner
- Collision of shells reduces RT, decreasing overall shell width at stagnation

- High transparency: ‘Current transfer’

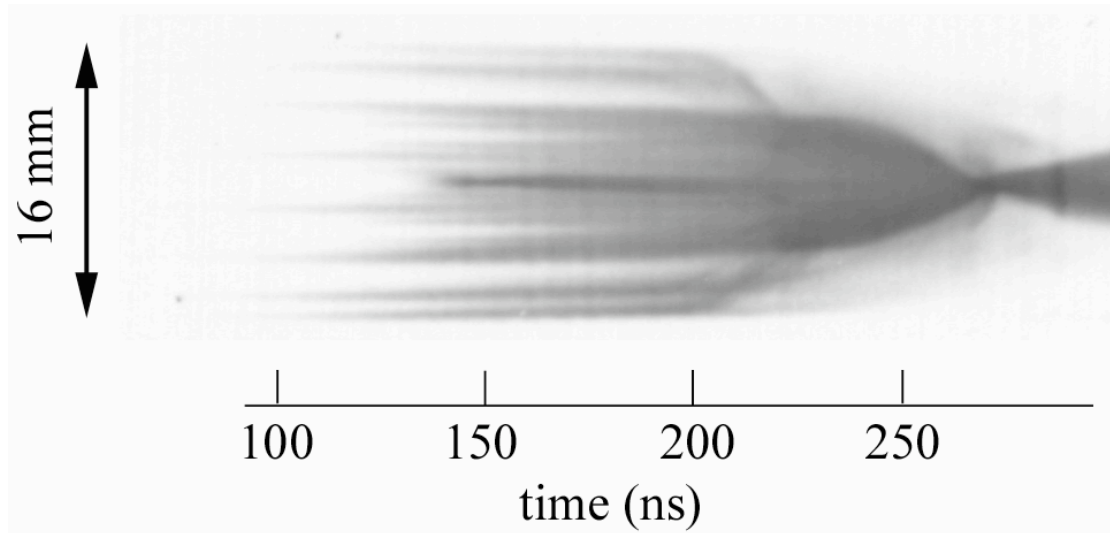


- Assumes inner shell is transparent
- Outer shell passes through inner, switch current but no momentum
- Outer shell coasts to axis, inner implodes rapidly

Answer: Use radial streak photography to observe implosion trajectory of nested arrays

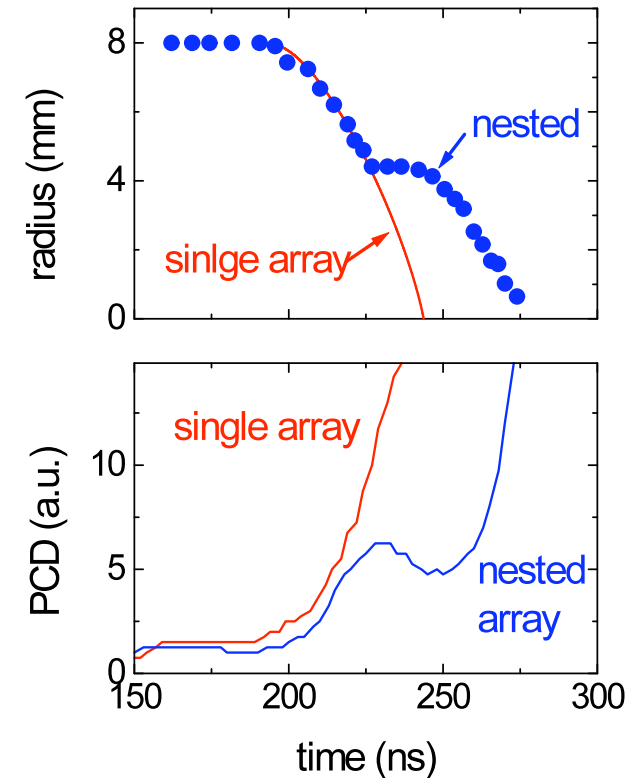
Nested arrays operate in “current transfer” mode

Streak shows no momentum transfer at interaction



- Implosion time of outer array starts at same time as for a single array – all current in outer array, none on the inner
- Interpenetration of the arrays and fast transfer of current to the inner array
- After interaction, decay of snowplough emission from outer array indicates all current has been switched (outer array is coasting in)

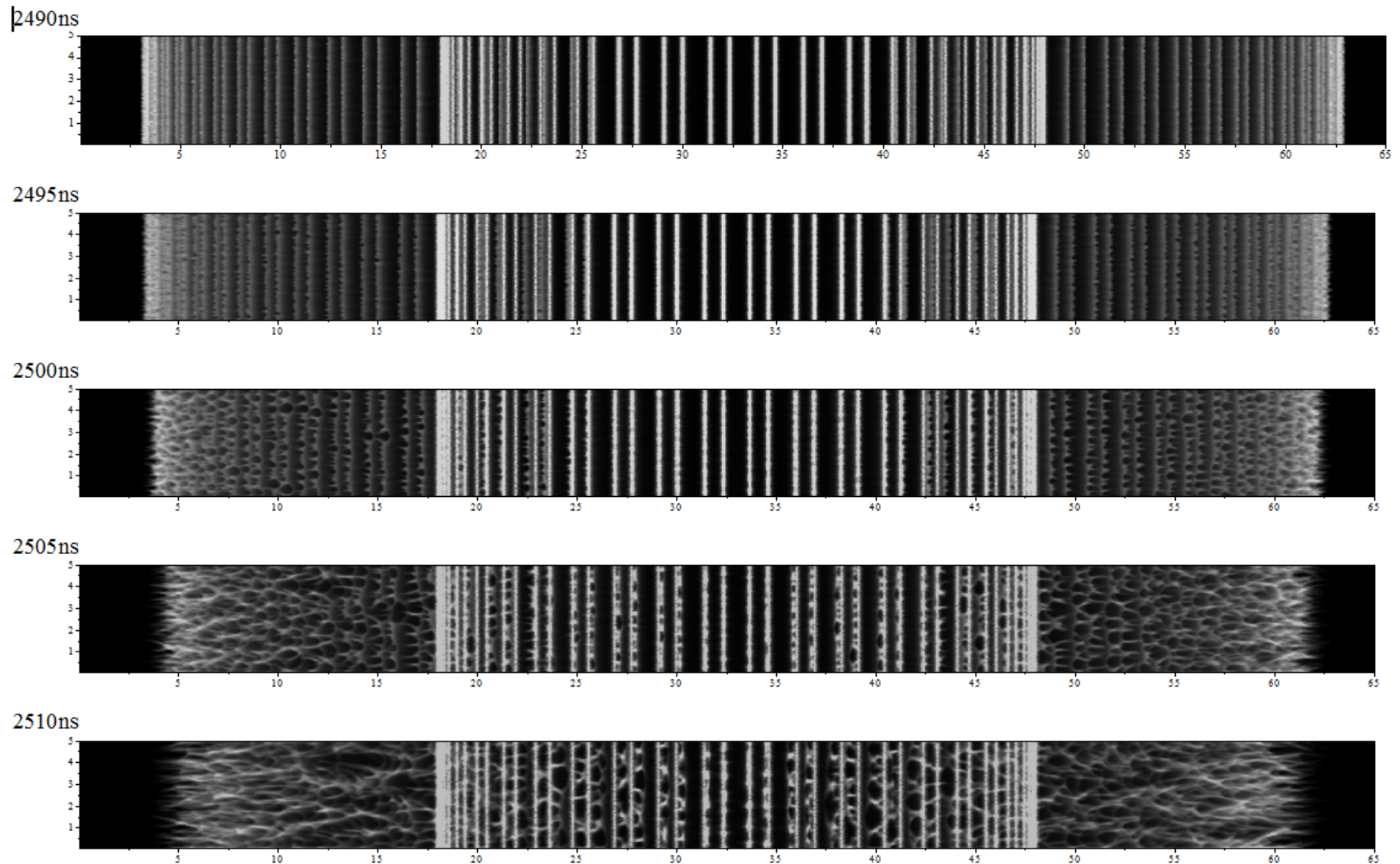
Trajectory and X-ray pulse



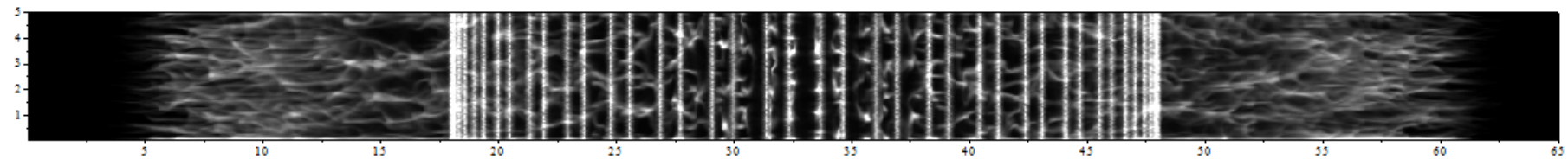
Davis et al., APL 1997, Deeney et al., PRL 1998, Terry et al. PRL 1999,
Lebedev et al., PRL 2000, Deeney et al., PRL 2004, Cuneo et al PRL 2005

Simulation of a Z-machine nested array

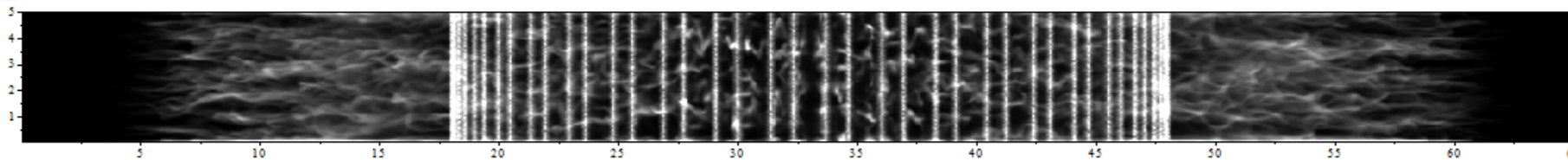
Radiative resistive MHD code GORGON (see talk by J. Chittenden) simulation of a Z-machine copper array. Series of synthetic radiographs (i.e. areal density) showing implosion dynamics.



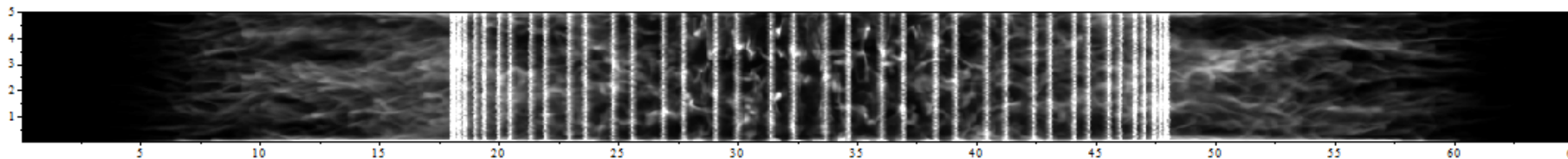
2515ns



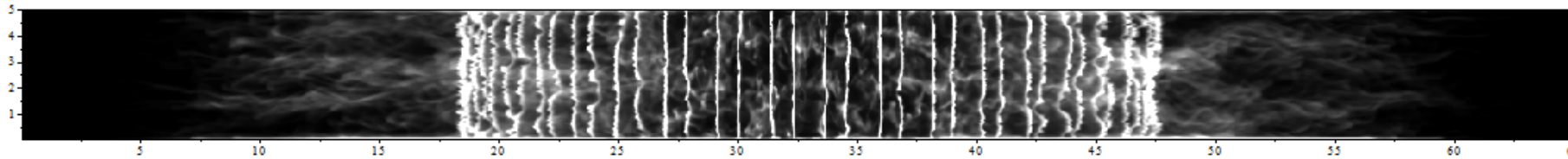
2520ns



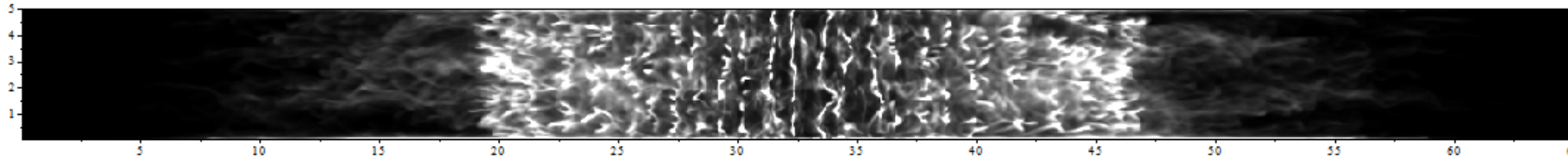
2525ns



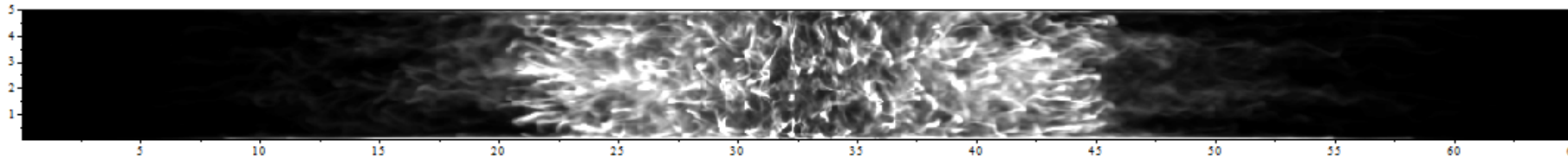
2530ns



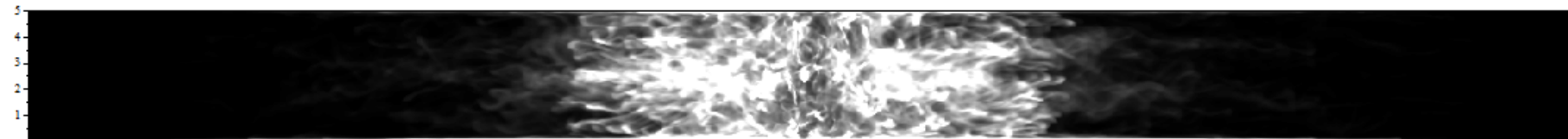
2535ns



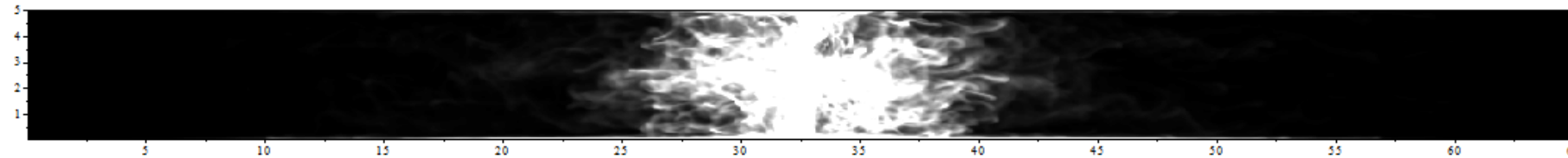
2540ns



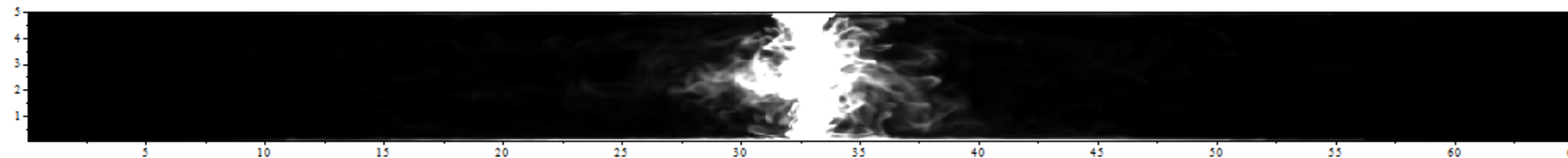
2545ns



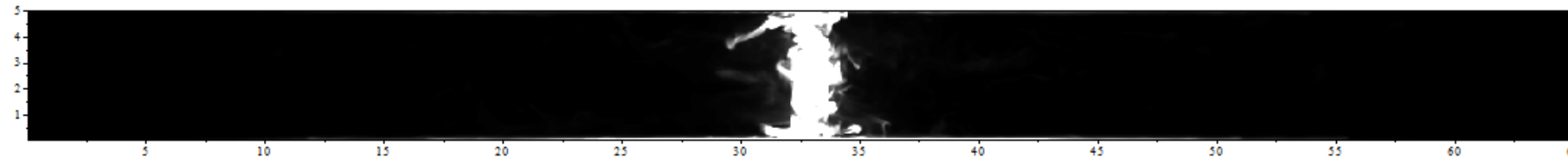
2550ns



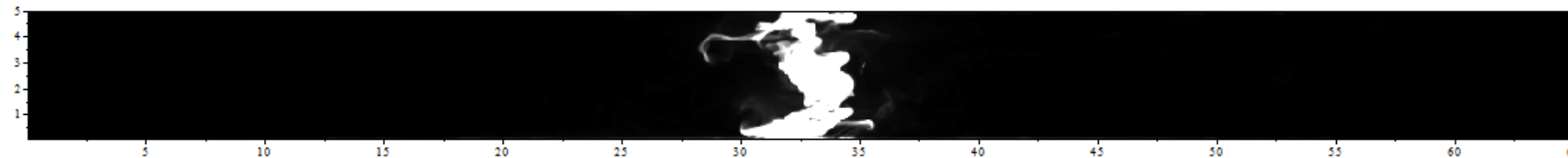
2555ns



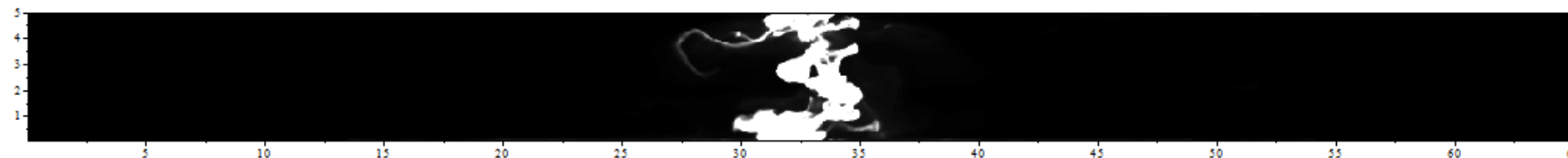
2560ns



2565ns

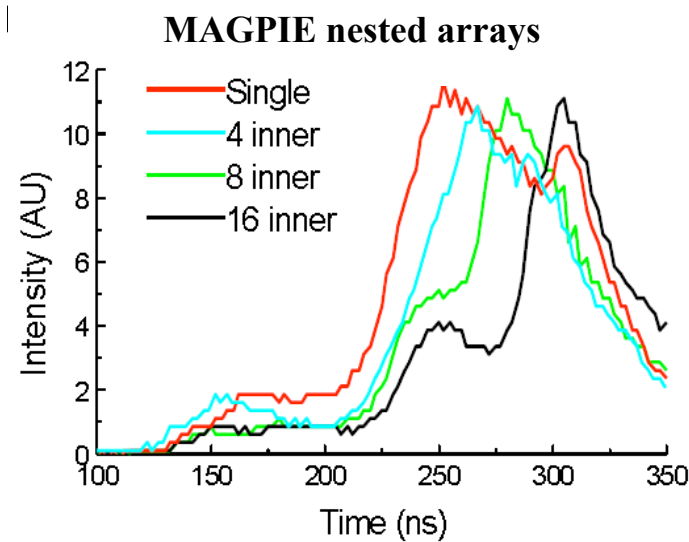


2570ns

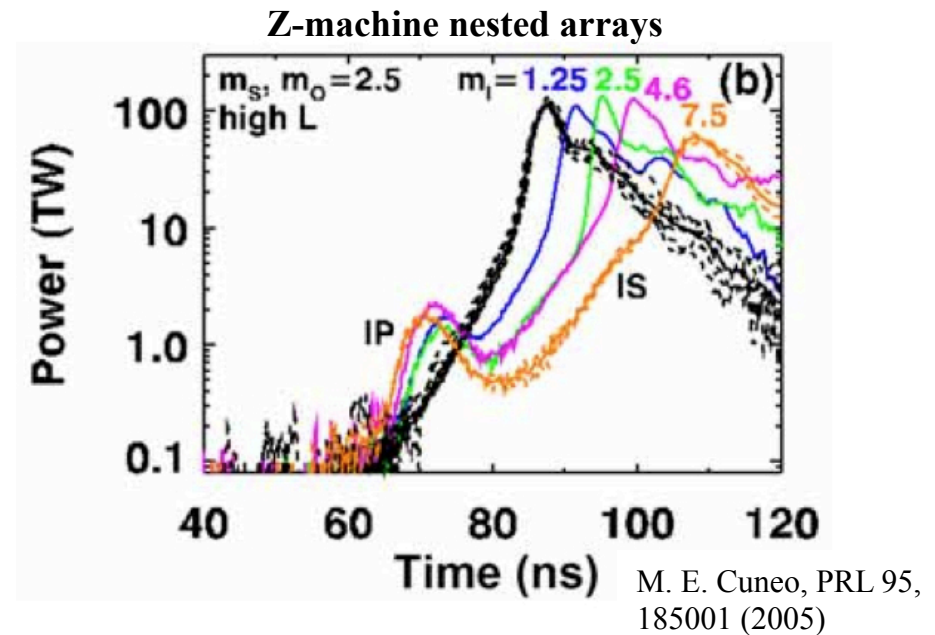


Nested arrays have many variables for pulse shaping

- Vary the number of wires on the inner array to change the contrast of the interaction pulse (this also changes inner array mass)

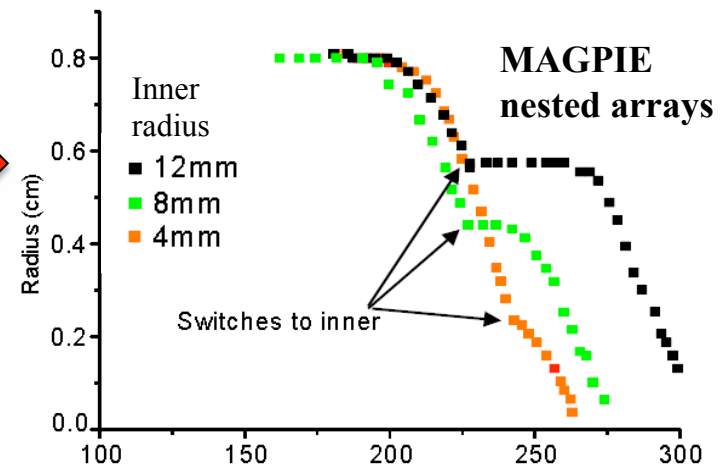
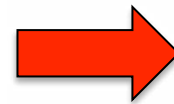


- Vary the mass of the inner array keeping everything else constant – keeps interaction pulse the same, but changes main pulse



Can also vary...

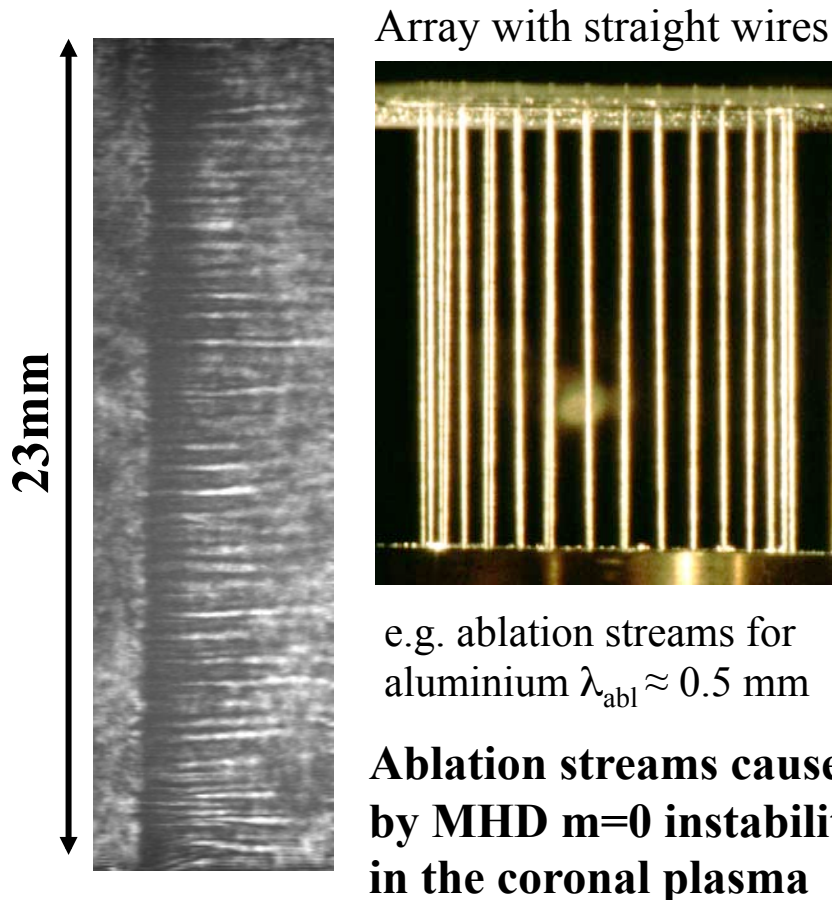
- Ratio of inner array to outer array – changes timing between all three shock features
- Number of nested arrays: recent experiments on Z have used triple nested arrays to add even more control to the pulse shaping.



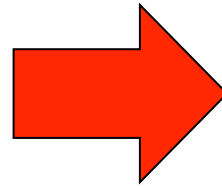
Other methods of changing implosion dynamics

- X-ray output and pinch structure is dependant on implosion dynamics, and implosion dynamics are dependant on ablation structure (streams which seeds the RT instability).
- Is performance (x-ray production, etc.) of wire-arrays limited by this ablation wavelength?

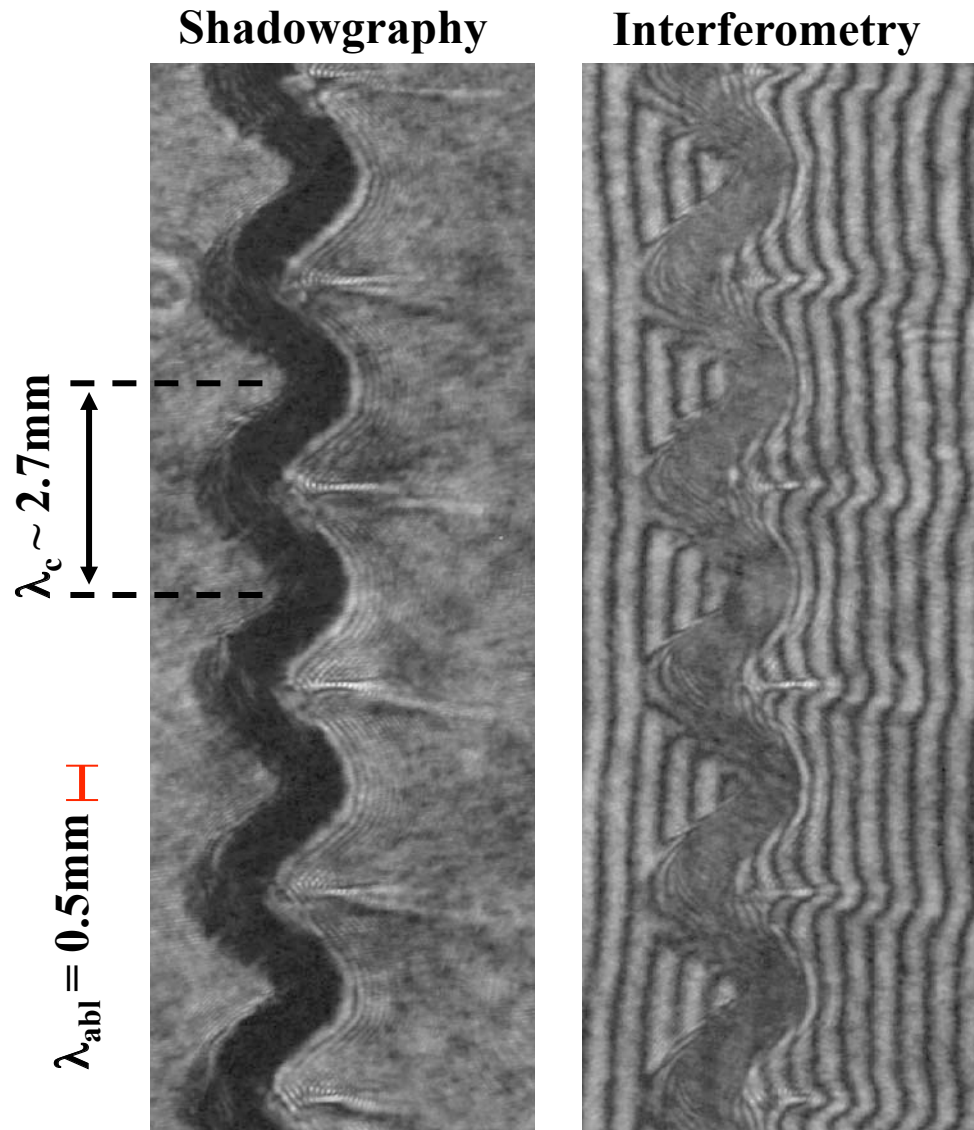
Change ablation structure and you change everything!



Change conditions for MHD growth by changing the magnetic field topology



Coiled arrays change the ablation structure



- Currently the only type of wire array that suppresses ablation streams at the “natural” wavelength, λ_{abl}
- Ablation streamers now occur at the coil wavelength λ_c
- Successfully demonstrated with coil wavelengths from 1.4mm to 4.5mm on MAGPIE (2.8 to 9 times the ablation wavelength in Al)
- Previously, ablation streams were in a random position, and so wire breakage was seeded at random positions. Now, can control where ablation and wire breakage occur.

Wire breakage occurs at the coil wavelength

Soft X-ray camera images

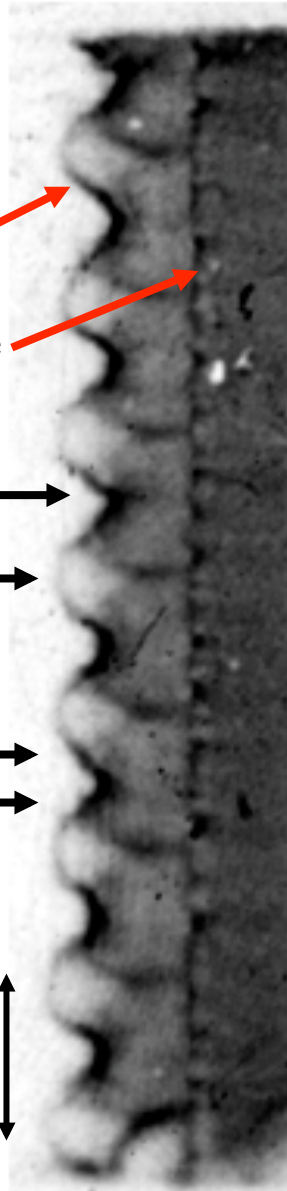
- 1 coiled wire $\lambda_c = 2.7\text{mm}$
- 1 straight wire

Inner edge →

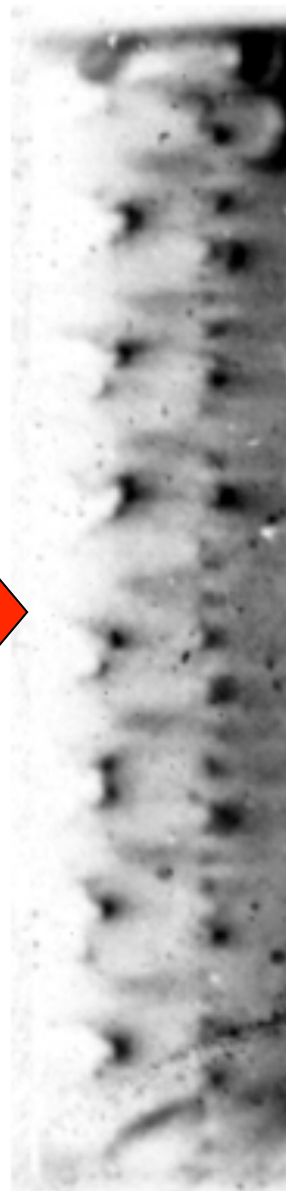
Outer edge →

Azimuthal edges ⇄

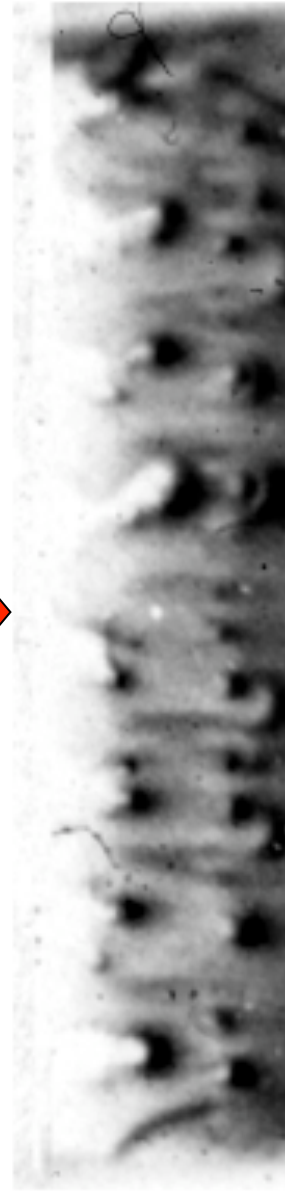
$\lambda_c \sim 2.7\text{mm}$



142ns



179ns



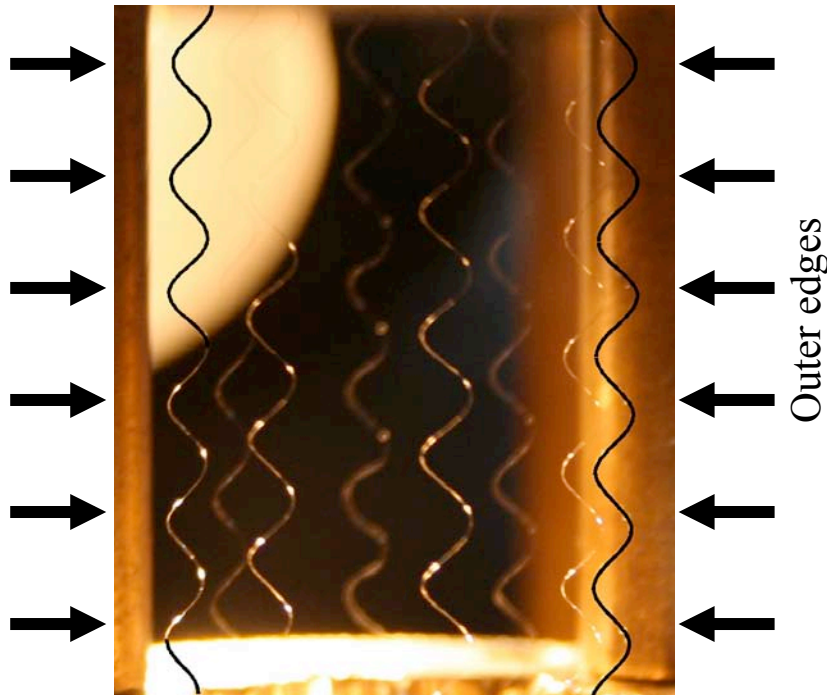
189ns

- Wire breakage first occurs at the azimuthal edges ($J \times B$ force is strongest here)
- The inner edge of the coil then also proceeds to implode.
- The outer edge remains as trailing mass.
- The straight wire breaks up at the “natural” wavelength. These perturbations seed the RT instability which rapidly grows in wavelength – **perturbations merge together**
- **With a large enough coil wavelength, perturbations in the implosion surface do not merge during implosion.**

Coiled arrays suppress RT growth

“Correlated” coiled array

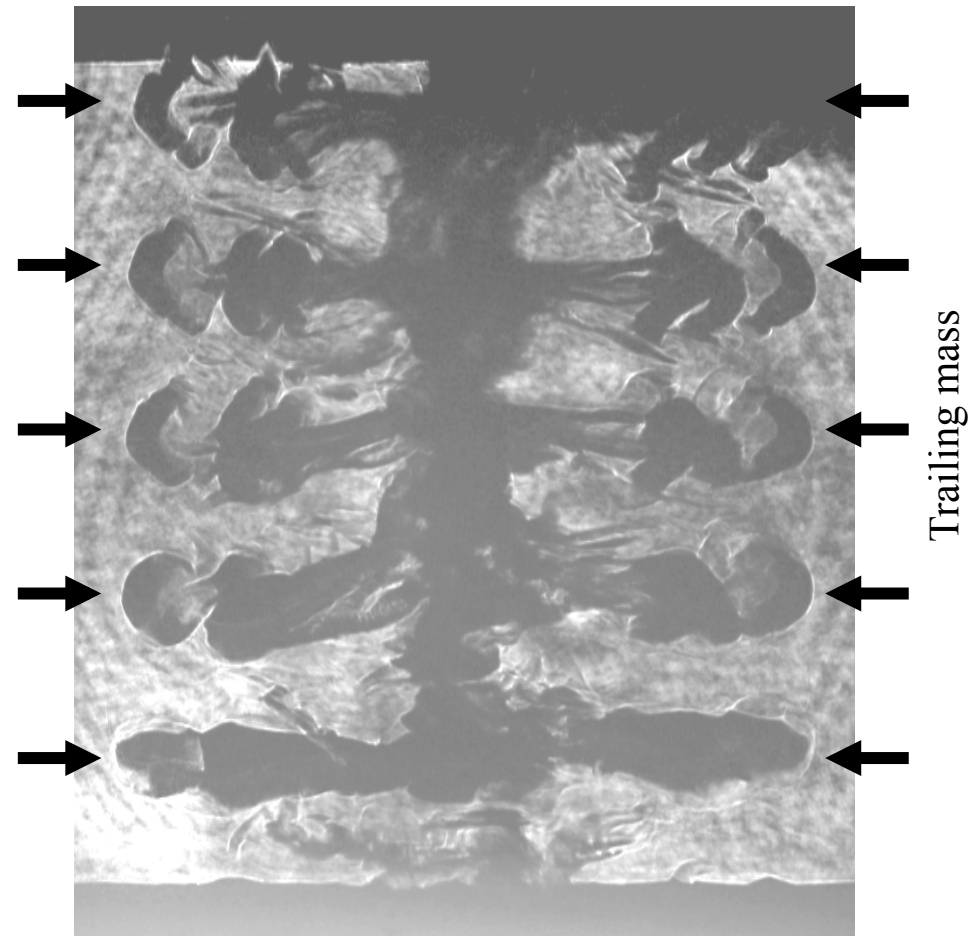
Outer edges (get left behind)
axially aligned for every wire



Al 8x20 μ m array on MAGPIE

“Organised” Implosion

Trailing mass is aligned around entire array



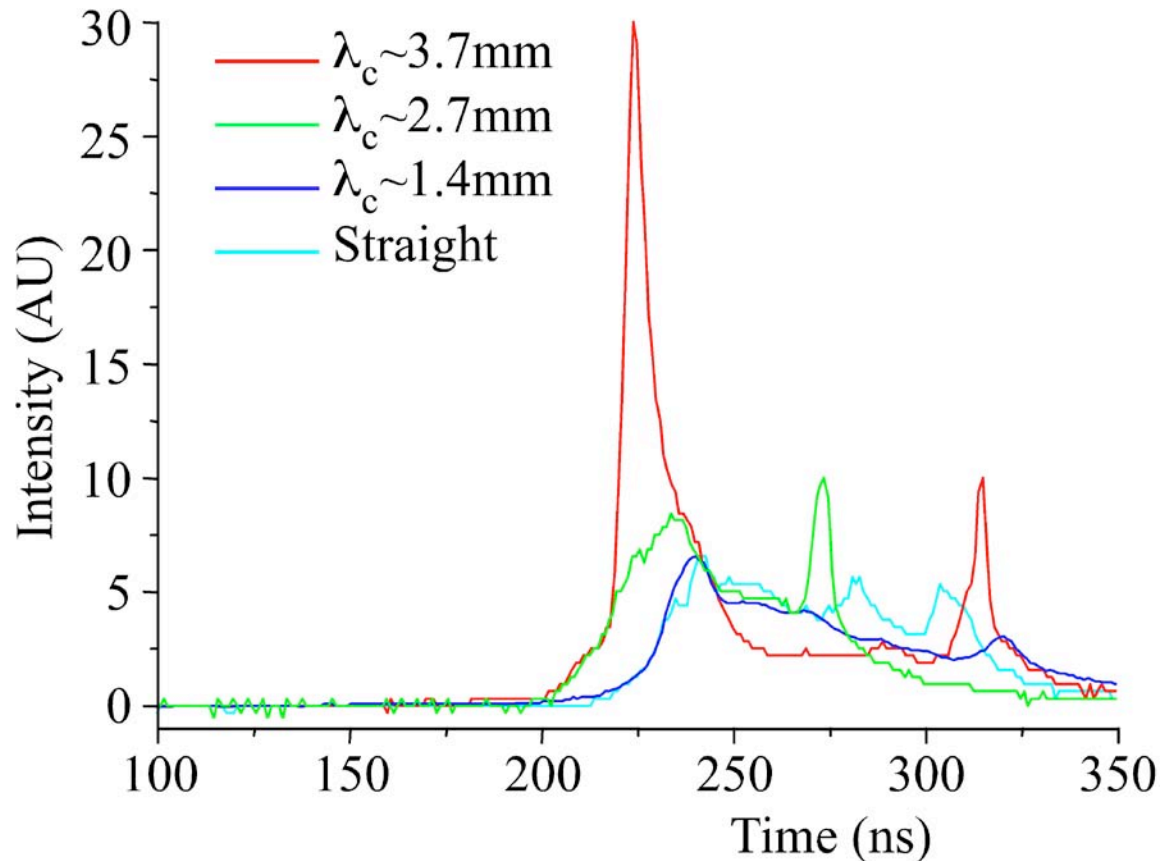
238ns

(2ns before peak current)

- Wavelength growth is suppressed (global structure remains at λ_c)
- Coiled arrays are a tool for controlling the global structure of the implosion.

Large coil wavelengths produce high x-ray powers

X-ray Intensity of Coiled and Straight Arrays



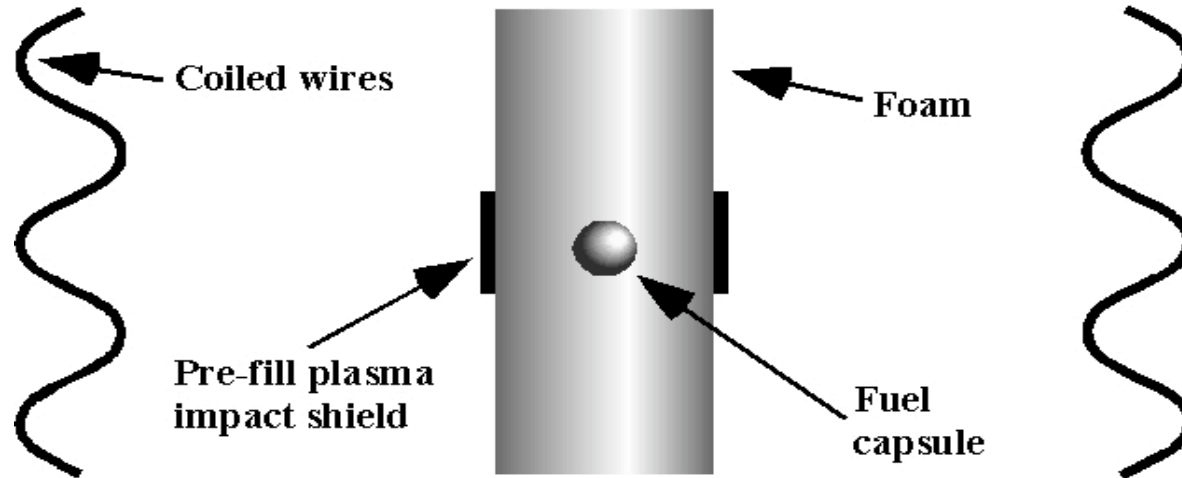
- **X-ray signal from long wavelength coiled arrays is 5-6 times more intense than 8-wire straight arrays, and higher even than 32 wire straight arrays.**

G. N. Hall *et al*, IEEE T Plasma Sci 37 520 (2009)

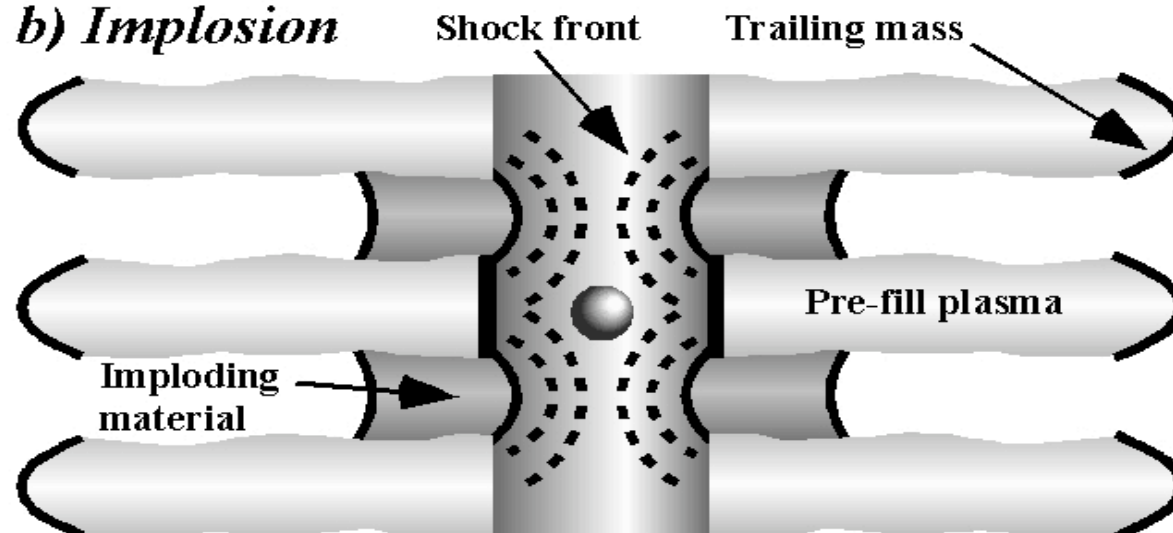
- Radial streak suggests continual acceleration: no pre-fill in front of the imploding section of the coil (implosion occurs *between* streamers). **No snowplough!**
- Final velocity reaches $\sim 3.5 - 4.5 \times 10^5$ m/s. A straight array usually reaches $\sim 2.5 \times 10^5$ m/s.
- Organised implosion results in axial alignment of imploding mass.
- Organised implosion leaves large, discrete gaps in trailing mass. Gaps contain very little plasma, reducing possibility of trailing current. Greater fraction of current driving implosion and stagnation?

Coiled array quasi-spherical dynamic hohlraum

a) Setup



b) Implosion



- New dynamic hohlraum concept being investigated

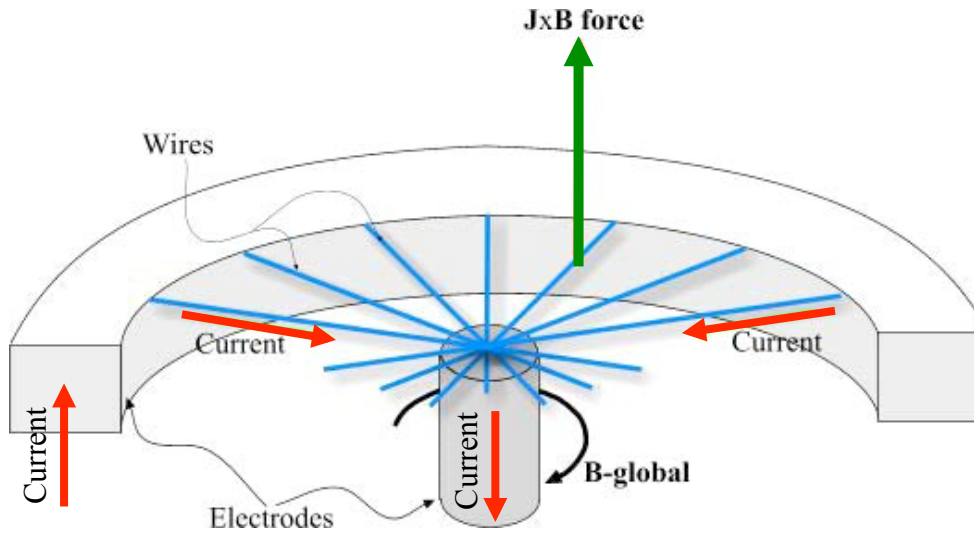
- Aims to overcome symmetry problem of traditional dynamic hohlraum by using coiled arrays

- Coiled arrays allow control of implosion positions, so “aim” implosion just above and below fuel capsule

- Impact of implosion drives quasi-spherical radiative shock into foam, creating better radiation symmetry.

Radial arrays

- Radial array: wires connected between central cathode and anode ring (spokes on a wheel)

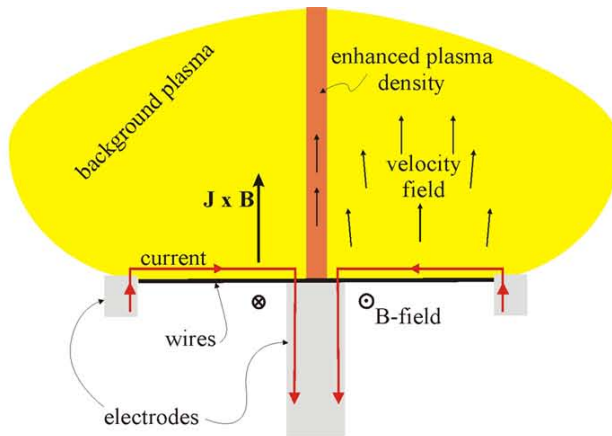


- Ablation rate: $dm/dt \sim \mathbf{J} \times \mathbf{B} \sim 1/R$
i.e. higher at small radii

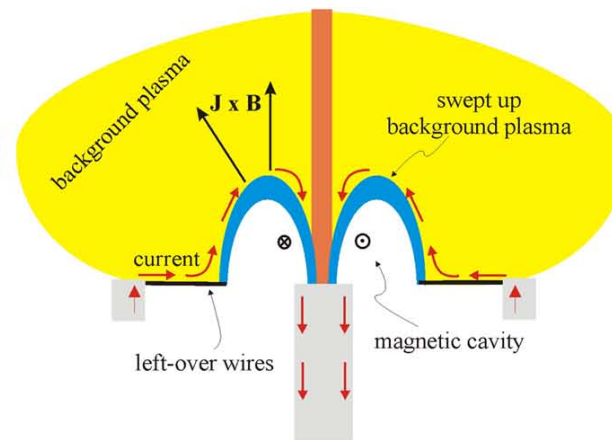
- Wires will break first at the cathode

- Dynamics are qualitatively similar to a plasma focus

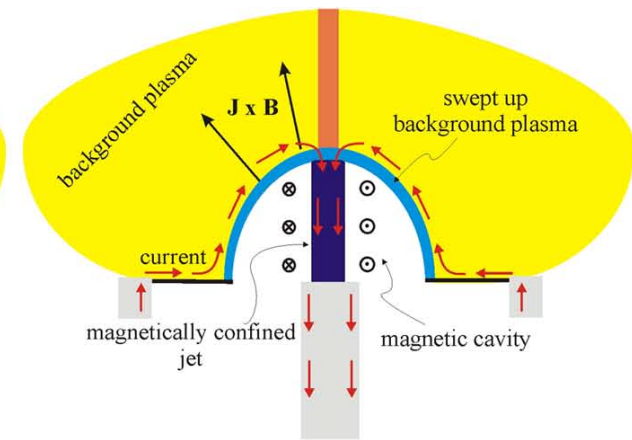
S. V. Lebedev, Mon. Not. R. Astron. Soc.
361, 97–108 (2005)



Background plasma forms
above array, jet on axis



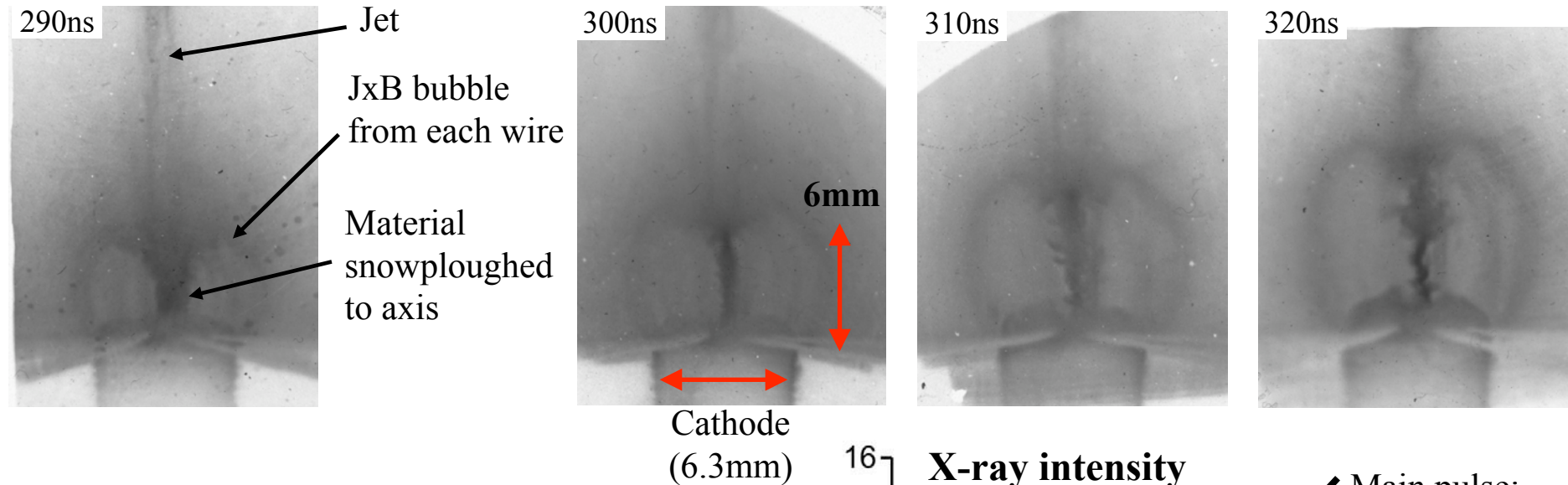
Wire breakage at cathode,
 $\mathbf{J} \times \mathbf{B}$ drives bubble upwards



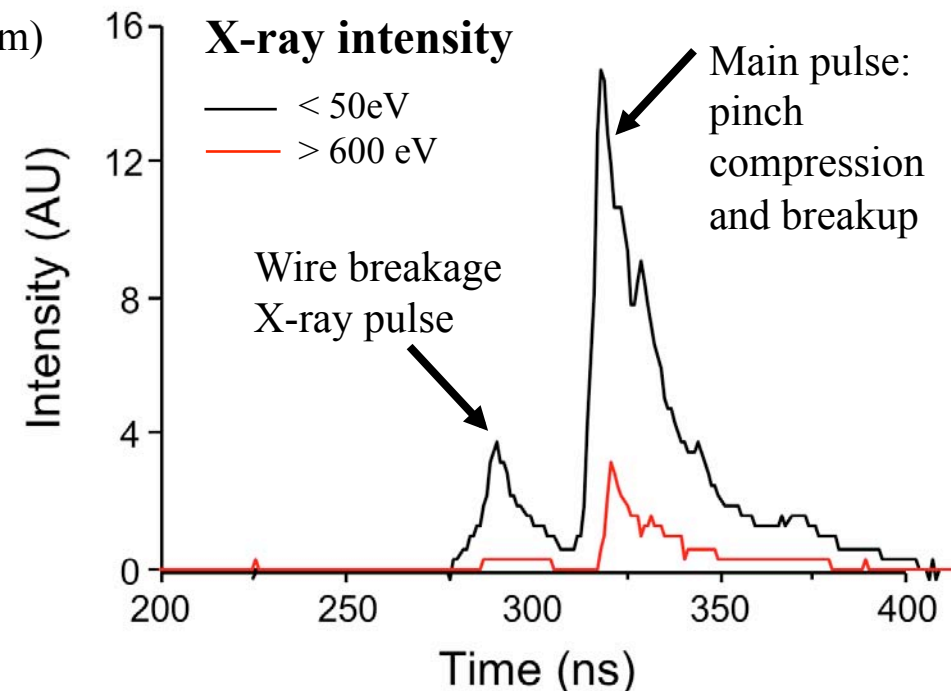
Bubble collapses onto jet,
pinches, X-ray pulse

Radial array dynamics and X-ray production

Soft x-ray camera ($>36\text{eV}$)



- Wire breakage produces first X-ray pulse
- Radiation continues to be emitted as bubble snowploughs through background plasma and towards axis
- Second, main pulse due to compression of pinch, formation of instabilities and break up of central column
- **Length of pinch (main pulse) ~same as cathode diameter**



Radial wire arrays as compact hohlraum source

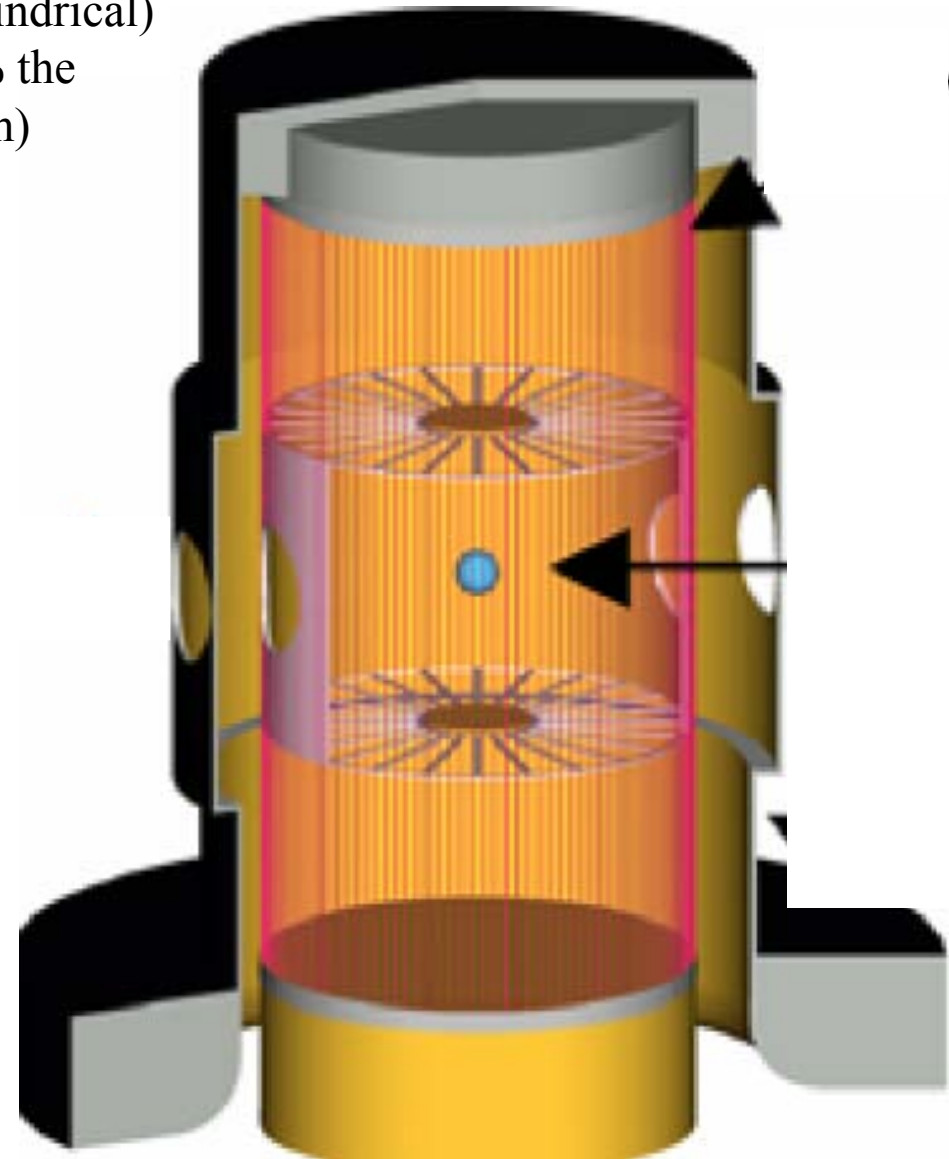
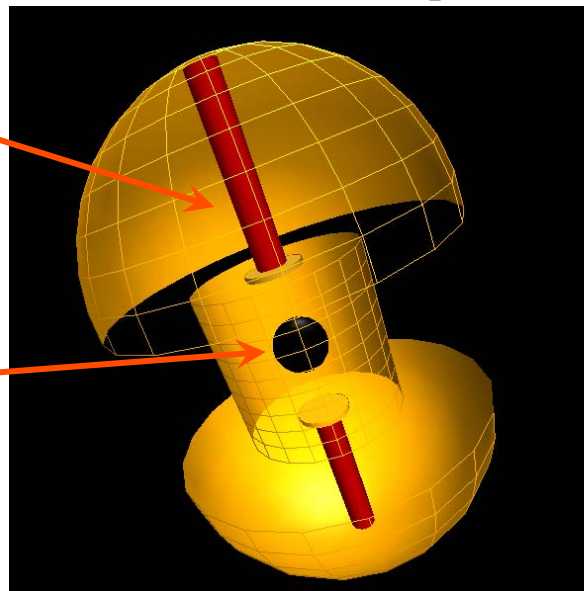
- Soft X-ray power is similar to cylindrical arrays
- X-ray yield is generally lower (~50% of cylindrical) but stagnating length can be as small as 25% the length of a cylindrical array (6mm c.f. 23mm)
- Yield per unit length is ~double for radials
- **Small pinch size = compact x-ray source**
- **Can make smaller hohlraum: higher temperature, more efficient**

**Large pinch = large hohlraum:
low temperature, inefficient**

Radial DEH concept

Radiation
source:
radial array
pinch

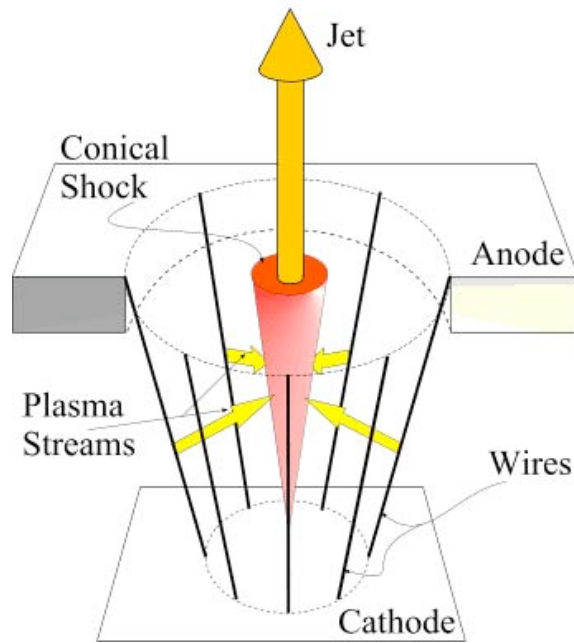
capsule
inside
cathode



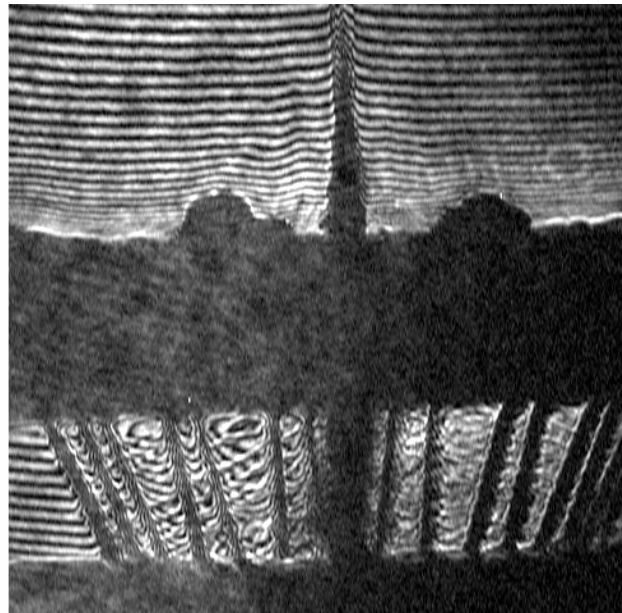
One non-ICF application of wire
arrays: Laboratory Astrophysics

Hydrodynamic jets from conical wire arrays

- Supersonic, radiatively cooled plasma jets can be produced from a conical wire array
- Converging plasma flow is re-directed by a standing conical shock



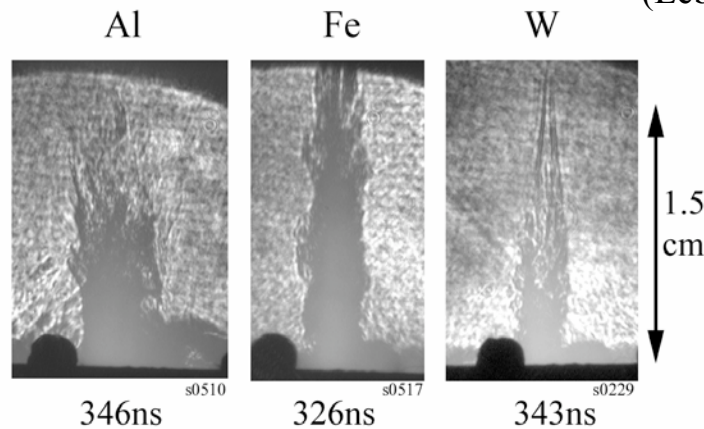
Interferometry



(Lebedev et al., ApJ, 2002)

- Radiatively cooled jet with Mach numbers >20
- Jet velocity $\sim 200\text{km/s}$
- Electron densities in the range $10^{18}\text{-}10^{19}\text{ cm}^{-3}$
- Reynolds number $\text{Re} > 10^4$
Peclet number $\text{Pe} > 10\text{-}50$

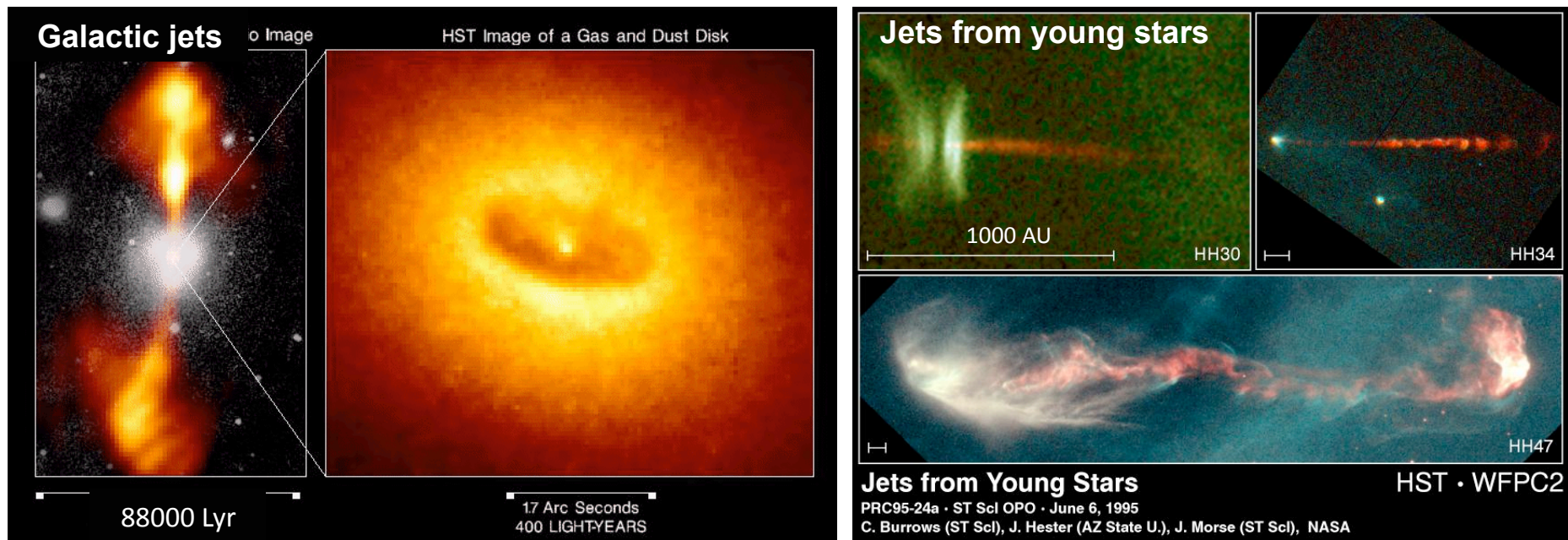
These parameters are highly relevant to jets observed in the universe



- Experiments with different materials demonstrate that radiative cooling affects jet collimation: presence of high Z elements increases radiative cooling rate, enabling collimation over greater distances

Jets and outflows in the universe

- Jets are observed from different types of astrophysical objects with vastly different spatial scales.
- Commonly studied with high-resolution observations and simulations.
- Open questions:
 - **Launching mechanism** close to the source?
 - How do they maintain their **collimation** far away from the source?



The role of experiments in astrophysics

- **Observations** can recover many parameters, but some others are difficult to measure or infer.
- **Experiments** have the advantage of:
 - Inherent **3-D geometry**, allowing to probe from different viewing angles.
 - Possible to **control and vary** the initial conditions.
 - **Provide new ideas!** or rule out theories of jet formation and propagation.
- It possible to scale jets in the laboratory to astrophysical jets, despite them having length and time scale differences of 15-20 orders of magnitude
 - Hydrodynamic and MHD scaling: Euler scaling
 - Dissipative processes are negligible (use ideal MHD)
 - Use **dimensionless parameters** to describe both systems, e.g. Mach number, Reynolds number (viscosity), Peclet number (heat conduction), density ratio, etc...

Plasma jet experiments

- Experiments can focus into 2 main regions:

Outflow region
(jet propagation,
interaction with
interstellar
medium)

Conical wire arrays

Hydrodynamical jet

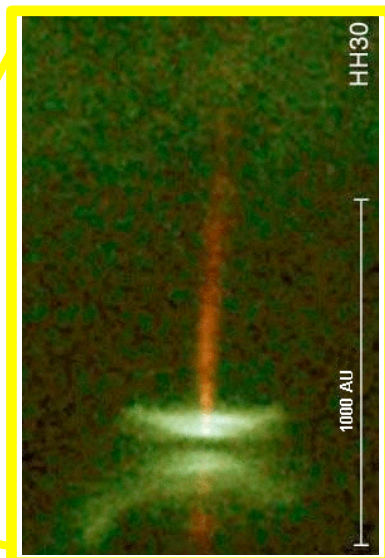
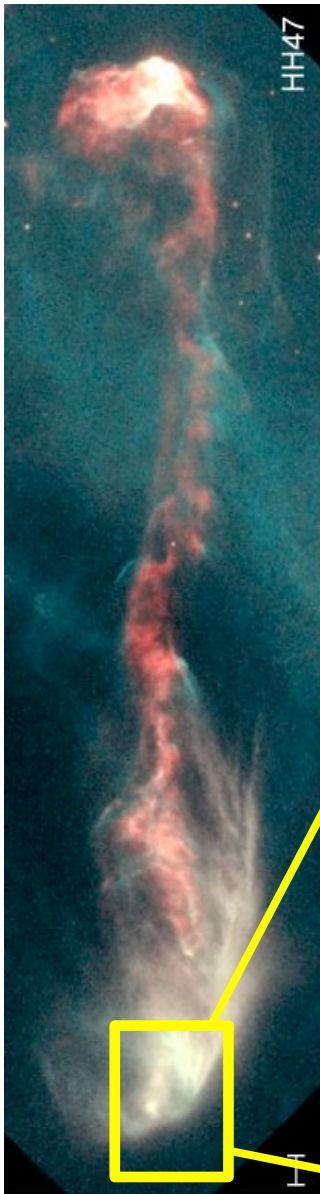
- Supersonic flow
- Radiatively cooled
- Shock from jet-ambient interaction

Radial wire arrays

**Launching /
driving region**
(star embedded
in accretion disk)

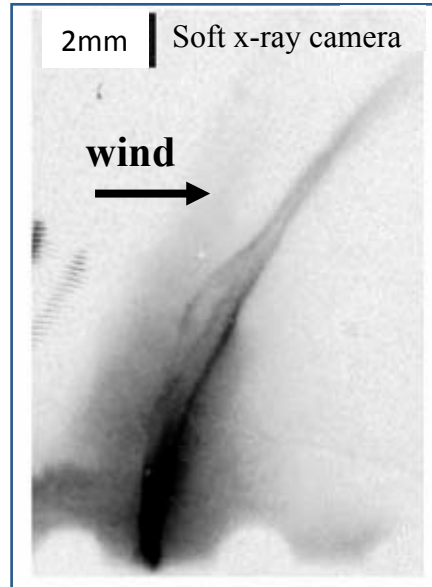
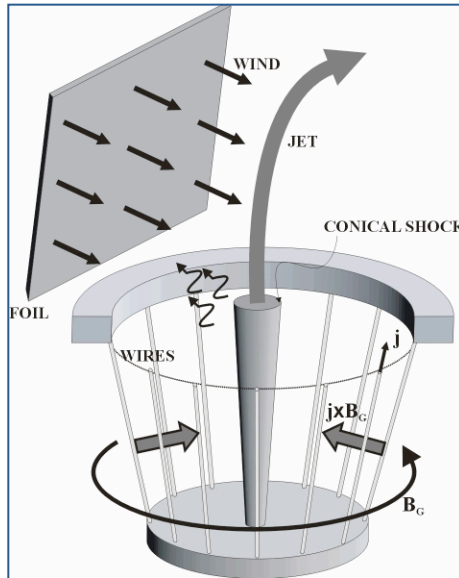
Magnetically-driven jet

- Collimation by toroidal B-field



Hydrodynamic jets from conical wire arrays

Effects such as the presence of interstellar wind and angular momentum can be investigated



Jet bending experiment

- Hydrocarbon foil placed off-axis above array
- Ultraviolet radiation from array photo-ionises foil, plasma blows off, simulating a wind
- Jet interacts with the plasma flow from the foil and trajectory is bent

Ampleford et. al, A&S.Sci, 2007

Jet rotation experiment

- Conical array is twisted to add angular momentum to the ablated plasma
- Jet has angular momentum, which reduces collimation

Ampleford et. al, PRL, 2008

(a) Untwisted (331ns)

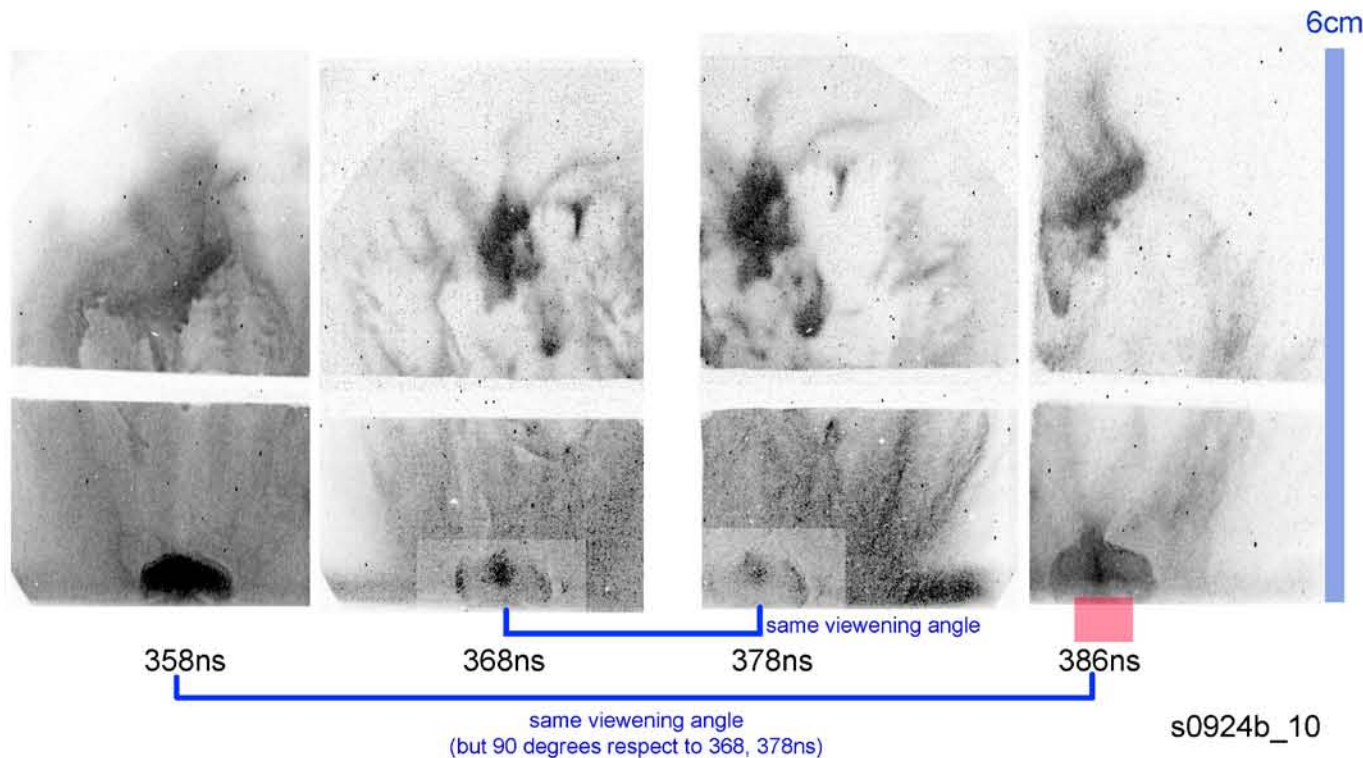
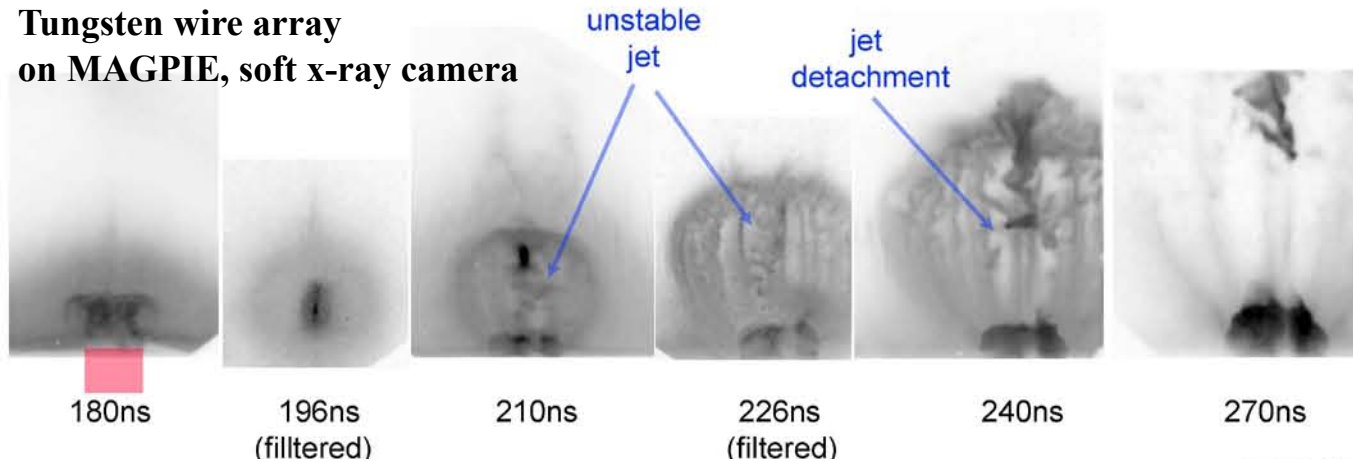


(b) Twisted (337ns)



Study launching / driving region with radial arrays

Tungsten wire array
on MAGPIE, soft x-ray camera



- Late time dynamics of radial wire arrays can be used to model astrophysical jet launching mechanisms

- Initially, jet forms inside cavity and is confined by toroidal magnetic field

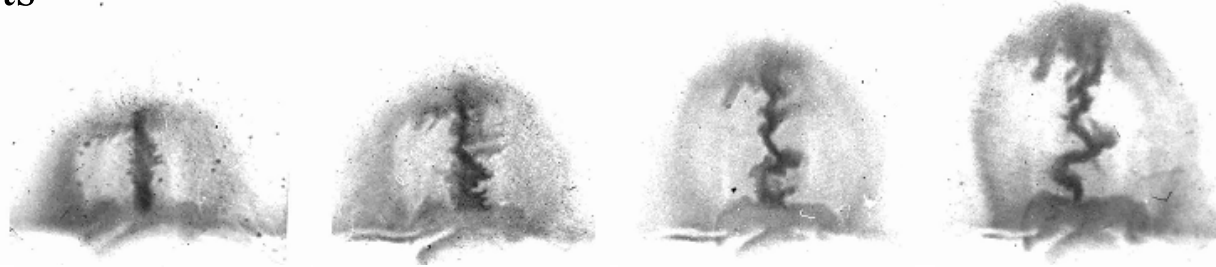
- As bubble breaks, jet is launched, but retains collimation – this suggests it carries magnetic field with it

F. Suzuki-Vidal, IEEE Trans Plasma Sci **38**, 4 (2010)

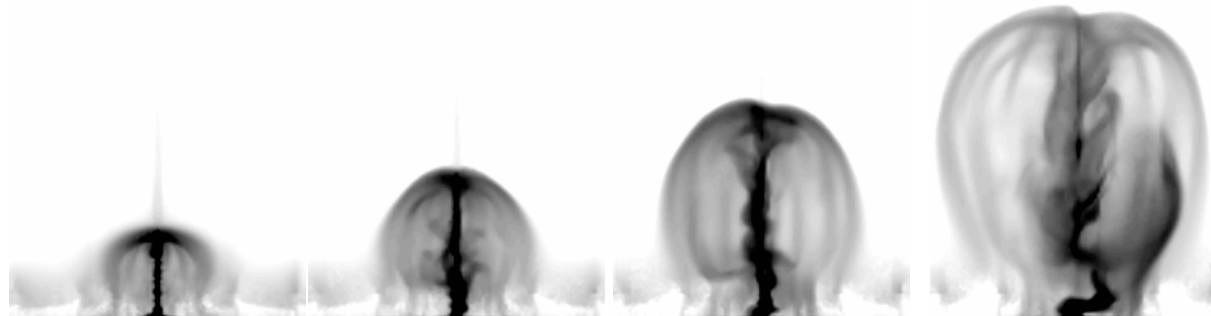
Laboratory astrophysics

Combining experiments with simulations for additional insights into physics of astronomical objects

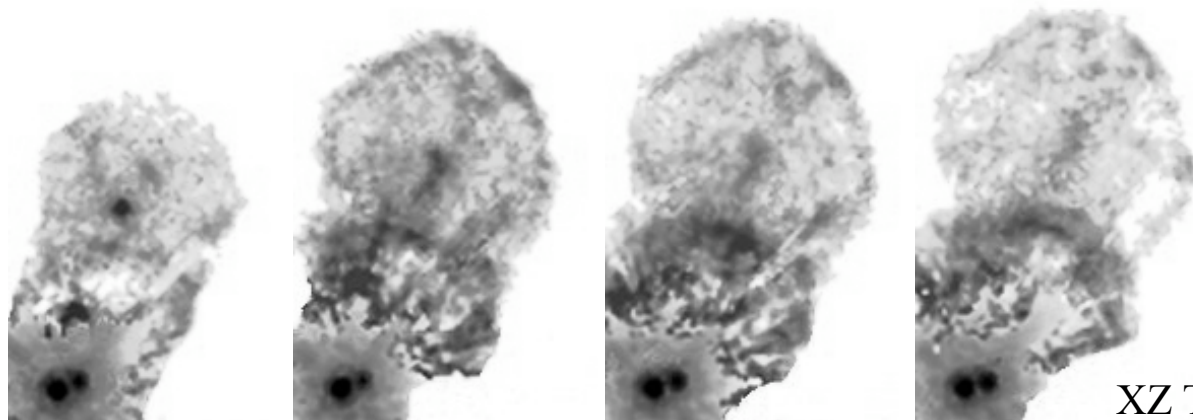
Experiments



Simulations



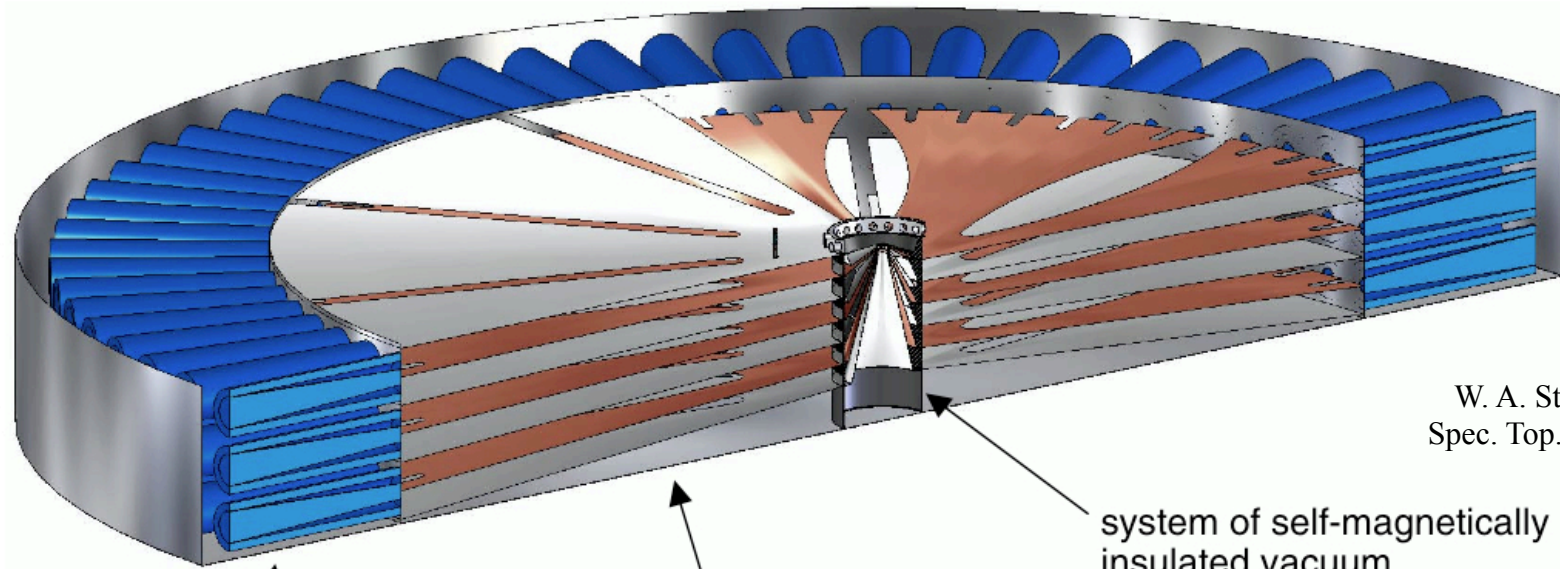
**Astronomical
Observations**



XZ Tauri

The future of wire array ICF

Next-generation pulsed-power machine



W. A. Stygar, Phys. Rev. Spec. Top. 10, 030401, 2007

linear-transformer-driver (LTD) modules (210 total)

radial-transmission-line impedance transformers

system of self-magnetically insulated vacuum transmission lines

Three-dimensional model of a 1000-TW LTD-based z-pinch accelerator. The model is approximately to scale. The diameter of the outer-tank wall is 104 m. The model shows a person standing on the uppermost water-section electrode, near the central vacuum section.

Accelerator and pinch parameters	Present Z accelerator	LTD-accelerator option 1
Outer tank diameter $2r_{\text{tank}}$	33 m	104 m
Number of pulse generators	36 5.4-MV Marx generators	210 11.4-MV LTDs
Initial energy storage	12 MJ	182 MJ
Peak electrical power at the stack P_s	55 TW	1050 TW
Effective peak pinch current I_{eff}	19 MA	68 MA
Actual peak pinch current I	19 MA	63 MA
Energy delivered to the stack at z-pinch stagnation	3.3 MJ	77 MJ
Length of the z-pinch load ℓ	10 mm	10 mm
Z-pinch mass m	5.9 mg	74 mg
Effective pinch implosion time $\tau_{i,\text{eff}}$	95 ns	95 ns
Nominal peak pinch implosion velocity v_p	47 cm/ μs	47 cm/ μs
Nominal peak pinch kinetic energy E_k	0.65 MJ	8.3 MJ
Estimated total radiated x-ray energy	1.6 MJ	20 MJ